UNIVERSITAT POLITÈCNICA DE VALÈNCIA

TISSUE ENGINEERING TECHNIQUES TO REGENERATE ARTICULAR CARTILAGE USING POLYMERIC SCAFFOLDS

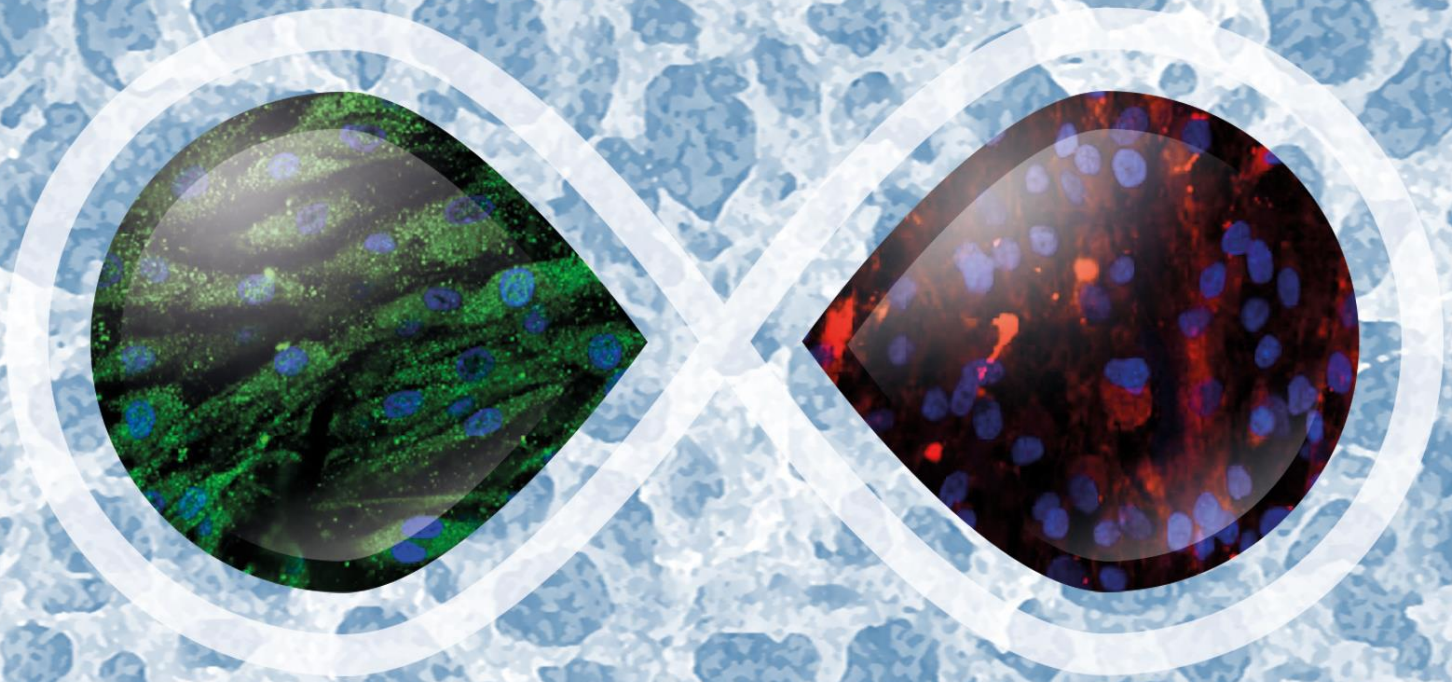

PhD Thesis presented by
Marcos Pérez Olmedilla

Supervisors:
Prof. Dr. José Luis Gómez Ribelles
Dr. Gloria Gallego Ferrer
Dr. Natàlia Garcia Giralt

Valencia, Spain. September, 2015

UNIVERSITAT POLITÈCNICA DE VALÈNCIA

Centro de Biomateriales e Ingeniería Tisular
Universidad Politécnica de Valencia

Tissue engineering techniques to regenerate articular cartilage using polymeric scaffolds

PhD thesis presented by

Marcos Pérez Olmedilla

Supervisors:

Prof. Dr. José Luis Gómez Ribelles

Dr. Gloria Gallego Ferrer

Dr. Natàlia Garcia Giralt

Valencia, Spain. September, 2015

A mis padres,
con amor y gratitud.

Acknowledgments

Durante los años que ha durado este proceso son muchas las personas que me han ayudado y apoyado. Quiero expresar mi más sincera gratitud a TODAS ellas. Nombrarlas a todas sería prácticamente el trabajo de una nueva tesis, por ello, en las próximas líneas mencionaré algunos nombres pero sabed que os doy las gracias a TODOS.

Primeramente, quiero agradecer a mis co-directores José Luis, Gloria y Natàlia, no sólo las enseñanzas a nivel científico sino también los aprendizajes a nivel humano con los que me quedo gracias a haberlos conocido y a haber tenido la posibilidad de trabajar con ellos. Gracias.

Agradezco a todos los compañeros del CBIT su ayuda, compañerismo y amistad. A José Carlos, Raúl, Ángel, Andrés, Carmen, Alberto, Bea, Harmony, Tatiana, Myriam, Amparo,… y un largo etcétera. A M. Salmerón, M. Monleón, Roser, Pepe, Jorge,… Quiero agradecer especialmente a Elisa todos los momentos compartidos en el Laboratorio de Cultivos.

Gràcies al personal del URFOA, el IMIM, el Hospital del Mar i la UPF amb els que vaig poder compartir temps de laboratori i "pasillo" durant les meues estades d'investigació a Barcelona.

I'd like to acknowledge Prof. Ursula Graf-Hausne and all her team for all the help received during my research stay in ZHW (Winterthur, Switzerland). Vielen Dank!

Agradezco al equipo del Dr. Soria, Cris y Olga, todos los consejos y ayuda prestada.

Gracias al Servicio de SEM de la UPV y a Alberto, del CIPF, por ayuda con el Confocal.

A mis compañeros de carrera con los que he seguido en contacto, a compañeros de trabajo en todo este periodo y a amigos en general… gracias por estar ahí y por hacerme saber que puedo contar con vosotros. A Dani, Laura, Burgui, Aurora, Edu, Martina, Rebeca, Pau, Venanci, Guillem, Eva, Mª Jesús, Nachete, Alex, Matteo, Vicente, Alejandra, Rosa, Raúl, Pachi, Marta, Lorena, Bea, Vela, Serrano, Ramses, Osele, JP, Dave, Paco, Alma, Diana, Erick, Amparo, Ivana, Yoli, Jochi, Ana, Esther, Susana, Eugenio, Roberto, Dory, Alegría, Elena, Regi, Vicky, Alberto, Sonia, Miquel,… y lo que sería un casi interminable etcétera (¡el tiempo pasa!)… a todos, gracias.

Quisiera agradecer a todos los compañeros de mi actual trabajo en la UV su paciencia y apoyo en la última etapa de esta tesis. Cabe mencionar de manera especial al inefable Mr. Signes; gràcies mestre.

A Cris, Laia, Isabel, Silvia, Alexandra… gracias por haberme acompañado en este periodo de mi vida.

Mónica, “thank you, more please”.

De manera muy especial quiero dar las gracias a mis padres, a Ana y al resto de mi familia por su apoyo incondicional.

Este trabajo fue financiado por el Ministerio de Ciencia y Tecnología del Gobierno de España a través del proyecto MCYT MAT2001-2678-C02-01, el cual también financió mi beca FPI.

Abstract

Articular cartilage is a connective tissue that consists of chondrocytes surrounded by a dense extracellular matrix (ECM). The ECM is mainly composed of type II collagen fibrils and proteoglycans (mainly aggrecans). The main function of articular cartilage is to provide a lubricated surface for articulation.

Articular cartilage damage is common and may lead to osteoarthritis. Articular cartilage does not have blood vessels, nerves or lymphatic vessels and therefore has limited capacity for intrinsic healing and repair.

Tissue engineering (TE) is a promising approach for healing degenerated cartilage. TE involves the use three-dimensional (3D) scaffolds to support cell and tissue growth. The scaffold provides a structure that facilitates chondrocyte adhesion and expansion while maintaining a chondrocytic phenotype and limiting dedifferentiation, which is a problem in two-dimensional (2D) systems.

Several materials have been tested as scaffolds for the transplantation of chondrocytes into the injured cartilage. Cell attachment to the scaffolds depends on the physical and chemical characteristics of their surface. Surface morphology, rigidity, equilibrium water content, surface tension, hydrophilicity and the presence of electric charges, have an impact on cell attachment and viability.

The primary aim of this thesis was to study the influence of different kinds of biomaterials (mainly scaffolds but also 2D substrates) on the response of chondrocytes to *in vitro* culture, including cellular adhesion, viability, proliferation, chondrocyte differentiation and ECM synthesis.

3D scaffold constructs must have an interconnected porous structure in order to allow for cell development through the network, to maintain their differentiated function, as well as to allow for the entry of nutrients and metabolic waste removal. Therefore, the effect of the hydrophilicity and pore architecture of the scaffolds was studied.

A series of polymer and copolymer networks with varying hydrophilicity was synthesised and biologically tested in monolayer culture. Cell viability, proliferation and aggrecan expression were quantified. When human chondrocytes were cultured on polymer substrates in which the hydrophilic groups were homogeneously distributed, adhesion, proliferation and viability decreased monotonously with the content of hydrophilic groups in the polymer chain. Nevertheless, copolymers in which hydrophilic and hydrophobic domains alternate showed better results than the corresponding homopolymers.

In order to further explore the study above, biostable and biodegradable scaffolds with different hydrophilicity and porosity were synthesised. To do so, a template of sintered microspheres (either poly(methyl methacrylate), PMMA, or poly(ethyl methacrylate), PEMA) of controlled size was used to obtain the interconnected porous structure. This technique allows the interconnectivity between pores and their size to be controlled. Highly periodic and regular pore architectures and very reproducible structures were obtained. The mechanical behaviour of the porous samples was significantly different from that of the bulk (non porous) material of the same composition. Cells fully colonised the scaffolds when the pores' size and their interconnection were sufficiently large.

Another objective was to assess the chondrogenic redifferentiation in a biodegradable 3D scaffold of polycaprolactone (PCL) of human mature chondrocytes previously expanded in monolayer. This study demonstrated that chondrocytes cultured in PCL scaffolds without fetal bovine serum (FBS) – but supplemented with insulin-transferrin-selenium (ITS) and ascorbate – efficiently redifferentiated, expressing a chondrocytic phenotype characterised by their ability to synthesise cartilage-specific ECM proteins.

The influence that pore connectivity and hydrophilicity of caprolactone-based scaffolds has on the chondrocyte adhesion to the pore walls, proliferation and composition of the ECM produced was also studied. Two series of caprolactone-based scaffolds were prepared, one of them of varying porosity and the other with copolymers in which the ratio of the hydrophilic/hydrophobic component varied. The number of cells inside polycaprolactone scaffolds clearly increased as porosity was increased. A minimum of around 70% porosity seems to be necessary for this scaffold architecture to allow for seeding and viability of the cells within. The results of this study suggest that some of the cells inside the scaffold adhered to the pore walls and kept the dedifferentiated phenotype characteristic of chondrocytes cultured in monolayer, while others redifferentiated.

In conclusion, the findings of this thesis provide valuable insight into the field of cartilage regeneration using TE techniques. The studies carried out shed light on the right composition, porosity and hydrophilicity of the scaffolds to be used for optimal cartilage production, which could be applied for future autologous chondrocyte transplantation in patients.

Resumen

El cartílago articular es un tejido conectivo compuesto por condrocitos rodeados por una densa matriz extracelular (MEC). La MEC se compone principalmente de fibras de colágeno tipo II y de proteoglicanos (mayoritariamente agrecanos). La función principal del cartílago articular es proporcionar una superficie lubricada para las articulaciones.

Las lesiones en el cartílago articular son comunes y pueden derivar a osteoartritis. El cartílago articular no tiene vasos sanguíneos, nervios o vasos linfáticos y, por tanto, tiene una capacidad limitada de auto-reparación.

La ingeniería tisular (IT) es un área científica multidisciplinar muy prometedora en la regeneración de las lesiones del cartílago. En la IT se utilizan en "andamiajes" (*scaffolds* en inglés) tridimensionales (3D) como soportes para el cultivo celular y tisular. Dichos *scaffolds*, en el caso de la IT del cartílago articular, tratan de proporcionar una estructura que facilite la adhesión y la expansión de los condrocitos, manteniendo un fenotipo condrocítico limitando su desdiferenciación; que es el mayor problema en los sistemas bidimensionales (2D).

Gran variedad de materiales están siendo probados como *scaffolds* para el trasplante de condrocitos en el cartílago lesionado. La adhesión celular a los *scaffolds* depende de las características físicas y químicas de su superficie. Características del material como la morfología de la superficie, la rigidez, el contenido de agua en equilibrio, la tensión superficial, la hidrofilicidad y la presencia de cargas eléctricas, influyen en la adhesión y la viabilidad celular.

El objetivo general de esta tesis fue estudiar la influencia de diferentes tipos de biomateriales (principalmente *scaffolds* pero también soportes 2D) en la respuesta de los condrocitos en cultivo *in vitro*. Las variables estudiadas incluyen la adhesión y viabilidad celular, así como la proliferación, la diferenciación de los condrocitos y síntesis de matriz extracelular.

Los *scaffolds* deben tener una estructura porosa interconectada con el fin de permitir el desarrollo celular a través de toda la estructura 3D. Además, los scaffolds, deben potenciar que los condrocitos mantengan su fenotipo así como permitir la entrada de nutrientes y la eliminación de desechos metabólicos.

Por todo ello, en este trabajo se ha estudiado el efecto de la hidrofilicidad y de la arquitectura de poro de los scaffolds. Se sintetizaron una serie de sustratos poliméricos de hidrofilicidad variable y se evaluó la respuesta biológica en cultivo en monocapa. Se cuantificó la viabilidad celular, la proliferación y la expresión de agrecano. Cuando los condrocitos humanos se cultivaron en sustratos poliméricos en el que los grupos hidrófilos se distribuyeron de manera homogénea, la adhesión, la proliferación y la viabilidad disminuyó monótonamente con el

contenido de grupos hidrófilo de la cadena polimérica. Sin embargo, los copolímeros en los que los dominios hidrófilos e hidrófobos se alternaban mostraron mejores resultados que los homopolímeros correspondientes.

Para completar el estudio anterior, se sintetizaron series de *scaffolds* acrílicos bioestables así como series de *scaffolds* biodegradables con diferente hidrofilicidad y porosidad. Para ello, se utilizó una plantilla de microesferas sinterizadas (de polimetilmetacrilato, PMMA, o de polietilmetacrilato, PEMA) de tamaño controlado para obtener la estructura porosa interconectada. Esta técnica permite tanto el control del tamaño del poro como de su interconectividad. Se obtuvieron arquitecturas de poros regulares y reproducibles. El comportamiento mecánico de las muestras porosas fue significativamente diferente de las muestras de material no poroso de la misma composición. Las células colonizaron el *scaffold* en su totalidad cuando los poros y la interconexión entre los mismos era lo suficientemente grande.

Otro de los objetivos fue evaluar la rediferenciación condrogénica de condrocitos adultos humanos, previamente expandidos en monocapa, sembrados en un *scaffold* biodegradable de policaprolactona (PCL). Este estudio demostró que los condrocitos cultivados en *scaffolds* de PCL con medio sin suero bovino fetal (FBS) (suplementado con insulina-transferrina-selenio (ITS) y ascorbato), se rediferenciaban de manera eficiente; expresando un fenotipo condrocítico, caracterizado por su capacidad de sintetizar proteínas de la MEC específicas de cartílago hialino.

Se estudió también la influencia de la hidrofilicidad y la conectividad de los poros de los *scaffolds* de caprolactona sobre la adhesión de los condrocitos a las paredes de los poros, su capacidad proliferativa y la composición de la MEC sintetizada. Se prepararon dos series de *scaffolds* basados en la PCL: en una de las series variando la porosidad y en la otra creando copolímeros en los que la relación de componente hidrófilo / hidrófobo variaba. Se observó de manera clara que el número de células aumentaba a medida que se aumentaba la porosidad del *scaffold*. Se comprobó que un mínimo de 70% de porosidad parece ser necesario para permitir la siembra de los condrocitos en el *scaffold* y su posterior viabilidad en el interior del mismo. Los resultados sugieren que parte de las células que se adherían a las paredes internas de los poros mantenían el fenotipo desdiferenciado de condrocitos cultivados en monocapa, mientras que otros se rediferenciaban.

En conclusión, los resultados de esta tesis aportan un avance en el campo de la regeneración de cartílago articular utilizando técnicas de IT. Los estudios realizados proporcionan directrices sobre la composición, la porosidad y la hidrofilicidad más adecuada para la óptima producción de cartílago hialino con la utilización de *scaffolds*, para su futuro uso en el trasplante autólogo de condrocitos en pacientes.

Resum

El cartílag articular és un teixit connectiu format per condròcits envoltats per una densa matriu extracel·lular (MEC). La MEC es compon principalment de fibres de col·lagen tipus II i de proteoglicans (majoritàriament agrecans). La funció principal del cartílag articular és proporcionar una superfície lubricada a les articulacions.

Les lesions en el cartílag articular són comuns i poden derivar en osteoartritis. El cartílag articular no té vasos sanguinis, nervis ni vasos limfàtics i, per tant, té una capacitat limitada d'auto-reparació.

L'enginyeria tissular (IT) és una àrea científica multidisciplinar prometedora en la regeneració de les lesions del cartílag. A la IT s'utilitzen en gran mesura "bastiments" (*scaffolds* en anglès) tridimensionals (3D) com a suports per al cultiu cel·lular i tissular. Aquests *scaffolds*, en el cas de la IT del cartílag articular, tracten de proporcionar una estructura que facilite l'adhesió i l'expansió dels condròcits, mantenint un fenotip condrocític limitant la seva desdiferenciació; que és el major problema en els sistemes bidimensionals (2D).

Gran varietat de materials estan sent provats com *scaffolds* per al trasplantament de condròcits al cartílag lesionat. L'adhesió cel·lular als *scaffolds* depèn de les característiques físiques i químiques de la superfície. Característiques del material com la morfologia de la superfície, la rigidesa, el contingut d'aigua en equilibri, la tensió superficial, la hidrofilicitat i la presència de càrregues elèctriques, influeixen en l'adhesió i la viabilitat cel·lular.

L'objectiu general d'aquesta tesi va ser estudiar la influència de diferents tipus de biomaterials (principalment *scaffolds* però també suports 2D) en la resposta dels condròcits en cultiu *in vitro*. Les variables estudiades inclouen l'adhesió, viabilitat i adhesió cel·lular, així com diferenciació dels condròcits i la síntesi de MEC.

Els *scaffolds* han de tindre una estructura porosa interconnectada per a permetre el desenvolupament cel·lular a través de tota l'estructura 3D. A més, els *scaffolds* han de potenciar que els condròcits mantinguen el seu fenotip, així com permetre l'entrada de nutrients i l'eliminació de productes metabòlics.

Per tot açò, en aquest treball s'ha estudiat l'efecte de la hidrofilicitat i de l'arquitectura de porus dels *scaffolds*. Es van sintetitzar una sèrie de substrats polimèrics d'hidrofilicitat variable i, posteriorment, es va avaluar la resposta biològica en cultiu en monocapa. Es va quantificar la viabilitat cel·lular, la proliferació i l'expressió de agrecà. Quan els condròcits humans es van cultivar en substrats polimèrics en els quals els grups hidròfils es van distribuir de manera homogènia, l'adhesió, la proliferació i la viabilitat van disminuir monòtonament amb el contingut de grups hidròfils de la cadena polimèrica. No obstant això, els copolímers en els

quals els dominis hidròfils i hidròfobs s'alternaven van mostrar millors resultats que els homopolímers corresponents.

Per completar l'estudi anterior, es van sintetitzar sèries de *scaffolds* acrílics bioestables així com sèries de *scaffolds* biodegradables amb diferent hidrofilicitat i porositat. Per fer això, es va utilitzar una plantilla de microesferes sinteritzades (de polimetilmetacrilat, PMMA, o de polietilmetacrilat, PEMA) de grandària controlada per a obtindre l'estructura porosa interconnectada. Aquesta tècnica permet tant el control de la mida del porus com de la seua interconnectivitat. Es van obtindre arquitectures de porus regulars i reproduïbles. El comportament mecànic de les mostres poroses va ser significativament diferent al de les mostres de material no porós de la mateixa composició. Les cél.lules van colonitzar el *scaffold* en la seua totalitat quan els porus i la interconnexió entre els mateixos era suficientment gran.

Altre objectiu va ser avaluar la rediferenciació condrogènica de condròcits adults humans, prèviament expandits en monocapa, en un *scaffold* biodegradable de policaprolactona (PCL). Aquest estudi va demostrar que els condròcits cultivats en *scaffolds* de PCL sense sèrum boví fetal (FBS) (suplementat amb insulina-transferrina-seleni (ITS) i ascorbat) es rediferenciaven de manera eficient, expressant un fenotip condrocític caracteritzat per la seua capacitat de sintetitzar proteïnes de la MEC específiques de cartílag hialí.

També es va estudiar la influència de la hidrofilicitat i la connectivitat dels porus dels *scaffolds* de caprolactona sobre l'adhesió dels condròcits a les parets dels porus, la seva capacitat proliferativa i la composició de la MEC sintetitzada. Es van preparar dues sèries de *scaffolds* amb base de PCL: en una de les sèries variant la porositat i en l'altra creant copolímers en els que la relació de component hidròfil / hidròfob variava. Es va observar de manera clara que el nombre de cèl·lules augmentava a mesura que s'augmentava la porositat del *scaffold*. Es va demostrar que un mínim de 70% de porositat sembla ser necessari per permetre la sembra dels condròcits en el *scaffold* i la seua posterior viabilitat al seu interior. Els resultats suggereixen que part de les cèl·lules que s'adherien a les parets internes dels porus mantenien el fenotip desdiferenciat de condròcits cultivats en monocapa, mentre que altres es rediferenciaven.

En conclusió, els resultats d'aquesta tesi proporcionen informació valuosa en el camp de la regeneració de cartílag utilitzant tècniques d'IT. Els estudis realitzats proporcionen directrius sobre la composició, la porositat i la hidrofilicitat més adequada per a una òptima producció de cartílag hialí amb la utilització de *scaffolds*; que podrien ser aplicats en futurs trasplantaments autòlegs de condròcits en pacients.

Table of Contents

List of Figures

List of Tables

Abbreviation List

2D	Two-dimensional
3D	Three-dimensional
ACI	Autologous chondrocyte implantation
ADSC	Adipose derived mesenchymal stem cell
AFM	Atomic force microscopy
AGC	Aggrecan
ANOVA	Analysis of variance
BMP	Bone morphogenetic protein
BMSC	Bone marrow mesenchymal stem cell
BrdU	Bromodeoxyuridine
BSA	Bovine serum albumin
CBIT	Centre for biomaterials and tissue engineering
CCI	Characterised chondrocyte implantation
CLMA	Caprolactone 2-methacryloyloxy ethyl ester
CPS	Culture polystyrene
DAPI	4',6-diamidino-2-phenylindole
DJD	Degenerative joint disease
DMA	Dynamic mechanical analysis
DMEM	Dulbecco's modified Eagle's medium
DMF	N,N-dimethylformamide
DMS	Dynamic mechanical spectroscopy
DMSO	Dimethyl sulfoxide
DNA	Deoxyribonucleic acid
DSC	Differential scanning calorimetry
EA	Ethyl acrylate
ECM	Extra-cellular matrix
EDTA	Ethylene diamine tetraacetic acid
EGDMA	Ethyleneglycol dimethacrylate
ELISA	Enzyme-linked immunosorbent assay
EMA	Ethyl methacrylate
ESC	Embryonic stem cell
EWC	Equilibrium water content

FBS	Faecal bovine serum
FCM	FBS containing medium
FGF	Fibroblast growth factor
GAG	Glycosaminoglycan
HEA	2-Hydroxyethyl acrylate
HEMA	Hydroxyethyl methacrylate
HUVEC	Human umbilical vein endothelial cells
ICM	ITS containing medium
IGF-1	Insulin-like growth factor-1
IHC	Immunohistochemistry
IL-1	Interleukin-1
iPSC	Induced pluripotent stem cell
ITS	Insulin-transferrin-selenium
MACI	Matrix-induced autologous chondrocyte implantation
mRNA	Messenger ribonucleic acid
MSC	Mesenchymal stem cell
MTT	3-(4,5,-dimethyl-2-thazolyl)-2,5-diphenyl-2H-tetrazolium bromide
MTS	(3-(4,5-dimethylthiazol-2-yl)-5-(3-carboxymethoxyphenyl)-2-(4-sulfophenyl)-2H-tetrazolium)
Mw	Molecular weight
OCT	Optimum cutting temperature compound
PBS	Phosphate-buffered saline
PCL	Poly-caprolactone
PCR	Polymerase chain reaction
PEA	Poly-ethyl acrylate
PEMA	Poly-ethyl methacrylate
PFA	Paraformaldehyde
PG	Proteoglycan
PHEA	Poly-hydroxyethyl acrylate
PHEMA	Poly-hydroxyethyl methacrylate
PLA	Poly-lactic acid
PLG	Polylactide-co-Glycolide
PLLA	Poly-L-lactic acid
PMMA	Poly-methyl methacrylate

PTFE	Polytetrafluoroethylene
PTHrP	Parathyroid hormone related peptide
rpm	Revolutions per minute
RT	Room temperature
SD	Standard deviation
SEM	Scanning electron microscope
TE	Tissue engineering
TGF-β	Transforming growth factor-β
TNF-α	Tumour necrosis factor-α
UV	Ultra violet
wt%	Weight percentage

Chapter 1

INTRODUCTION

"Science is much more than a body of knowledge. It is a way of thinking. This is central to its success. Science invites us to let the facts in, even when they don't conform to our preconceptions. It counsels us to carry alternative hypotheses in our heads and see which ones best match the facts. It urges on us a fine balance between no-holds-barred openness to new ideas, however heretical, and the most rigorous skeptical scrutiny of everything — new ideas and established wisdom. We need wide appreciation of this kind of thinking. It works. It's an essential tool for a democracy in an age of change. Our task is not just to train more scientists but also to deepen public understanding of science."

Carl Sagan (astronomer and science communicator. 1934-1996)

1.1 ARTICULAR CARTILAGE TISSUE

Cartilage is a specialised form of connective tissue composed of cells (chondrocytes) embedded in an extracellular matrix (ECM) that provide its mechanical and physical properties. Intercellular components predominate over the cells, which are isolated in small pockets (lacunae) within this matrix.

Cartilage ECM is composed mainly of two components: the collagenous network, responsible for the tensile strength of the cartilage matrix, and the proteoglycans (mainly aggrecan), responsible for the osmotic swelling and the elastic properties of the cartilage tissue. It can be defined as a dynamic network of molecules secreted by cells that in turn regulate cell behaviour by modulating their proliferation and differentiation, providing structural strength to cartilage and maintaining a complex architecture around the cells [1].

Except in the places where the cartilage is in contact with the synovial liquid in the joints, cartilage is always surrounded by a fibrous membrane of conjunctive tissue. This membrane, called perichondrium, plays a major role in the regeneration of cartilage. Perichondrium is joined to the cartilage in one side and with the adjacent connective tissue on the other side.

The cells of the chondrogenic inner layer of perichondrium are constantly differentiating into chondrocytes while simultaneously secreting matrix around them and supplying cells to the surface of new cartilage ECM. This type of growth is called appositional growth.

The other mechanism for growth is when the cells divide by mitosis generating new and identical cells while at the same time secreting new matrix between the daughter cells separating them. This process, which occurs mainly in immature cartilage, results in the expansion of the cartilage from the inside and is called interstitial growth [2].

According to the relative amounts of its components, three kinds of cartilage can be identified (**Figure 1.1**): hyaline cartilage, fibrocartilage and elastic cartilage [2].

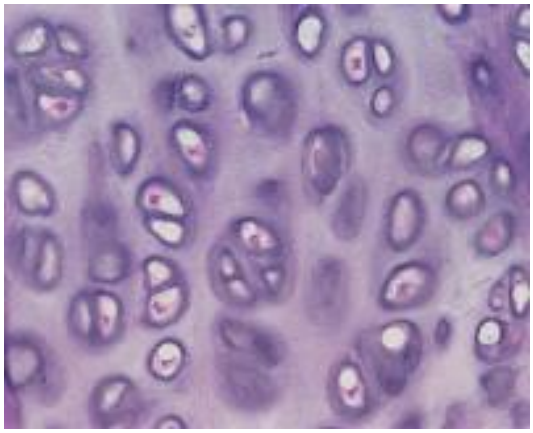

Hyaline cartilage. Cells located in lacunae surrounded by ECM containing fine collagen fibres.

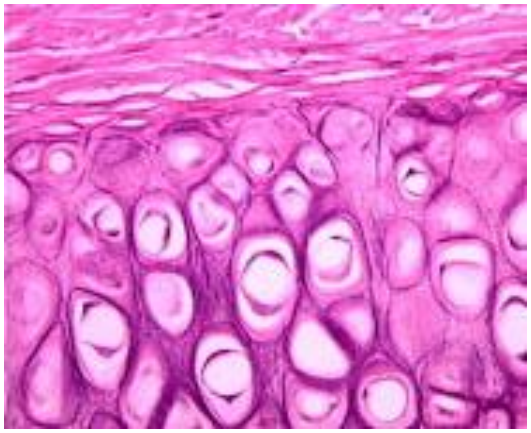

Elastic cartilage. Fine collagenous and elastic fibres in the ECM.

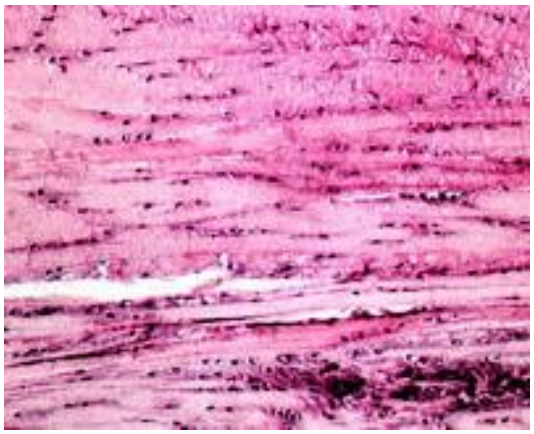

Fibrocartilage with many large collagenous fibres in the ECM.

Figure 1.1 Types of cartilage

Adapted from [3]

Unlike other connective tissues, cartilage does not have blood or lymphatic vessels and the nutrition of the cells diffuses through the matrix. In the same way, cartilage has no nerve endings and is therefore insensitive and exposed to a harsh biomechanical environment. Most importantly, articular cartilage has a limited capacity for intrinsic healing and repair, so preservation of this type of cartilage is essential for proper joint health [4].

The focus of this thesis is the articular cartilage, which is a highly specialised hyaline cartilage. This cartilage is found in the synovial or diarthrodial joints and has unique viscoelastic properties. In the following sections, the functions, histology and structure of articular cartilage are described.

1.1.1 Articular Cartilage Functions

The principal function of the articular cartilage is to provide a smooth, lubricated surface for articulation and to facilitate the transmission of loads with a low frictional coefficient.

Friction is the force that opposes the direction of motion. There are two types of friction: static, when objects are at rest, and kinetic, when objects move against each other. Static friction tends to be greater than kinetic friction.

The coefficient of friction (μ) is calculated as the ratio of friction over normal force:

$$\mu = f/N$$

As far as the cartilage **coefficient of friction** is concerned, this is especially low compared to that of other materials (**Table 1.1**). Some factors can decrease this coefficient, such as the quality of **synovial** fluid, the elastic deformation of cartilage and the formation of a layer of fluid or liquid from the outpouring of cartilage. In the same way, there are factors that can increase the coefficient; for example, the cartilage fibrillation, in which the cartilage loses its normal structure and with it, its function [5].

Table 1.1 Friction coefficients of different materials [5]

Materials	Coefficient
Steel-steel	0.6
Polytetrafluoroethylene(PTFE)-steel	0.04 – 0.2
PTFE-PTFE	0.04 – 0.2
Cartilage-cartilage	0.002 – 0.02

It must be noted that human cartilage supports enormous forces, up to 10 times the body weight (in the case of knee and hip, in an area of 3 cm^2) and it does so constantly and over long periods of time (it is estimated to be more than one million supports per year). In addition to this, every joint is subjected to rotation and sliding forces at some point in their function. During these movements, the surfaces are protected with a lubricating layer directly adhering to the cartilage. A protein called proteoglycan 4 or lubricin, which is present in the synovial fluid and on the surface of articular cartilage, is responsible for joint lubrication and the mechanical properties of the surfaces involved [5].

1.1.2 Articular Cartilage Histology

Articular cartilage consists of a dense ECM, principally composed of water, collagen and proteoglycans, along with other non-collagenous proteins and glycoproteins. We can also find chondrocytes present in lesser amounts and with a sparse distribution. Together, these components help to retain water within the ECM, which is critical for maintaining its unique mechanical properties.

A more detailed explanation of the components of articular cartilage is presented below:

Extracellular Matrix (ECM)

The ECM is responsible for the mechanical characteristics of the cartilage. It consists of (**Figure 1.2**):

- **Water (60-80%)**

It allows for the deformation of the cartilage in response to stress by flowing in and out of it. There is more water in the surface (80%) that in depth (60%). Water is very important for cartilage nutrition and for joint lubrication. In cases of osteoarthritis, the water level increases up to 90%. This increase causes an increase in permeability and a decrease in both resistance and Young's modulus. Also known as the tensile modulus or elastic modulus, Young's modulus is a measure of the stiffness of an elastic material and is used to characterise materials.

- **Collagen (10-20%)**

It is mainly collagen type II (90-95%), which gives the cartilage its significant tensile strength. There are also small amounts of collagen type I, V, VI, IX, X and XI. Type VI collagen is found in early osteoarthritis and type X collagen appears only during endochondral ossification (both types of collagen are associated with cartilage calcification).

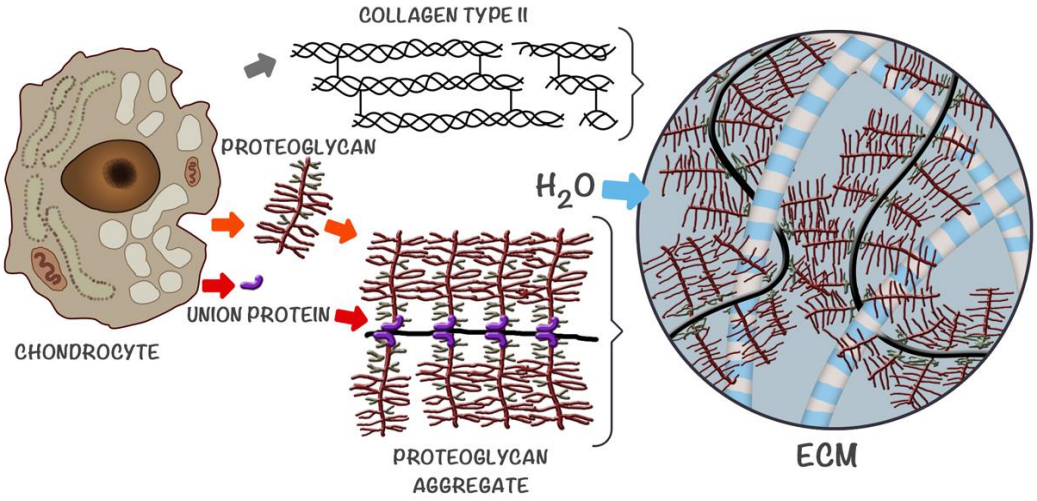

Figure 1.2 Chondrocyte synthesis collagen and proteoglycans

Collagen and proteoglycans interact forming the ECM of the cartilage, which is capable of retaining significant amounts of water. Figure adapted from [5]

- **Glycoproteins**

Proteoglycans (PGs) are the most abundant glycoproteins in the ECM (10-15%). These complex macromolecules are responsible for the compressive strength of the cartilage. They are secreted by chondrocytes and consist of subunits called glycosaminoglycans (GAGs), which bond to a protein core forming more complex molecules called aggreccans. The most common GAG is the chondroitin sulphate, which can be divided in two subtypes, chondroitin-4-sulfate and chondroitin-6-sulfate. Other GAGs commonly found are keratin sulfate (or keratan sulfate) and dermatan sulfate. Chondroitin 4-sulfate is the most abundant and its amount decreases with age, whilst chondroitin-6-sulfate remains constant and keratin increases with age. Less abundant PGs are biglycan, decorin and fibromodulin.

Agreccans are joined by binding proteins to hyaluronic acid, which is another non-sulphated GAG. The PGs (**Figure 1.3**) have an average life of three months, can retain large amounts of water and are responsible for the "porous" structure of the cartilage.

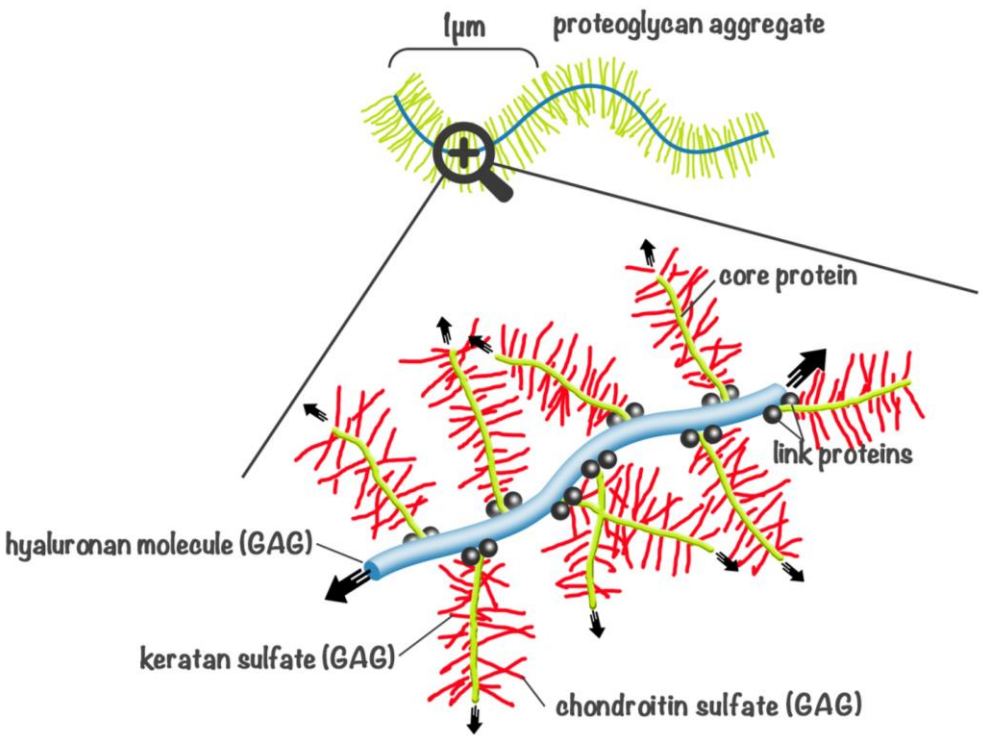

Figure 1.3 Proteoglycans aggregates
Figure adapted from [6]

Other glycoproteins (anchorin CII, fibronectin, laminin). These glycoproteins have binding functions between the ECM and the chondrocytes.

The continuous renewal of the components of the ECM depends on a number of intra- and extracellular proteases. Under normal conditions, cartilage has high levels of inhibitors of these proteases. Alteration of this balance between enzymes and inhibitors may be one of the causes of the onset of osteoarthritis, the main degenerative disease of articular cartilage.
The ECM composition varies depending on the cartilage layer and its location with regard to the chondrocytes [7]. These differences in composition are described in the next section (**1.1.3**), Structure of Articular Cartilage.

Chondrocytes

These specialised cells account for approximately 10% of cartilage weight and are located in lacunae within the ECM, to which they are adapted. They produce the adjacent ECM, though they are also able to depolymerise and remove the ECM to widen its lacunae. This is observed very clearly in the process of endochondral ossification. Cell function is determined by multiple factors: age, pressure variations in the cell membrane, certain growth factors and changes in the ECM itself – for example, the loss of proteoglycan determines functional activation of chondrocyte [4].

1.1.3 Structure of Articular Cartilage

Depending on the structure and function of the sections of the ECM, the articular cartilage can be divided in zones and/or regions, which are described below.

Zones

The macrostructure of the articular cartilage consists of four regions associated with cartilage ECM: superficial, middle, deep, and calcified zone [4, 8, 9] (**Figure 1.4**). This organisation is closely linked to function, as described below.

- **The superficial zone (tangential)**

This thin superficial layer (40 μm) comprises 10% to 20% of the articular cartilage tissue [4]. It is in contact with synovial fluid and is responsible for most of the tensile properties of the cartilage. Thus, the integrity of this layer is crucial for protecting deeper layers from shear stresses [4].

In this zone, the collagen fibres (primarily type II) are densely packed and oriented parallel to the cartilage surface [10].

This layer contains the highest cellular density. Cell density gradually decreases through the intermediate and deep zones to about one-third the density of the superficial layer [11].

In this zone, chondrocytes have a flattened shape, whilst in the rest of the zones they maintain the characteristic round morphology of chondrocytes [11].

The proteoglycan content of this zone is relatively low [9].

- **The middle (transitional) zone**

This layer is the thickest of the zones (500 μm) and represents 40% to 60% of the total cartilage volume [4]. The middle zone provides an anatomic and functional bridge between the superficial and deep zone, functioning as the first line of resistance to compressive forces [4]. In this layer, the collagen fibres are thicker and organised obliquely. The cell density of this zone is lower than it is in the superficial zone and the chondrocytes are rounder. This zone contains the highest amount of proteoglycans [9].

- **The deep zone**

The deep zone represents approximately 30% of articular cartilage volume. It provides the greatest resistance to compressive forces, as the collagen fibrils are arranged perpendicular to the articular surface.

This zone contains the largest diameter collagen fibrils, the highest proteoglycan content and the lowest water concentration. Chondrocytes are typically arranged in columnar orientation, parallel to the collagen fibres and perpendicular to the joint line [4, 8].

- **The calcified layer**

The calcified zone is separated from the deep zone by the tidemark. This layer plays an integral role in securing the cartilage to bone, by anchoring the collagen fibrils of the deep zone to subchondral bone [4].

The cell population in this zone is scarce and chondrocytes are small and distributed randomly [4, 8].

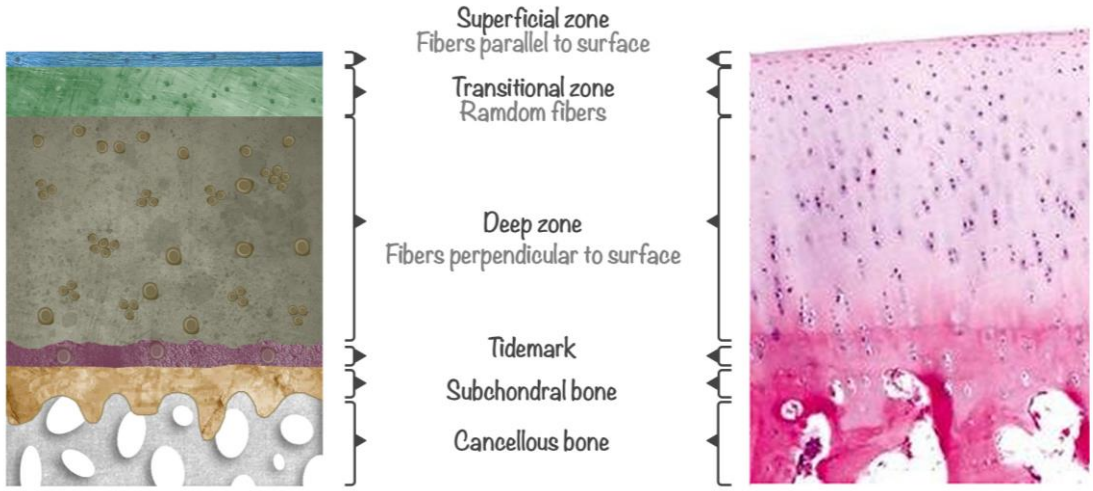

Figure 1.4 Articular cartilage layers
Figure adapted from [5]

Regions

In addition to the horizontal zonal organisation associated with cartilage ECM, the matrix consists of several distinct regions based on proximity to the chondrocyte. The ECM can be divided into three regions: pericellular, territorial, and interterritorial [4, 8, 9]**.** These regions are represented in **Figure 1.5** and their main characteristics are summarised below.

- **Pericellular matrix**

This region completely surrounds the chondrocyte, forming a thin layer around the cell membrane. The function of this region may be to initiate signal transduction within cartilage with load bearing [12].

The pericellular matrix contains mainly PGs, as well as glycoproteins and other non-collagenous proteins [4].

- **Territorial matrix**

The territorial matrix surrounds the pericellular matrix and is thicker than it. This region may protect the cartilage cells from mechanical stress and may contribute to the resilience of the articular cartilage structure and its ability to withstand substantial loads [4, 8].

This region is composed mostly of fine collagen fibrils, forming a fibrillar network around the cells [8].

- **Interterritorial region**

This is the largest of the three matrix regions and contributes most to the biomechanical properties of the articular cartilage.

This region is composed of large collagen fibrils and the majority of PGs. The collagen fibrils change orientation depending on the zone of articular cartilage: parallel to the surface in the superficial zone, obliquely in the middle zone, and perpendicular to the joint surface in the deep zone [4, 8].

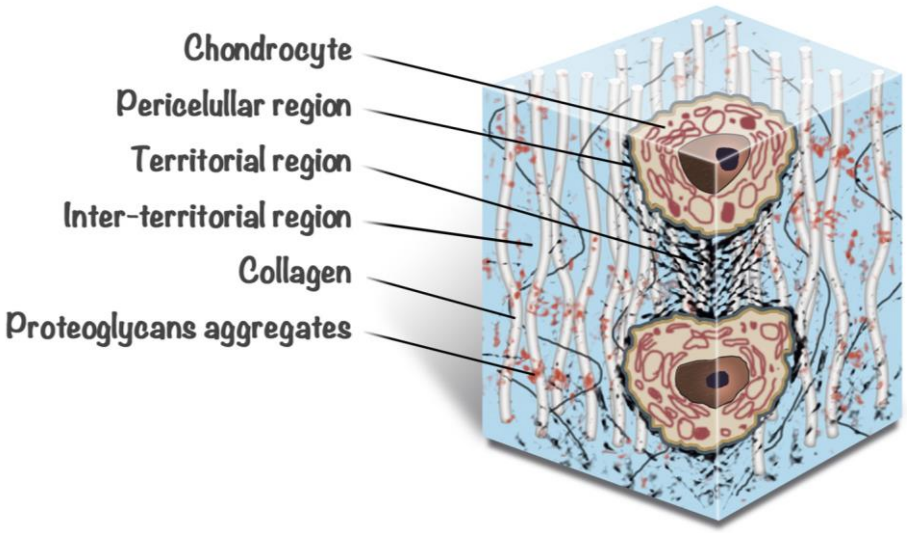

Figure 1.5 Regional organisation of ECM regarding proximity to chondrocytes

Figure adapted from [5]

1.2 ARTICULAR CARTILAGE REGENERATION

Chondrocytes regulate the development, maintenance, and repair of the ECM. A variety of factors can affect the metabolic activity of chondrocytes. For instance, proinflammatory cytokines, such as interleukin-1 (IL-1) and tumour necrosis factor-α (TNF-α), play a role in the degradation and synthesis of the matrix macromolecules [13]. The homeostasis of ECM metabolism compensates for the degradation of certain macromolecules with their replacement by newly synthesised products. Nevertheless, several studies indicate very little turnover of the matrix as a whole, lasting several decades [14].

The composition of the ECM and the organisation of chondrocytes and their response to external cues, such as cytokines, changes with ageing [15]. With increasing age, zonal changes in the distribution of chondrocytes are detected even though the quantity of chondrocytes remains almost unchanged. Chondrocyte density in the superficial region tends to decrease, whereas in the deeper layers the quantity of cells tends to increase.

Other changes due to ageing are a decrease in the hydration of collagen and in the concentration of GAGs, as well as a decrease in the size of proteoglycans. PGs are modified as a result of proteolytic divisions that occur at all ages. The age-related changes in articular cartilage will result in an ECM with a reduced capacity for coping with the normal loads supported during normal functioning of the joint. These changes may have implications for the underlying subchondral bone and can also affect the pore size distribution and the solute permeability. There is also an increased ratio of keratin sulfate to chondroitin sulfate. The concentration of hyaluronan increases with age but this is the result of the gradual accumulation of partially degraded hyaluronan rather than increased synthesis [16].

Furthermore, joint changes that come as a result of injuries of the articular cartilage are characterised by the level of affectation of the composition of the ECM, which damages the chondrocytes.

The three typical articular cartilage injuries are the following [17]:

1. **Blunt trauma:** characterised by the loss of components of the matrix, mostly PGs, without harming the chondrocytes. If the damage is not long lasting, chondrocytes may be able to restore the cartilage by repairing the proteoglycans and the matrix components.
2. **Fractures of cartilage or chondral injuries**: these are the result of a traumatic penetration that alters articular surface by injuring the subchondral plate. The pathophysiological response is a chondrocyte proliferation and synthesis of ECM

protein. This will result in an incomplete repair due to the impossibility for chondrocytes to migrate to the injured area.

3. **Osteochondral fractures**: in these injuries the damage affects not only the cartilage but also the subchondral bone, including the bone marrow cells. There is an inflammatory response as the vascular structures are also affected. In these injuries, an initial repair tissue is formed, though it has the characteristics of fibrocartilage and is actually not functional articular cartilage. After several phases of remodelling, the repaired tissue has a lower content of proteoglycans and a higher content in collagen type I than type II in the ECM. Therefore, the resulting repair is sometimes of low quality resulting in a poor joint function [18].

Furthermore, cartilage lesions can be divided into partial thickness defects when there is no penetration of subchondral bone and no spontaneous repair, and full thickness defects, with penetration of subchondral bone and a partial repair potential depending on the size and locations of the defect (**Figure 1.6**).

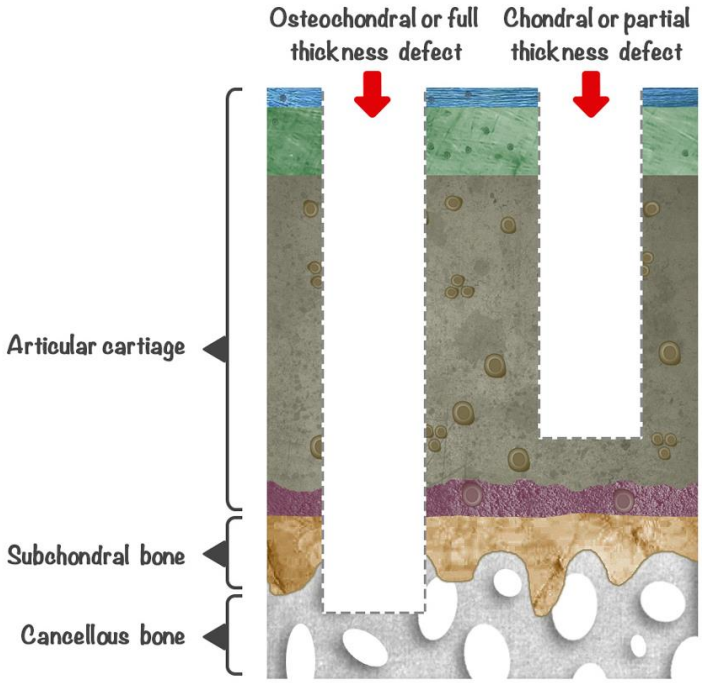

Figure 1.6 Classification of cartilage defects

Chondral defects affect only the articular cartilage layer. Osteochondral defects reach the subchondral bone. Figure adapted from [19].

Outerbridge [20] classified these focal chondral defects into different stages (**Figure 1.7**), based on the severity of the defect. However, such large focal defects, if left untreated, ultimately lead to premature end-stage osteoarthritis.

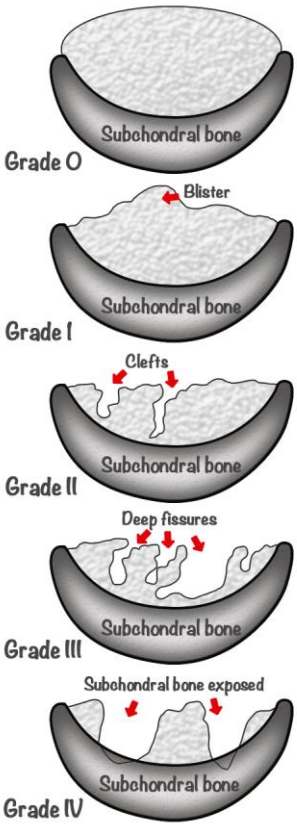

Outerbridge Classification	
Grade	Description
0	Normal cartilage
I	Cartilage with softening and swelling
II	Fragmentation and fissuring in an area of half an inch or smaller in diameter
III	Fragmentation and fissuring in an area larger than half an inch
IV	Erosion of cartilage down to bone

Figure 1.7 Outerbridge classification of articular cartilage lesions

Figure adapted from [21] and [22]

1.2.1 Osteoarthritis

Osteoarthritis, which is also known as osteoarthrosis or degenerative joint disease (DJD), is a progressive disorder of the joints caused by gradual loss of cartilage and resulting in the development of bony spurs and cysts at the margins of the joints [23].

ECM replacement is relatively low and chondrocytes are able to synthesise the necessary elements to maintain homeostasis and joint integrity. When a chronic trauma or a disease alters its homeostasis, articular cartilage may undergo a progressive degeneration. This imbalance between synthesis and degradation maintains the progression of articular cartilage damage and promotes osteoarthritis [24].

During the initial stage of osteoarthritis, chondrocyte proliferation takes place with an increased synthesis of the ECM. This is similar to the response that occurs in subchondral injury of the articular cartilage [25].

Chondrocyte activity is partly stimulated by the release of growth factors such as insulin-like growth factor-1 (IGF-1). However, the newly synthesised proteoglycans have an abnormal composition, where the keratan sulfate concentration is decreased and the ratio of chondroitin 4-

sulfate and chondroitin 6-sulfate is increased. In the same way, the newly synthesised proteoglycans subunits show abnormal aggregation of hyaluronic acid.

Cytokines such as IL-1 and TNF-α can cause a loss of matrix by proteolytic degradation. IL-1 also stimulates chondrocytes and synovial cells to release arachidonic acid metabolites such as PGE, leukotriene B4 and tromboxane. The synovial inflammation is present in the established osteoarthritis, although to a lesser extent than in other joint diseases.

One of the early changes detected in osteoarthritis is the increase in the hydration (2-3%) of the articular cartilage. The functional collagen network is broken, allowing proteoglycans to have an increased amount of water, leading to inflammation of the cartilage, which becomes obvious in early osteoarthritis.

In the progression of osteoarthritis, necrosis of chondrocytes appears, as well as a strong imbalance between the synthesis and the degradation of the ECM. Collagen network suffers processes leading to disorganisation and disintegration.

Removing the functional PGs of the ECM results in a decrease of water content in the cartilage and in a loss of their biomechanical properties, such as elasticity and resilience. Therefore, chondrocytes undergo mechanical stress and trauma, which accelerate the osteoarthritic process [26].

Nowadays, in cases of end-stage knee osteoarthritis, the most commonly available treatment is prosthetic replacement of the articular surface (arthroplasty). However, arthroplasty is indicated for elderly people (more than 60 years of age) with a sedentary lifestyle. Thus, patients younger than 45 years of age are not ideal candidates for the total knee replacement, so another technique must be applied in this case [27].

1.2.2 Repair Techniques for Articular Cartilage

The ageing human population is experiencing increasing numbers of symptoms related to its degenerative articular cartilage. Cartilage injuries of the knee affect approximately 900.000 US citizens annually, resulting in more than 200.000 surgical procedures [28].

This fact has been verified by several studies. In one massive knee arthroscopy study (more than 30.000 knee arthroscopies were reviewed), it was found that 63% of patients had chondral injury [29]. This kind of injuries affect not only the elderly but also children and adolescents, some of whom requiring surgery.

This circumstance has stimulated the investigation of methods for regenerating or repairing articular cartilage. However, repair and regeneration should be differentiated. Repair refers to the restoration of a damaged articular surface with a neo-cartilage tissue that resembles the

native cartilage but does not necessarily duplicate its structure, composition and function. Regeneration refers to the formation of tissue, indistinguishable from the native articular cartilage [30].

Articular cartilage repair techniques seek to prevent early joint degeneration and ensure pain-free movement. The main objectives of these techniques are defect filling and restoration of the articular surface with the best possible repair tissue, which is to say that this tissue must have long-lasting biomechanical properties and has to resemble hyaline cartilage with full integration into the surrounding articular cartilage [31].

1.2.3 Bone Marrow Stimulation Techniques

Some of the therapeutic interventions in the treatment of osteoarthritis attempt to induce a forced regeneration of the articular cartilage. These techniques are based on bone marrow stimulation by the penetration of subchondral bone.

Bone marrow stimulation is one of the oldest and most commonly used methods for stimulating regeneration of neo-cartilage. This method is suited for a full thickness chondral defect with an exposed subchondral bone. The penetration of the subchondral bone plate disrupts the subchondral blood vessels, which leads to the formation of a "super clot" or fibrin clot on the surface of a chondral defect. If the defect is protected from loading at this stage, then the primitive bone marrow mesenchymal stem cells (MSCs) migrate into the super clot to proliferate and differentiate into cells that resemble morphologically with the chondrocytes.

The techniques most commonly used to produce bone marrow stimulation are: microfracture, abrasion arthroplasty and subchondral drilling. These techniques were introduced more than 20 years ago, when no alternative or better strategies were available; in the years since, a considerable body of clinical experience has been gained with them.

Although these surgical solutions can reduce symptoms, the repair tissue formed in response to these procedures is fibrocartilage, which has biomechanical properties that are markedly different from articular cartilage. Fibrocartilage does not have the biochemical composition or structural organisation necessary to provide proper mechanical function within the joint environment and will degrade over time because of insufficient load-bearing capacity [9]. In fact, on the basis of the results obtained, a long-term cure cannot be expected from performing abrasion arthroplasty, Pridie drilling or the microfracture technique. The success rates are variable and depend on many factors, such as the patient's age and activity level, the severity of the arthritic condition and the follow-up period [26].

1.2.3.1 Microfracture

The microfracture technique (**Figure 1.8**) was introduced in the 1980s and its main goal consists of stimulating the growth of new articular cartilage by creating a new blood supply. In this technique a sharp tool called an awl is used to make multiple holes in the joint surface. The holes are made in the bone beneath the cartilage, in the subchondral bone. These perforations create a healing response so that new blood supply can reach the joint surface and bring with it new cells that will form the new cartilage [32].

After the damaged cartilage is removed (debridement of the defect), conical holes 0.5-1 mm in diameter and 4 mm deep are punched all over the defect at a distance of 3-4 mm apart with specialised, tapered awls. Consequently, a blood clot fills the defect followed by ingrowth of bone marrow cells.

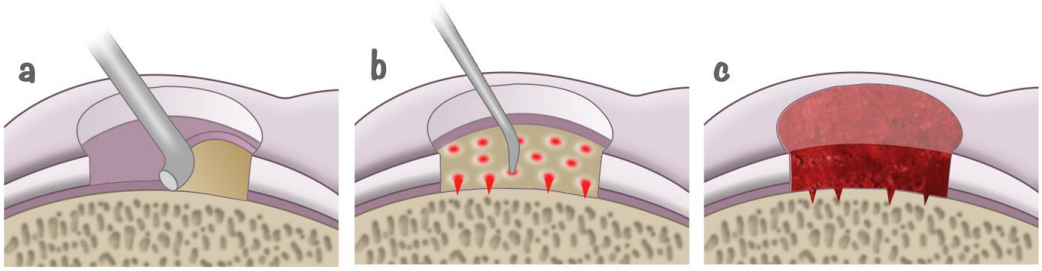

Figure 1.8 Microfracture technique

Steps: **a.** Removal of damaged cartilage. **b.** Holes in the subchondral bone. **c.** Healing response with new cells. Figure adapted from [33]

1.2.3.2 Drilling

Drilling, like microfracture, stimulates the production of cartilage. Multiple holes are made through the injured area in the subchondral bone with a surgical drill or wire. The subchondral bone is penetrated to create a healing response. This technique can be done with an arthroscope. However, it is less precise than microfracture and the heat of the drill may cause injury to some of the tissues [34].

Pridie [35] described a drilling of the subchondral bone preceded by careful removal of all the loose pieces of cartilage. In clinical practice, joint debridement is usually combined with other marrow stimulation techniques, such as drilling or microfracture. Thus, debridement should be considered as a first step in any marrow stimulation techniques.

Microfracture has some advantages over drilling in that there is reduced thermal damage to subchondral bone and a rougher surface is created to which repair tissue might adhere more easily. It should be also mentioned that during an arthroscopic procedure, it is easier to penetrate a defect perpendicularly with a curved awl than with a drill [36].

1.2.3.3 Abrasion arthroplasty

Abrasion arthroplasty is similar to drilling but instead of drills or wires, high-speed burrs are used to remove the damaged cartilage and reach the subchondral bone. Abrasion arthroplasty can be done using an arthroscope [37].

In the same way, this technique involves surgical access to the bone-marrow spaces, which, together with other vicinal compartments (such as the vascular and perivascular spaces, the bone tissue itself and adipose tissue) are consequently stimulated.

1.2.3.4 Spongialisation

Spongialisation is a modification of debridement and drilling but it is applied predominantly in patellar surgery for the treatment of highly localised defects. This technique involves complete removal of the subchondral bone plate at the lesion site and the exposing of the cancellous bone or spongiosa. This removal causes bleeding with a subsequent formation of the fibrous cartilage [38]. Due to the difficulties in removing the subchondral plates, this is usually done during patellar surgery.

1.3 TISSUE ENGINEERING IN ARTICULAR CARTILAGE REGENERATION

Bone marrow stimulation techniques have been enormously useful for many years for repairing cartilage surface. However, these techniques have several limitations, such as the formation of fibrocartilage tissue, which is inferior to hyaline cartilage tissue and consequently it deteriorates months after surgery [39]. These limitations prompted scientists to develop new methodologies for the regeneration of cartilage tissue. In this regards, Tissue Engineering (TE) has proven to be a promising technique in the development of functional cartilage.

1.3.1 Definition of Tissue Engineering (TE)

Langer and Vacanti [40] defined TE as "an interdisciplinary field that applies the principles of engineering and life sciences toward the development of biological substitutes that restore, maintain, or improve tissue function or a whole organ".

TE involves working with biomaterials, growth factors, cell populations and the interaction of all of them in a controlled way for the purpose of achieving functional improvement in the restoration of a tissue or organ. TE of articular cartilage has been a high priority for scientists for several reasons: this tissue does not regenerate by itself after injury, the annual health care costs associated with musculoskeletal diseases and injuries are extremely high, and an effective reparative solution (more successful than the bone marrow stimulation techniques) would improve the quality of life for millions of people suffering from this lesion. These facts, joined with the number of young patients undergoing arthroscopy, has increased the need for creating a repair tissue that can last several decades [9].

Nowadays important developments in TE have given way to new possibilities for tissue replacement parts and implementation strategies. There have been numerous scientific advances in biomaterials, stem cells, growth and differentiation factors and biomimetic environments that have created opportunities for manufacturing tissues in the laboratory, combining engineered extracellular matrices (scaffolds), cells and biologically active molecules.

The application of TE in the healing of the damaged cartilage involves the synthesis of cartilaginous constructs capable of restoring the normal functions of native cartilage.

For instance, one way TE can solve problems is by using living cells. These could be artificial skin that includes living fibroblasts, cartilage repaired with living chondrocytes or other types of cells used in other ways. We shall focus on the developments of several methods using TE to heal degenerated cartilage [41-45].

1.3.2 Cell Based Repair: Autologous Chondrocyte Implantation (ACI)

The irregular results of microfracture inspired the development of autologous chondrocyte implantation (ACI), which now represents one of the first TE applications for the regeneration of the articular cartilage surface.

This technique (**Figure 1.9**) has been in use for almost 30 years and consists of the enzymatical isolation of chondrocytes from a biopsy of healthy articular cartilage on a minor weight bearing area of the knee joint. Once extracted, the chondrocytes are expanded in a monolayer culture and then injected under an autologous periosteal flap, which is sutured onto cartilage defect [46].

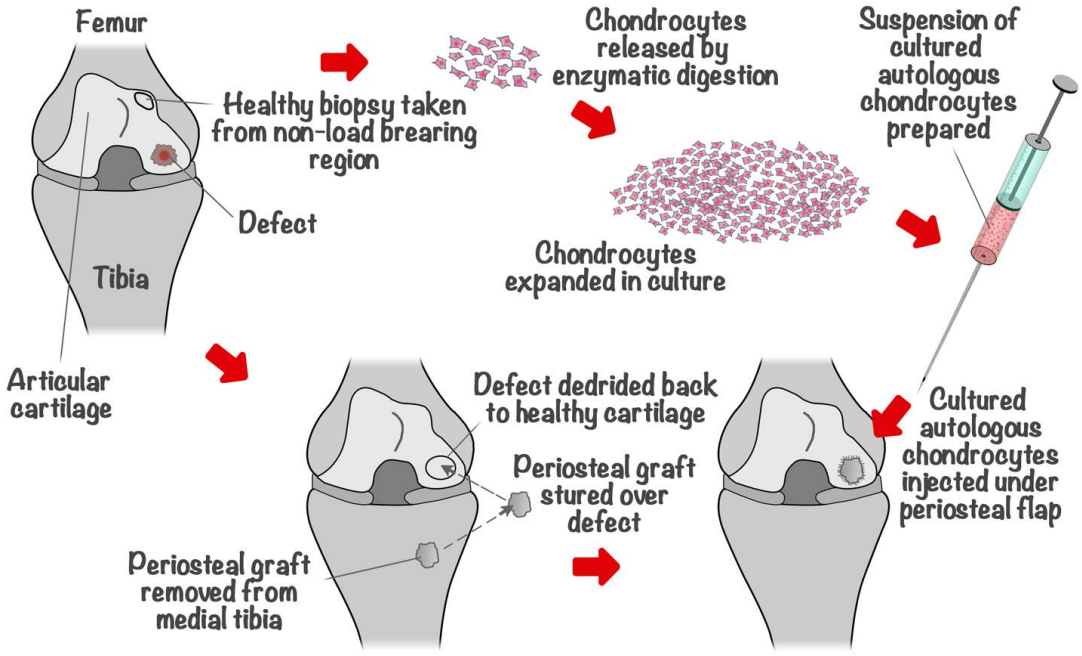

Figure 1.9 Autologous chondrocyte implantation

Figure adapted from [47]

This procedure has potential disadvantages, such as the reacquisition of phenotype of dedifferentiated chondrocytes in a monolayer culture, the risk of leakage of transplanted chondrocytes from the cartilage defects and an uneven distribution of chondrocytes in the transplanted site due to gravity [48]. In the same way, as a surgical technique, the main drawbacks are: two operations are needed, a long recovery time (6–12 months) is required to ensure neotissue maturation and achieve improved clinical scores from baseline, and the multistage, complex procedure it requires. The most frequently reported adverse event after ACI, using a periosteal flap to seal the implanted cells in the cartilage defect, is hypertrophy of the flap [49]. Due to this deficiency, there have been developments towards the use of an

alternative membrane to seal the cartilage defect, such as the collagen-membranes. Although these alternative membranes avoid hypertrophy, injected chondrocytes are not properly stimulated and the tissue they regenerate is fibrocartilage lacking proper function.

1.3.3 Cell Based Repair: Matrix-Induced Autologous Chondrocyte Implantation (MACI)

In order to overcome the irregular distribution of chondrocytes within the defect and to properly stimulate injected cells, biocompatible scaffolds (biodegradable or biostable) seeded with chondrocytes have been developed. A further advantage of this method of cell delivery is that the scaffold may act as a mechanical support capable of inducing chondrocyte re-differentiation and avoiding fibrocartilage repair.

Matrix-induced autologous chondrocyte implantation (MACI) is a technique that was eventually developed by combining chondrocytes and a scaffold (matrix). The use of a scaffold provides a structure that facilitates chondrocyte adhesion and expansion while maintaining a chondrocytic phenotype limiting dedifferentiation, which has been observed in two-dimensional (2D) systems [50]. In **Figure 1.10** several cartilage regeneration techniques can be observed, including MACI.

Although MACI has demonstrated good healing response with better repair than ACI, a major drawback of this approach is the inability to treat large chondral defects as well as the inherent donor site morbidity due to chondrocyte harvesting from cartilage tissue [50]. Furthermore, there is still a long way left to go before finding the ideal membrane or 3D support to adequately stimulate implanted chondrocytes, so that the regenerated tissue is of the same quality as the native.

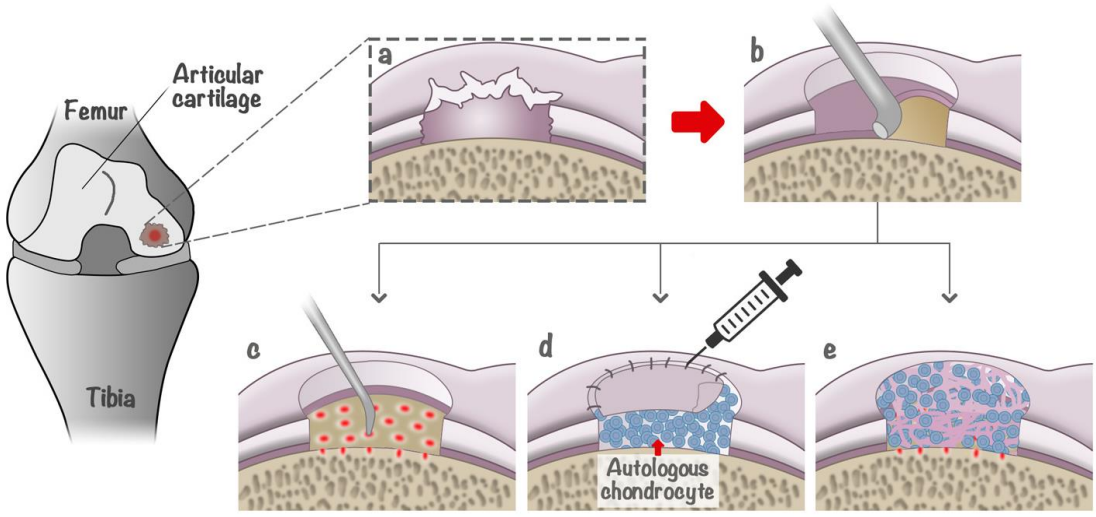

Figure 1.10 Cartilage regeneration techniques

Figure adapted from [49]

a. A full-thickness focal **chondral lesion**.

b. The lesion is **debrided** to ensure healthy, stable margins for integration of the host tissue with the neotissue.

c. Microfracture: Channels are created using a 45° awl, spaced 3–4 mm apart, and 3-4 mm deep to penetrate the subchondral bone, allowing mesenchymal stem cells to migrate from the marrow to the cartilage defect.

d. ACI: The debrided lesion is filled with 12–48 million autologous chondrocytes and covered with a periosteal flap or mixed collagen type I and type III membrane.

e. MACI: The autologous chondrocyte population is expanded *in vitro* and then seeded for 3 days onto an absorbable three-dimensional (collagen types I and III or hyaluronic acid) matrix prior to implantation. The cell-seeded scaffold is then secured into the lesion with fibrin glue.

1.3.4 Cell Source

1.3.4.1 Mature Chondrocytes

Chondrocytes have shown themselves to be a good guarantee for a long-term repair of articular cartilage lesions, but, as it has been mentioned before, they have some drawbacks that hold back their use in TE:

- Cell-based procedures utilising chondrocytes, such as ACI, are limited by the size of defects (2–10 cm^2 diameter). In these cases, the required number of cells is high (10,000 cells per microlitre) and therefore large quantities of autologous tissue harvested from healthy regions of joints are needed, with the resulting risk of creating secondary critically-sized defects as well as donor site morbidity.

- Another drawback associated with the use of chondrocytes is the requirement for monolayer expansion prior to implantation in ACI procedures. This expansion period can be detrimental to the phenotype of chondrocytes and their capacity for synthesising cartilage-like tissue is diminished as a result. Moreover, the lengthy period of expansion is not a financially viable option.

As a result, the use of alternative sources of cells for cartilage defect repair has been widely investigated and, for this reason, researchers have several options when choosing a cell source. The choice of cell type often depends on the initial condition of the cartilage tissue; in cases of extensive degradation or disease, the use of autologous chondrocytes is not an option. The use of allogeneic chondrocytes from donor tissue is a good alternative if this tissue is available. However, difficulties regarding tissue availability for humans and possible disease transmission or immune response can arise [9].

So in selecting an ideal cell source, scientists have to consider whether cells fulfil the following features:

- Easy access to/harvesting of the source
- Extensive self-renewal or expansion capability of the cells for generating sufficient quantities of cells for large scale TE
- Ability to readily differentiate into the chondrocytic lineage when induced
- Lack of or minimal immunogenicity or ‘tumourigenic’ tendencies

Other cell sources for cartilage tissue engineering, apart from chondrocytes are: induced pluripotent stem cells (iPSCs), mesenchymal stem cells (MSCs), embryonic stem cells (ESCs). All these have been explored for their potential as a viable cell source for cartilage repair (**Table 1.2**).

MSCs are also promising candidates for tissue engineering, and several types of adult MSCs are used as a cell source for cartilage tissue engineering. Nevertheless, the two most commonly used MSC sources are adipose tissue and bone marrow. Unlike other sources such as embryonic tissue, there are few ethical issues associated with harvesting and using these tissues in research and development. Additionally, bone marrow MSCs (BMSCs) and adipose derived stem cells (ADSCs) are relatively easy to source compared with synovium-derived- or periostium-derived MSCs [51].

Table 1.2 Advantages and disadvantages of various cell types in cartilage repair [52]

Cell type	Cell sources [53]	Advantages	Disadvantages
Autologous chondrocyte	– Articular – Auricular – Costal – Nasoseptal	✓ Native phenotype ✓ Minimal risk of immunological problem	x Small initial cell number x Dedifferentiation on expansion
Allogeneic chondrocyte		✓ Larger cell number ✓ Off-the-shelf solution	x Limited donor availability x Risk of disease transmission
Adult MSCs	– Bone-marrow derived – Adipose-derived – Muscle-derived – Synovium-derived – Periosteum-derived	✓ Potential to produce large numbers ✓ Various harvest sites ✓ Additional paracrine signalling potential	x Potential for hypertrophy x Heterogeneous population of cells x Stable and reproducible differentiation still problematic
iPSC		✓ Large source of patient specific cells ✓ Multiple cell types can be produced	x Stable and reproducible differentiation still problematic x Potential for teratoma
ESC		✓ Off-the-shelf solution ✓ Multiple cell types can be produced	x Stable and reproducible differentiation still problematic x Potential for teratoma x Ethical considerations

1.3.4.2 Mesenchymal Stem Cells (MSCs)

A stem cell is a cell from the embryo, foetus, or adult that, under certain conditions, can reproduce for long periods. It can also give rise to specialised cells of body tissues and organs. For this reason culturing undifferentiated (stem/progenitor) cells in cartilage TE has become promising.

Differentiation of such cells can be obtained *in vitro* by changing the culture conditions after their expansion or *in vivo* as a consequence of the new 'physiological' microenvironment in the transplant area [54].

Adult MSCs are multi-potent cells with an extensive self-renewal capacity and a useful ability for differentiating into a variety of connective tissue cells, including cartilage-like cells. They are also able to secrete a range of trophic factors such as cytokines and growth factors, which

mediate cellular activity, from differentiation to immunological response. Therefore, MSCs are considered an alternative to chondrocytes in the repair of cartilage lesions. They can be obtained from several sources such as bone marrow, adipose tissue, fat pad as well as synovium tissue [50, 55, 56].

The process by which a stem cell is differentiated into a mature chondrocyte is called chondrogenesis and it includes the following stages: MSC condensation, the rise of chondroprogenitors, chondrogenesis, terminal differentiation of progenitor cells and in skeletal development ossification (**Figure 1.11**).

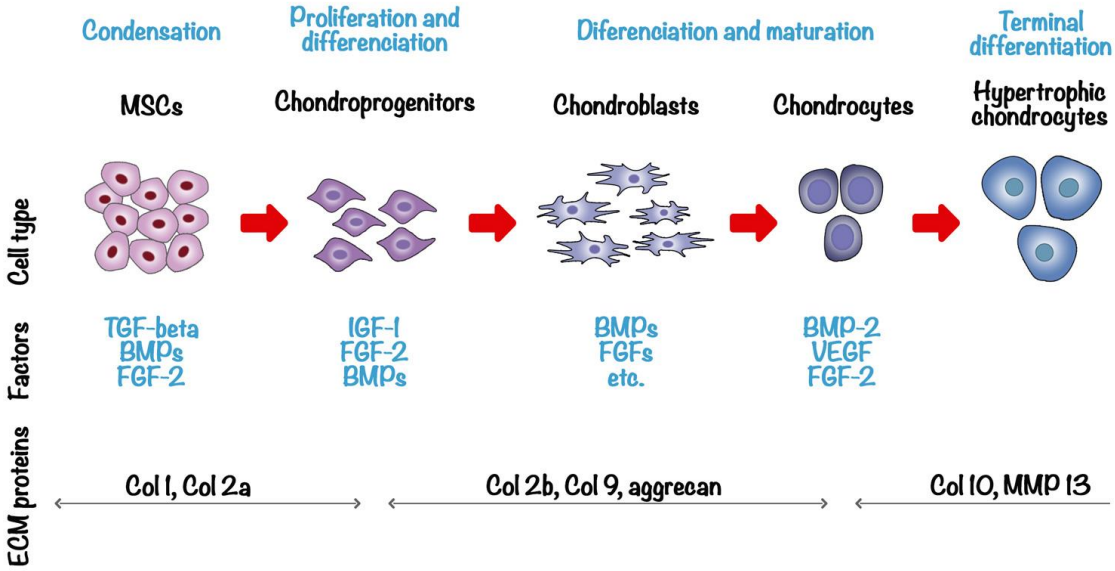

Figure 1.11 Schematic diagram of the stages of chondrogenesis

The main growth factors involved in each stage of chondrogenesis and the accompanying alterations in ECM are represented. Figure adapted from [57]

1.4 PHENOTYPE CHANGES IN MATURE CHONDROCYTES DURING THE DIFFERENT STAGES IN CARTILAGE ENGINEERING

1.4.1 Chondrocyte Expansion

This thesis focuses on the use of matrix autologous chondrocyte implantation (MACI) for the regeneration of articular cartilage. This technique is an evolution of autologous chondrocyte implantation (ACI), in clinical use since 1987. Either in ACI or MACI, the first step is to obtain a high enough number of chondrocytes from a biopsy of a small healthy cartilage area from the same patient. During the expansion of chondrocytes via repeated monolayer culture *in vitro*, they undergo a loss of the chondrogenic phenotype, which results in an overall fibroblast like phenotype [58].

The progressive change of chondrocytes to rounded morphology and the gradual loss of chondrogenic capacity with further monolayer culture is known as dedifferentiation.

The dedifferentiation of chondrocytes causes alterations in the synthesis of the ECM. For instance, the synthesis of collagen types specific to the cartilage, such as collagen II and IX, are down-regulated during expansion of chondrocytes in monolayer. In contrast, the synthesis of collagen type I, which is abundant in fibrotic tissues and normally not present in hyaline cartilage, is increased [59].

In addition, aggrecan, the major proteoglycan component of the cartilage, is down-regulated. Contrarily, other proteoglycans such as decorin, biglican and versican are up-regulated [59].

The synthesis of other collagen types, proteoglycans, glycoproteins, cell markers, *etc*. is also affected during dedifferentiation [59]. The ratio of collagen type II/I or aggrecan/versican are proposed as a dedifferentiation index [60].

When chondrocytes of hyaline cartilage, or those of fibrocartilage, are cultured in monolayer they will dedifferentiate up to the level at which they become morphologically indistinguishable [61, 62]. Dedifferentiation and proliferation in monolayer culture is closely related to cell-substrate adhesion, which in turn highly depends on factors such as the chemical structure of substrate's surface, amount and conformation of the proteins adsorbed to it and the surface microtopography, among others [63-68]. The composition of the culture medium and the presence of growth factors also affect growth and differentiation of chondrocytes [69]. For instance, the addition of insulin-transferring-selenium (ITS) has been proven to prevent chondrocyte dedifferentiation in monolayer culture [70].

It has been shown [71] that dedifferentiation for cartilage regenerative applications is considered an adverse phenomenon; therefore, it can be prevented by using the isolated chondrocytes in relatively early passages, when cells are not fully dedifferentiated yet, or by inducing redifferentiation by means of selected medium supplements. Moreover, the culture of chondrocytes in 3D constructs such as alginate or other gels preserve hyaline chondrocyte rounded morphology, although the ability of expansion is low [72]. Clearly, these considerations are limited by the relatively high number of cells required for this therapy.

1.4.2 TE for Chondrocytic Redifferentiation

After expansion chondrocytes should condense and produce a tissue with the composition (with collagen type II and aggrecan as main components of the ECM), morphology (with cells isolated in lacunae that protect them from the high compression loading to which articular cartilage is subjected) and functional characteristics of hyaline cartilage [61, 62]. This process is what we call redifferentiation. Chondrocytes should recover their original phenotype.

It has been proven that chondrocytes expanded in monolayer culture can redifferentiate when seeded in a 3D construct. Different types of 3D environments can be used, from gels to macroporous scaffolds [81, 82].

Chondrocyte phenotype can be characterised by using a variety of techniques listed in **Table 3.3** (section **3.3.8)**.

Animal models and clinical practice of autologous chondrocyte transplantation indicates that the correct regeneration of hyaline cartilage after implantation in the site of the defect needs a 3D support, a scaffold that protects the cells in the first stages of regeneration of the imposed loads and organises the regenerated tissue. A lot of different scaffold materials with different pore architecture and seeding protocols have been used in research work: *in vitro, in vivo* in animal models [73-78] and in clinical use as well [79, 80].

One of the key aspects in redifferentiation of expanded chondrocytes is the biomechanical environment the cells meet either *in vivo* or *in vitro*. In this sense, the advance of MACI technique with respect to the first generations of ACI therapies is expected to come from the role of the scaffold in stress transmission to the cells after implantation in the cartilage defect [81, 82].

1.5 SCAFFOLDS IN TISSUE ENGINEERING

1.5.1 Macroporous Scaffolds

This thesis is based on four articles, each of them compiling the results of studies carried out using biocompatible polymeric biomaterials for the synthesis of 2D supporting materials and 3D scaffolds for the cell culture of chondrocytes. In these papers, some of the mechanical properties of the scaffolds used have been studied, as well as the consequences that varying these properties have in human chondrocytes culture. Porosity is one of the properties that are highly important to consider when designing a scaffold.

Porous scaffolds are of primary importance in TE as they offer a 3D environment where cells and regenerative factors work in a controlled way with the goal of repairing the damaged cartilage. High porosity enables larger volume for cell infiltration and ECM formation but it is inversely related to the mechanical properties, which will decrease the higher the porosity becomes. Pore interconnectivity is also a very important issue for a good design of the scaffold as it allows for ECM infiltration, as well as the entry of nutrients and metabolic waste removal [83-85]. The pore geometry and interconnectivity depends on the material selected.

Besides porosity, when selecting biomaterials it must be also taken into consideration that cell attachment to polymer substrates depends on the physical and chemical characteristics of the surface. Properties such as surface morphology [86], rigidity, equilibrium water content [87], surface tension [88-90], hydrophilicity and the presence of electric charges [91], adsorbed proteins [92] and specific binding sites can be correlated with the cell attachment, growth, spreading and viability.

The scaffold 3D structure can be obtained by different methods known to generate a porous structure in a polymer matrix: using gases [93], fibre templates [94], employing water soluble particles such as NaCl as porogen [95], solvent casting [96], polymerisation in the presence of a solvent [97, 98] and others [99-102].

1.5.2 Materials and their Properties

For the reasons stated above, the use of 3D supportive structures is of crucial importance in tissue regeneration. They should enable the proliferation of cells, chondrogenic differentiation and 3D tissue formation. Scaffolds must also withstand physiological loading until sufficient tissue regeneration occurs. Moreover, the material must be sufficiently porous to allow for effective transport of nutrients. Finally, it should be biocompatible and, if biodegradable, degrade as the tissue matrix is produced, leaving only nontoxic degradation products [103].

When using biomaterial scaffolds in tissue-engineered constructs, the 3D environment of the ECM is being imitated. Scaffolds also give structural support to the regenerated and surrounding tissues.

Scaffold design should seek to hold the following properties regarding the cells they are going to host (see **Table 1.3** for further details):

- Cell attachment and migration
- Deliver and retain cells and biochemical factors
- Nutrient and waste products permeation
- Apply mechanical/biological influences to modify cell response.

Furthermore, since scaffolds represent the space available for the tissue developing and the physical support for cell growth, they should meet some mechanical requirements [104]:

- If biodegradable, degrade with non-toxic by-products
- Provide mechanical integrity
- Enable tissue regeneration
- Capacity to fix to the defect site
- Show porosity and interconnectivity.

Table 1.3 Generic scaffold design requirements[a]

Scaffold Requirements	Biological and material basis
Biocompatibility	To prevent adverse inflammatory or immune responses
Cell attachment	To optimise cell seeding for delivery and retention of cells and promote maintenance of chondrogenic phenotype
Porous 3D environment	Support cell migration, proliferation and ECM production. High surface area to volume ratio.
Interconnected/permeable	Maximise nutrient/waste exchange and limit oxygen gradients
Biodegradation	Preferably in harmony with desired repair or regeneration process, whereby, by-products are metabolised or excreted from the body without eliciting an inflammatory response
Bioactivity/gene delivery	Act as a cell carrier or control the release of growth factors, transfection vectors and/or genetically modified cells
Mechanical integrity and integration	Sufficient to support or match surrounding native tissue at site of implantation, as well as mediate mechanical stimulus to cells during loading
Structural anisotropy	Promote native anisotropic tissue structure
Size and Shape	Reproducibly create scaffold of clinically relevant size and shape
Surgical application	Preferably allow minimally invasive techniques using injectable/flexible scaffold strategies, which can be reshaped/resized by surgeon to fit the specific defect. Press-fit solutions require mechanical integrity

[a]Scaffold design requirements are related to the repair of chondral and osteochondral articular cartilage defects [105]

Biomaterials used in TE can be sorted into three main categories [9] (see (**Table 1.4**):

- **Natural polymers**. These are found in living organisms and can be extracted and processed into functional biomaterials. They are preferred for biological applications because of their little or no immune response. Examples of these materials are alginate, agarose, chitosan, fibrin glue, type I and II collagen, hyaluronic acid-based materials, and reconstituted tissue matrices.
- **Synthetic polymers**. These are created using chemical processes, which allow for extensive customisation of material properties. They support essential cell functions in addition to mimicking the biomechanical properties of host tissues, whilst avoiding host immune

responses. Poly-glycolides, poly-lactides, poly-acrylates, poly-methacrylates, poly-caprolactone (PCL) and their copolymers are commonly used for scaffold materials and other biomedical applications.

- **Composites**. They combine two or more materials into one scaffold to take advantage of special characteristics intrinsic to each substance.

In **Figure 1.12**, a summary of the practice of articular cartilage tissue engineering can be seen. In tissue regeneration different types of scaffolds, cells and signalling molecules are involved.

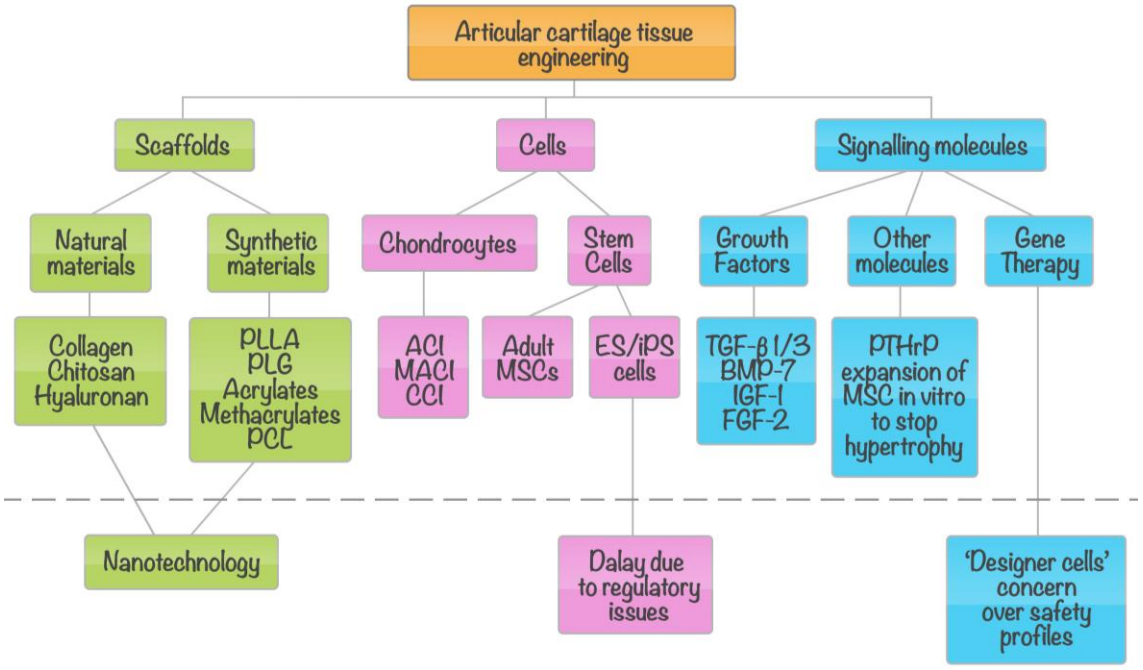

Figure 1.12 Articular cartilage tissue engineering

Figure adapted from [104]. **PLLA**, Poly-L-Lactic Acid; **PLG**, Polylactide-co-Glycolide; **ACI**, autologous chondrocyte implantation; **MACI**, matrix assisted chondrocyte implantation; **CCI**, characterised chondrocyte implantation; **MSC**, mesenchymal stem cell; **ES**, embryonic stem cell; **iPS**, induced pluripotent stem cell; **TGF-β**: transforming growth factor beta; **BMP**, bone morphogenetic protein; **IGF**: insulin like growth factor; **FGF**: fibroblast growth factor; **PTHrP**: parathyroid hormone related peptide

As can be seen in **Figure 1.12**, there are many kinds of materials that can be used in the manufacturing of scaffolds for the repair of articular cartilage defects or any other cartilage TE applications. In particular, in this work we are dealing with biostable acrylic scaffolds and scaffolds based in polycaprolactone, the following sections describe briefly the state of the art of the application of these materials in TE.

Table 1.4 Types of scaffolds[a]

NATURAL BIOMATERIALS:
▪ Protein-based polymers
Fibrin
Collagen
Gelatine
▪ Carbohydrate-based polymers
Hyaluronan
Agarose
Alginate
Chitosan
SYNTHETIC BIOMATERIALS:
Polylactic acid
Polygycolic acid
Polycaprolactone
Dacron (polyethylene terephthalates)
Teflon (polytetrafluoroethylene)
Carbon fibers
Polyesterurethane
Polybutyric acid
Hydroxyapatite
Polyacrylates
Polymethacrylates
WITHIN/BETWEEN CLASSES:
Crosslinkage
Chemical modifications
Geometrical modifications (to produce fibrillar forms or foams)
Matrix combinations

[a]Table adapted from [37]

1.5.3 Acrylic Scaffolds

A method based on the use of templates for generating the porous structure was adapted for the construction of the acrylic scaffolds presented in this thesis. First of all, a bonded micro-sphere template was built and then dissolved after the polymerisation process of the forming material in the free spaces of the template. This technique allows the interconnectivity between pores and their size to be controlled. There are examples in literature where the 3D architecture can be controlled in such a way, such as scaffolds obtained by rapid prototyping technologies [106, 107] and others fabricated using a technique similar to the one developed in our laboratory at the Centre for Biomaterials and Tissue Engineering (CBIT) but using biodegradable materials [108-110].

The influence of the hydrophilic/hydrophobic ratio on cell attachment in polycrylates and polymethacrylates has been the subject of several studies. While hydrophilic polymers such as poly(hydroxyethyl methacrylate), PHEMA [87, 88, 111], and poly(hydroxyethyl acrylate), PHEA [92, 112], are not adhesive for fibroblasts and other cell lines, hydrophobous polymers of the same series such as poly(methyl methacrylate), PMMA, or poly(ethyl methacrylate), PEMA, allowed for cell anchorage. The hydrophilicity can be varied monotonously by synthesising random copolymers using hydrophilic and hydrophobic comonomers. Much work has been done in order to understand the dependence of cell attachment on the composition of P(HEMA-co-EMA). It has been shown that cell attachment, spreading and growth increases monotonously with the content of EMA units in the copolymer. This behaviour was related to the water content or the surface energy and even critical upper equilibrium water content (EWC) has been proposed for cell anchorage.

1.5.4 PCL Scaffolds

Other artificial scaffolds can be composed of biodegradable polymers, for instance, poly-caprolactone (PCL) or polylactic acid (PLA). These materials have been shown to support cell attachment, proliferation, and matrix production for a variety of cells, including chondrocytes, osteoblasts and mesenchymal stem cells [113-115].

PCL is a semi-crystalline material that has good mechanical properties and degrades slower than other polyesters [116]. Because of the mechanical and degradation properties of PCL [117], it can be used for long-term *in vitro* cell culture before implantation into the injury site. A PCL scaffold would thus maintain its architectural integrity and mechanical properties during the preimplantation period while chondrocytes are both redifferentiating and synthesising new cartilage matrix [118].

In previous works of our group [119], human chondrocytes were seeded in PCL scaffolds and cultured *in vitro* in FBS and ITS supplemented culture medium. Inmunostaining of the components of the extracellular matrix and gene expression studies using real time-PCR proved that chondrocytes maintained their differentiated phenotype in PCL 3D scaffolds and produced cartilage specific ECM components.

In this thesis, the capacity of chondrocytes cultured in this PCL scaffold for generating cartilage for future animal implantation has been evaluated. The scaffold was characterised in terms of chondrocytic redifferentiation and synthesis of hyaline-specific ECM proteins. The influence that pore connectivity and hydrophilicity of modified ε-caprolactone scaffolds has also been studied. In particular, chondrocytes adhesion to the pore walls, as well as their proliferative ability and ECM composition was determined.

Chapter 2

OBJECTIVES

“If I cannot reach my destination now, I will accept it with joy, even if I do not get there within ten million years, I will wait cheerfully, too.”

“Of any success, however small, one day a larger effort will emerge that will complete it.”

Walt Whitman (poet, essayist and humanist. 1819-1892)

OBJECTIVES

This thesis is focused on articular cartilage regeneration using tissue engineering techniques. The work deals with MACI, which entails two different stages. The first stage involves the expansion of autologous chondrocytes isolated from a small portion of articular cartilage obtained in a biopsy from a healthy portion of the patient's tissue. In this first stage, a significant number of cells are obtained but they lose their characteristic phenotype. The second stage is the redifferentiation of the chondrocytes cultured in a three-dimensional (3D) scaffold. In both stages, flat substrates or macroporous 3D biomaterials are required.

The general objective of this work is to contribute to the study of the influence of the biomaterial's characteristics, particularly hydrophilicity and pore architecture, on the chondrocyte response in *in vitro* culture, including cellular adhesion, viability, proliferation and chondrocytic differentiation.

Specifically, the following aspects of the cartilage engineering process have been considered:

Objective 1: Study of the influence of hydrophilicity and distribution of hydrophilic domains in cell-material interaction and chondrocytes expansion in monolayer culture.

- To reach this objective, a series of biomaterials with varying hydrophilicity have been synthesised in the form of flat substrates. Human mature chondrocytes were isolated and cultured on these substrates to assess the influence of the hydrophilic/hydrophobic ratio on cell attachment, cell spreading and cell growth.

Objective 2: Study of the behaviour of chondrocytes in 3D macroporous biomaterials with interconnected pores in terms of cell viability and condrogenic redifferentiation.

- In this study, polymer scaffolds have been synthesised in such a way that the geometric characteristics (pore size, connectivity and porosity) and the physico-chemical properties of the resulting material can be independently controlled.

- Human chondrocytes, previously expanded in monolayer, were seeded in the 3D scaffolds and cultured *in vitro* to assess cellular viability, proliferation and gene expression of type II collagen and aggrecan.

- The influence of the cell culture medium on the development of chondrocytic phenotype was studied, in particular, the induction of collagen II and aggrecan expression of cells cultured in polycaprolactone scaffolds without Fetal Bovine Serum (FBS) but supplemented with Insulin-Transferrin-Selenium (ITS).

Chapter 3

MATERIALS AND METHODS

"Desde la infancia me veía obligado a concentrar mi atención más allá de mí mismo. Esto me causaba mucho sufrimiento, pero, tal y como lo veo ahora, fue una bendición disfrazada, puesto que me enseñó a apreciar el valor inestimable de la introspección a la hora de preservar la vida, y como modo de progresar. La presión de nuestras ocupaciones y la incesante corriente de impresiones que se vierten en nuestra conciencia a través de todas las puertas del conocimiento hacen que la existencia moderna sea arriesgada en muchos modos. La mayoría de las personas están tan absortas en la contemplación del mundo exterior que son totalmente ajenas a lo que está pasando dentro de sí mismas".

Nikola Tesla (ingeniero eléctrico y físico. 1856-1943)

3.1 BIOMATERIAL SYNTHESIS

Artificial biomaterials (2D substrates and scaffolds) can be composed of a variety of materials, such as biostable acrylic polymers or biodegradable polymers (*i.e.* poly-caprolactone, PCL). These polymers have promoted cell adhesion, proliferation and matrix production for a variety of cells, including chondrocytes, osteoblasts and mesenchymal stem cells [113-115].

Monomers, polymers, solvents and reagents used in this study:

- **HEMA**: hydroxyethyl methacrylate (98% pure, Scharlau, Spain).
- **HEA**: 2-hydroxyethyl acrylate (96% pure, Sigma-Aldrich, Spain).
- **EA**: ethyl acrylate (98% pure, Scharlau, Spain).
- **EMA**: ethyl methacrylate (96% pure, Sigma-Aldrich, Spain).
- **CLMA**: caprolactone (2-methacryloyloxy)ethyl ester (Sigma-Aldrich, Spain).
- **Medium molecular weight PCL:** poly-caprolactone (Polysciences, Molecular weight (MW)=50,000).
- **Low molecular weight PCL:** poly(ε-caprolactone) (Polysciences, MW: 10,000 – 20,000, density = 1.145 g/cm^3;)
- **Benzoin** (98% pure, Scharlau, Spain).
- **Ethanol** (99.5% pure, Sigma-Aldrich, Spain).
- **EGDMA**: ethyleneglycol dimethacrylate, (99% pure, Sigma-Aldrich, Spain).
- **DMF**: N,N-dimethylformamide.
- **PEMA-2003**: poly(ethyl methacrylate). Elvacite 2003, Lucite International.
- **PEMA-2043**: poly(ethyl methacrylate). Elvacite 2043, DuPont.
- **PMMA**: poly (methyl methacrylate). Colacryl DP 300 (Lucite International Inc., England).

3.1.1 Polymer and Copolymer Networks (2D)

For the synthesis of several series of hydrophilic and hydrophobic copolymers by bulk free radical copolymerisation, purchased monomers were used without further purification.

Polymer or copolymer networks were polymerised via ultraviolet light, at room temperature (RT), using 2 wt% EGDMA, as cross-linking agent and 0.13 wt% benzoin as photoinitiator.

Low molecular weight substances were extracted from the polymer networks by boiling in ethanol for 24 h and then drying them in vacuum to constant weight.

The composition of the different samples is given in **Table 3.1**.

Samples were obtained in the form of disks, 0.5 mm thick and with a diameter around 5 mm.

Table 3.1 Composition of the samples of biomaterials used in section 4.1

Sample	Composition	Description
A1	PEA	Poly(ethyl acrylate)
A2	P(EA-co-HEMA) 70/30 wt%	Copolymer of ethyl acrylate and hydroxyethyl methacrylate
A3	P(EA-co-HEMA) 50/50 wt%	Copolymer of ethyl acrylate and hydroxyethyl methacrylate
A4	P(EA-co-HEMA) 30/70 wt%	Copolymer of ethyl acrylate and hydroxyethyl methacrylate
A5	PHEMA	Polyhydroxyethyl methacrylate
B1	PEMA	Poly(ethyl methacrylate)
B2	P(EMA-co-HEA) 70/30 wt%	Copolymer of ethyl methacrylate and hydroxyethyl acrylate
B3	P(EMA-co-HEA) 50/50 wt%	Copolymer of ethyl methacrylate and hydroxyethyl acrylate
B4	P(EMA-co-HEA) 30/70 wt%	Copolymer of ethyl methacrylate and hydroxyethyl acrylate
B5	PHEA	Poly(hydroxyethyl acrylate)
C1	PEA	Poly(ethyl acrylate)
C2	P(EA-co-HEA) 70/30 wt%	Copolymer of ethyl acrylate and hydroxyethyl acrylate
C3	P(EA-co-HEA) 50/50 wt%	Copolymer of ethyl acrylate and hydroxyethyl acrylate
C4	P(EA-co-HEA) 30/70 wt%	Copolymer of ethyl acrylate and hydroxyethyl acrylate
C5	PHEA	Poly(hydroxyethyl acrylate)
CPS Control		Culture polystyrene well with cells
No-Cells		Culture polystyrene well without cells

3.1.2 3D Scaffolds

3.1.2.1 Acrylic scaffolds

The method used in the synthesis of these scaffolds is based on the use of templates for generating the porous structure. First, a bonded sintered micro-sphere template is built and then dissolved after the polymerisation of the forming material in the free spaces of the template. This technique allows the interconnectivity between pores and their size to be controlled.

Firstly, PMMA porogen spheres are introduced between two plates and sintered by keeping the temperature at 180ºC for one hour at a constant pressure. After cooling the template at room temperature, a monomer solution is introduced in the empty space between the PMMA spheres.

A wide range of hydrophilic/hydrophobic materials were prepared by changing the percentage of EA and HEMA in the original solution; in addition, 1 wt% of benzoin and 2 wt% of EGDMA is always added to the corresponding monomer solution.

The copolymerisation is carried out up to limiting conversion under a UV radiation source at room temperature.

Five monomer feed compositions were chosen, given by the weight fraction of HEMA in the original mixture: 1, 0.7, 0.5, 0.3 and 0 (pure EA). After polymerisation took place, the PMMA matrix was removed by Soxhlet extraction with ethyl acetate for a 24 h period. After this stage, the PMMA template is completely removed.

The porous sample was kept for an additional 24 h in a Soxhlet with ethanol in order to remove low molecular weight substances completely. Samples were dried in vacuum to constant weight before characterisation.

3.1.2.2 Caprolactone-based scaffolds

These scaffolds were synthesised by a CBIT's colleague, Jorge Luis Escobar Ivirico.

Modified caprolactone copolymer networks with different hydrophilicity were synthesised by radical polymerisation in solution using DMF as solvent (50 wt%), with different proportions of both (co)monomers, CLMA, and HEA (**Table 3.2** and **Figure 3.1**). In the text, the copolymers are referred to as P(CLMA-co-HEA).

Table 3.2 Composition of the feeding mixture

Sample designation	HEA (wt%)
PCLMA	0
P(CLMA-co-HEA) 70/30	30
P(CLMA-co-HEA) 50/50	50
P(CLMA-co-HEA) 30/70	70
PHEA	100

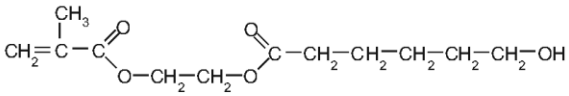

Caprolactone 2-(methacryloyloxy)ethyl ester

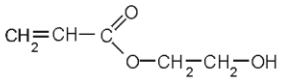

2-hydroxyethyl acrylate

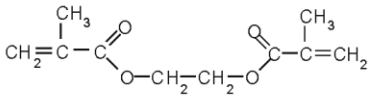

Ethyleneglycol dimethacrylate

Figure 3.1 Chemical structures of monomer units and crosslinking agent employed to prepare the P(CLMA-co-HEA) scaffolds.

Porogen microspheres (PMMA) were introduced between two plates and sintered by keeping temperature at 180ºC for 1h at a constant pressure.

After cooling that template at room temperature, a (co)monomer solution was introduced in the empty space between the PMMA spheres. A whole set of hydrophilic/hydrophobic materials was prepared by changing the percentage of HEA and CLMA in the original solution; in addition, 1wt% benzoin and 2wt% EGDMA was always added to the corresponding monomers solution.

The copolymerisation was carried out up to limiting conversion under a UV radiation source at room temperature. Once polymerisation took place, the PMMA template was removed by Soxhlet extraction with ethyl acetate for a 24 h period.

After this stage, the porogen template was completely removed. The porous sample was kept another 24 h in a Soxhlet with ethanol in order to completely remove remaining low molecular weight substances.

Samples were dried in vacuum to constant weight before use. The measured volume fraction of pores in the scaffolds of this series was 77 ± 3% independent of the HEA content of the copolymer. It was determined from the weight increase of samples after immersion in water for 24 h (see section **3.2.6** for details).

For more details on the copolymer synthesis see reference [129].

3.1.2.3 PCL scaffolds

Medium molecular weight PCL scaffolds were synthesised by a CBIT's colleague, Myriam Lebourg and were used in section **4.4**.

Details of the synthesis are described in Lebourg *et al*. [130]. Briefly, templates for the scaffolds were manufactured by sintering of PEMA-2003 microspheres at 140ºC. The porosity of the templates was changed by varying the compression degree to which the templates are submitted.

If the temperature and the pressure applied to sinter the porogen microspheres are higher, the contact surface between microspheres increases. These contact surfaces will generate pore throats in the scaffold, thus, mechanical and thermal treatments in template fabrication determine porosity and pore connectivity in the scaffold.

PCL scaffolds were obtained by injecting melt PCL (Mw=50,000) at 110ºC into the templates by means of a custom-made injection device. The pressure of nitrogen gas in the device forces the melted PCL to enter the template. Thereafter, the porogen was leached out by repeated washings in ethanol.

The scaffolds used in section **4.3** were manufactured by a CBIT's colleague, Raúl Izquierdo Escrig. A low molecular weight PCL was used in their preparation.

PCL (Mw: 10,000–20,000) was employed to develop the porous materials. PEMA-2043 beads, which have a size of around 200 ± 25 μm, were used as the porogen material. In addition, ethanol was used to leach out the filler material from the PCL. Each of these materials was employed as received.

For the fabrication of these scaffolds, glass tubes with diameters ranging between 5 and 7 mm were sealed with porous stoppers and filled with PEMA beads. A sintering treatment was then applied, at 130ºC for 60 min. Once the beads were sintered, PCL was placed over them and fused at 80ºC for 45 min. After that, the bottom of the tube was connected to a vacuum pump,

while keeping the whole system at 80ºC until the end of the infiltration. Once this operation was completed, the sample was taken out of the glass tube and the filler removed by leaving it in ethanol (changed daily) for 96 h, the result being porous polymeric scaffolds.

Cylinders about 6 mm in diameter and 4 mm in height were prepared. For further details see [119].

3.2 CHARACTERISATION OF MATERIALS

3.2.1 Equilibrium water content (EWC)

The equilibrium water sorption of the samples was measured by weighing after immersion of the sample in liquid water for 24 h. The EWC was measured on dry basis, i.e. mass of absorbed water per unit mass of polymer.

Five replicates of each sample were prepared to determine their equilibrium water content. They were cut into squares measuring about 2 cm each side. Dried samples of known weight were immersed in water at 37 ºC for 24 h. Then each sample was weighed after gently removing the excess water on their surface with a filter paper. The equilibrium water content (EWC) was calculated as follows:

$$EWC(\%) = \frac{m_{swollen} - m_{dry}}{m_{dry}} \cdot 100 = \frac{m_{water}}{m_{dry}} \cdot 100$$

3.2.2 Dynamic-mechanical analysis (DMA)

Dynamic mechanical analysis (DMA) (also known as Dynamic mechanical spectroscopy – DMS) is a technique used to study and characterise materials. It is most useful for studying the viscoelastic behaviour of polymers. A sinusoidal stress is applied and the strain in the material is measured, allowing the complex modulus to be determined. The temperature of the sample or the frequency of the stress are often varied, leading to variations in the complex modulus; this approach was used to locate the main relaxation of the material, as well as to identify transitions corresponding to other molecular motions.

In our studies, tensile dynamic-mechanical analysis, DMA, was performed at a heating rate of 1ºC/min in a Seiko DMS210 instrument from -150 to 200ºC at a frequency of 1 Hz. Samples for DMA experiments were rectangular, approximately 15 × 3 × 1 mm^3.

3.2.3 Atomic force microscopy (AFM)

Atomic force microscopy [131] (AFM) or scanning force microscopy (SFM) is a very high-resolution type of scanning probe microscopy, with demonstrated resolution on the order of fractions of a nanometre.

AFM was performed in a NanoScope III from Digital Instruments operating in the tapping mode in air. Sicantilevers were used with force constant of 42 N/m and resonance frequency of 290 kHz.

All the experiments in this thesis were performed with the instrument mounted on a vibration isolation system.

AFM was used to determine the surface roughness of the 2D materials.

3.2.4 Scanning electron microscopy (SEM)

A scanning electron microscope (SEM) is a type of electron microscope that produces images of a sample by scanning it with a focused beam of electrons. The electrons interact with atoms in the sample, producing various signals that can be detected and that contain information about the sample's surface topography and composition. The electron beam is generally scanned in a raster scan pattern, and the beam's position is combined with the detected signal to produce an image.

The morphology of the resulting scaffolds was observed by scanning electron microscopy (SEM) (Jeol JSM-5410) in a Hitachi S-3200N device.

Dry scaffolds were cut in a half with a scalpel. Prior to analysis, samples were mounted in the microscope carriers and coated with gold using a BAL-TEC SCD 005 Sputter Coater. Both, the interior (core) and surface of the scaffolds were observed.

Pore connectivity was characterised by measuring the diameter of the pore throats observed in SEM pictures of the scaffold cross-sections. Mean value and standard deviation were calculated from 45 measurements from three different SEM pictures for each sample.

3.2.5 Contact angle measurements

Contact angle measurements were performed in a Dataphysics OCA instrument. Samples were previously swollen to equilibrium in distilled water at room temperature to simulate the state of the polymeric substrate during culture.

The contact angle of drops of glycerol, diiodomethane, ethyleneglycol and formamide were used to calculate the surface tension γ_s of the wet samples and its polar γ^p and dispersive γ^d components following the method of Owens and Wendt [132]. Contact angle measurements were performed with five replicas.

3.2.6 Porosity of the material

The volume fraction of pores in the scaffold, *i.e*. porosity (P), was determined gravimetrically by swelling the sample in water using a vacuum accessory. The porosity P is defined as

$$P = \frac{V_{pore}}{V_{pore} + V_{polymer}},$$

where V_{pore} is the part of the volume occupied by pores and $V_{polymer}$ is the volume occupied by the polymer. Let m_s^{sw} be the mass of the scaffold swollen in water and m_s^{d} the mass of the dry scaffold. Water sorbed in the scaffold is distributed between two phases: water in pores and water sorbed in the polymer that forms the scaffold.

Assuming that the equilibrium water content measured on dry basis (mass of water absorbed in equilibrium divided by the mass of dry polymer), w^*, of the material that constitutes the scaffold is the same as that of the bulk material of the same composition, the mass of water located in pores m_w^{pores} is

$$m_w^{pores} = m_s^{sw} - m_s^{d} - m_w^*,$$

where m_w^* is the mass of water absorbed in the polymer that forms the scaffold, *i.e.*,

$$m_w^* = m_s^{d} \cdot w^*.$$

Taking into account the density of water (ρ_w), the amount of water located in pores gives their volume,

$$V_{pore} = \frac{m_s^{sw} - m_s^{d}(w^* + 1)}{\rho_w}$$

On the other hand, the volume of the scaffold occupied by the polymer was obtained by measuring the density of the corresponding bulk material ρ_b

$$V_{polymer} = \frac{m_s^{d}}{\rho_b}.$$

ρ_b is determined by weighing each one of the samples both in air and immersed in n-octane at 25ºC.

A Mettler AE240 balance (sensitivity 0.01 mg) with density accessory Mettler ME3360 was employed. Porosity measurements were taken in at least three different samples of each one of the compositions.

Porosity was calculated as the quotient of the volume of pores and the total volume of the scaffold.

The samples were weighed dry, filled with distilled water, and then subsequently weighed again. Water was injected in a chamber containing the scaffold under vacuum. Around 20 min was allowed for equilibration after immersing the samples in water. Water filled the pores nearly instantaneously and since bulk PCL is very hydrophobic, no further water absorption is expected.

3.3 CELLULAR AND MOLECULAR BIOLOGY

3.3.1 Chondrocyte isolation

Human articular cartilage was obtained from osteoarthritic knee joints after prosthesis replacement. Cartilage is extracted from the finest conserved region of the osteoarthritic knee although it cannot be considered to be normal cartilage.

The cartilage was dissected from subchondral bone, finely diced, and then washed with supplemented [100 U penicillin, 100 µg streptomycin (Biological Industries) and 0.4% fungizone (Gibco)] Dulbecco's modified Eagle's medium (DMEM; Life Technologies).

Cartilage digestive enzymes were also prepared with this supplemented DMEM.

For chondrocyte isolation, the diced cartilage was incubated for 30 min with 0.5 mg/mL hyaluronidase (Sigma-Aldrich) in a shaking water bath at 37ºC.

The hyaluronidase was subsequently removed and 1 mg/ml pronase (Merck, VWR International SL) was added. After 60 min incubation in a shaking water bath at 37ºC, the cartilage pieces were washed with supplemented DMEM. After removal of the medium, digestion was continued by addition of 0.5 mg/mL of collagenase-IA (Sigma-Aldrich) in a shaking water bath kept at 37ºC overnight.

The resulting cell suspension was filtered through a 70 µm pore nylon filter (BD Biosciences) to remove tissue debris.

Cells were centrifuged and washed with DMEM supplemented with 10% foetal bovine serum (FBS; Invitrogen SA).

Finally, the cells were cryopreserved in liquid nitrogen with DMEM containing 20% FBS and 10% dimethyl sulfoxide (DMSO) (Sigma-Aldrich) until use or plated in tissue culture flasks for immediate chondrocyte culture.

3.3.2 Cell culture and seeding on materials

After isolating or thawing, cells were plated in culture flasks (T75, Becton-Dickinson) at high density in DMEM supplemented with 10% FBS and 50 mg/ml ascorbic acid (Sigma-Aldrich) at 37ºC in a 5% CO_2 humidified atmosphere. The medium was changed every 2–3 days.

In parallel, polymer scaffolds were pre-sterilised with 25 kGy gamma radiation and placed into culture polystyrene 96-well plate (Nunc A/S, Denmark). Material were premoistened with Hanks' Balanced Salt Solution (Sigma-Aldrich) using a precision syringe before they were seeded.

After 7–14–28 days, adherent cells were harvested by incubation with tripsyn/EDTA (Biological Industries) and seeded into porous scaffolds by injection of 500,000 cells in 50 µL of supplemented culture medium with 10% FBS and 50 µg/mL ascorbic acid. After cell injection, medium was gently added to ensure that the material was covered.

To test only the cells attached onto the sample material, the biomaterials were changed to a new well after 1–2 days. Cells were cultured with DMEM supplemented with 10% FBS [FBS containing medium, (FCM)] or with 1% ITS [ITS containing medium (ICM); BD Biosciences] and 50 µg/mL ascorbic acid, according to experimental conditions. The corresponding medium was changed every 2-3 days.

In monolayer cultures on the polymeric materials, cell culture was initiated at a density of 10,000 cells per disk and, after 2 days, the polymer disks were changed to a new well to test only the cells attached onto the sample material as explained above.

First or second passage chondrocytes were used in all experiments in order to avoid their total de-differentiation to fibroblastic cells.

3.3.3 Pellet preparation

After harvesting the cells from the culture flasks, resuspended cells were transferred to a 15 mL polystyrene centrifuge tube (1,000,000 cells per tube), and 1 mL culture medium was added.

The cell suspension was centrifuged for 4 min at 1200 rpm. The resulting pellet was cultured with DMEM supplemented with 10% FBS or 1% ITS and 50 µg/mL ascorbic acid at 37 ºC in a 5% CO_2 humidified atmosphere. Medium was changed every 2-3 days.

Pellet cultures were used as a 3D positive control of hyaline-specific ECM proteins in some of the experiments.

3.3.4 SEM

Cell morphology was observed by SEM (Jeol JSM-5410). The scaffolds with the cultured cells were fixed in 2% paraformaldehyde, 2.5% gluteraldehyde solution in PBS, then cut in half (longitudinal axis) with a sterilised surgical scalpel. The pieces obtained were maintained in PBS in a 96-well cell culture plate. After that, samples were dehydrated using series of ethanol/water solutions (30%, 50%, 70%, and 90% of ethanol) for 15 min with final dehydration in absolute ethanol for 30 min (twice). The cut pieces of the scaffolds were then dried at room temperature overnight. Prior to analysis, samples were mounted in the microscope carriers and coated with gold using a BAL-TEC SCD 005 Sputter Coater.

Both, the interior (core) and surface of the scaffolds were observed.

3.3.5 Histology

The ability of chondrocytes to synthesise GAG in the porous PCL scaffold was monitored by Alcian blue staining at 7, 14, and 28 days of culture. Scaffolds were embedded in optimum cutting temperature (OCT) compound (Tissue-Tek, Sakura Finetek), frozen in liquid nitrogen and cryosectioned (8-µm thick). Cryosections were fixed in acetone for 10 min at 4ºC and air-dried before staining, or they were stored at -20ºC until use. Sections were stained with Alcian blue, counterstained using Mayer's hematoxylin, and then analysed by optical microscopy.

3.3.6 Immunohistochemistry

Immunohistochemistry (IHC) refers to the process of detecting proteins in a tissue section by exploiting the principle of antibodies binding specifically to antigens in biological tissues. This method was used to detect specific proteins found in chondrocytes or in the ECM that was being formed. Specific antibodies of the target protein were used. These antibodies were then made visible using secondary fluorescent antibodies that bond to primary antibodies. Antibody-epitope complexes were evaluated using confocal microscopy.

3.3.6.1 Inmunofluorescence of the chondrocyte-cultured scaffolds

To perform this technique, biomaterials with cultured cells were fixed with 4% PFA in PBS 0.1 M at pH 7.5 for 20 min, rinsed in PBS, and blocked in 10% FBS/0.1% Triton X-100 at room temperature (RT) for 1 h.

The following antibodies were incubated overnight in 0.1% FBS/0.1% Triton X-100 at 4ºC: polyclonal rabbit antihuman collagen I (Chemicon International, no AB745, 1:50); monoclonal mouse antihuman collagen II (Chemicon International, no MAB1330, 1:50); monoclonal mouse antihuman Aggrecan (Invitrogen, n_ AHP0022, 1:50), and monoclonal mouse antihuman Ki-67 (DAKO, no M7240, 1:50).

Biomaterials were then incubated for 2 h at RT with secondary antibodies: Alexa Fluor 488 goat antimouse (Invitrogen, 1:200), Alexa Fluor 555 goat antimouse (Invitrogen, 1:200) or Alexa Fluor 488 goat anti-rabbit (Invitrogen, 1:200). Subsequently, constructs were washed 3 times for 10 min with PBS at RT and cut in half by using microsurgical instruments in order to have a view of the internal part. Samples were then prepared with mounting medium for fluorescence with 4',6-diamidino-2-phenylindole (DAPI) (Vectashield, VECTOR, no H-1200) as a counterstaining of the cell nuclei. Finally, samples were analysed by inverted microscope (Leica, DM IRB) and confocal microscope (Leica, TCS SP2 AOBS - Leica Microsystems Heidelberg GmbH, Mannheim, Germany).

3.3.6.2 Immunohistochemistry of the chondrocyte-cultured scaffolds

In the scaffolds embedded in OCT and cryosectioned after 7, 14, and 28 days of seeding (as explained above in section **3.3.5**), immunohistological analysis was used to detect the synthesis of type II collagen, the expression of S-100 (chondrocyte differentiation marker) and the expression of Ki-67 (proliferation marker).

Sections were incubated for 1 h at RT with a 1:100 dilution of type II collagen antibody (Chemicon), 1:100 dilution of Ki-67 antibody (Dako Cytomation), or prediluted S-100 antibody (Dako Cytomation).

Antigen–antibody complexes were detected colorimetrically using the EnVision Dual Link Kit (Dako Cytomation) and counterstained with Mayer's hematoxylin.

3.3.6.3 Cell viability and proliferation assay in 2D biomaterials

Cell viability and proliferation were monitored by cell staining, MTT test and BrdU assay at 7 and 14 days from the seeding.

Cell staining was performed with Mayer's haematoxylin and analysed with optical microscopy.

The cell viability was evaluated by MTT assay based on the cleavage of the yellow tetrazolium salt to purple formazan crystals by metabolic active cells (Roche Diagnostics GmbH). Crystals were solubilised and the resulting coloured solution was quantified using an ELISA reader (A_{550}).

Proliferation was determined using a colorimetric immunoassay based on the measurement of BrdU incorporation during DNA synthesis (Roche Diagnostics GmbH). The absorbance was measured at 450 nm in an ELISA reader. In this case, cells were synchronised by incubation in serum-free medium with 0.1 bovine serum albumin (BSA) for 2 days. Serum-containing medium was added 24 h before the BrdU addition. In every experiment, cells cultured on polystyrene of a 96-well plate (without biomaterial) were used as a control (CPS; culture polystyrene).

The chondrocytic phenotype was assessed for synthesis of aggrecan by means of immunoassay (Human Aggrecan ELISA Kit; Biosource).

3.3.7 RNA extraction and real-time PCR

The polymerase chain reaction (PCR) is used to amplify a single or a few copies of a piece of DNA across several orders of magnitude, generating thousands to millions of copies of a particular DNA sequence.

Real-time PCR is an advanced form of PCR used to perform truly quantitative analysis of gene expression. Real time PCR makes possible to amplify and quantify gene-specific products from very small samples and allows for quantification of mRNA with high accuracy, reproducibility, and sensitivity in a wide dynamic range [60, 122].

In this work, this quantitative PCR was used to assess the gene expression of the type II collagen and aggrecan in cells from PCL scaffolds, monolayer, and pellet cultures at 7, 14, and 28 days of culture. Specimens were suspended in 0.5 mL of Tri Reagent (Molecular Research Centre) and homogenised by vortexing. The RNA was then extracted according to Tri Reagent manufacturer's instructions.

Total RNA was tested by agarose gel electrophoresis, and 7 µL were used to synthesise the DNA complementary strain according to the protocol of TaqMan® Reverse Transcription Reagents (Applied Biosystems, Foster City, CA). The product was then diluted by half with RNAse-free pure water, and 1 µL of the resulting solution was used for quantitative PCR. Real-time PCR was conducted in a volume of 20 µL containing gene-specific Assay on Demand primers and TaqMan-MGB probe, and TaqMan Universal PCR MasterMix (Applied Biosystems). The PCR reaction had the following sequence: 2 min at 50ºC, followed by 50 cycles of 15 s at 95ºC and 60 s at 60ºC each cycle in 384-well plates with the ABI PRISM 7900 HT Detection System (Applied Biosystems).

The results were analysed using SDS TM software 2.1 (Applied Biosystems), and the expression levels were calculated against 18S expression and then normalised to an internal sample (relative quantification) using arbitrary units.

All real-time PCR reactions for each sample were performed in triplicate. The sample used to normalise each experiment was one pellet at 28 days post-seeding that had been cultured in the same experiment and had been run on the same PCR plate. Real-time PCR for 18S was carried out under the same conditions, using an 18S endogenous control Assay on Demand (Applied Biosystems).

3.3.8 Summary of biological parameters for cartilage engineering

The biological parameters used in this thesis to characterise chondrocyte phenotype and hyaline cartilage are summarised in **Table 3.3**.

Table 3.3 Chondrocyte biological parameters in TE

Chondrocyte biological parameters	Chondrogenic marker	Evaluation techniques
Chondrocyte cell viability		MTT assay
Chondrocyte cell proliferation		DNA quantification [71, 123, 124]
Chondrocyte cell adhesion		Fluorescence microscopy [125]
Chondrocyte morphological analysis	Rounded morphology: positive marker	Microscope: phase-contrast microscopy [64] SEM [64, 123-126] Confocal Microscopy [125]
Collagen II	Positive marker	IHC Real time PCR [123, 124, 126-128]
Collagen I	Negative marker	IHC Real time PCR[123, 124, 126, 128]
Aggrecan	Positive marker	Histology (Alcian blue staining) IHC Real time PCR [123, 124, 126, 128]
S-100	Positive marker	IHC Real time PCR [123, 124]

3.4 STATISTICAL ANALYSIS

Quantitative data were statistically analysed with SSPS 10.0 software. Data from every assay were expressed as mean ± standard deviation (SD).

Data from each independent experiment were normalised to one of the materials within the experiment. Each experiment was performed in triplicates and repeated at least three times using different chondrocyte populations. An asterisk in the figures emphasises the data that show statistically significant differences as a result of variance analysis (ANOVA test) with $p = 0.05$ and, as a consequence, are considered significantly different from them.

Real-time PCR results were normalised using the endogenous control 18S and the same sample was used for relative quantification. Differences between PCL, pellet, and monolayer cultures were evaluated using the Mann-Whitney U-test. The p-values less than 0.05 were considered significant.

Chapter 4

RESULTS AND DISCUSSION

“Te quejas de las censuras de tus maestros, émulos y adversarios, cuando debieras agradecerlas. Sus golpes no te hieren; te esculpen.”

“Nada me inspira más veneración y asombro que un anciano que sabe cambiar de opinión.”

“Al carro de la cultura española le falta la rueda de la ciencia.”

Santiago Ramón y Cajal (médico y científico. 1852-1934)

4.1 RESPONSE OF HUMAN CHONDROCYTES TO A NON-UNIFORM DISTRIBUTION OF HYDROPHILIC DOMAINS ON POLY (ETHYL ACRYLATE-CO-HYDROXYETHYL METHACRYLATE) COPOLYMERS

This chapter is based on the work of M. Pérez Olmedilla, N. Garcia-Giralt, M. Monleón Pradas, P. Benito Ruiz, J.L. Gómez Ribelles, E. Cáceres Palou, J. C. Monllau García. *Response of human chondrocytes to a non-uniform distribution of hydrophilic domains on poly(ethyl acrylate-co-hydroxyethyl methacrylate) copolymers.* Biomaterials 27, 1003-1012 (2006). Some results and discussion have been updated with recent published literature in order to complete the arguments of the original work.

It is widely known that the surface hydrophilicity significantly affects cellular response in monolayer culture. However, the way in which this surface hydrophilicity affects cellular response depends on the cell type and the kind of material where cells are seeded. Moreover, it is difficult to find a clear correlation between the parameters that are used to characterise the hydrophilicity - such as equilibrium water content (EWC), wettability or surface tension - and the factors characterising cell adhesion. Hence, this study aims to understand the mechanism by which the presence in the substrate surface of groups capable of binding water molecules through hydrogen bonds (thereby increasing hydrophilicity) can affect mature human chondrocytes cultures.

4.1.1 Results

4.1.1.1 Culture substrates with modulated hydrophilicity

For this study three series of copolymers were designed and synthesised combining a monomeric unit containing hydroxyl groups (HEA or HEMA) with a monomeric unit not containing such groups (EA and EMA). On the other hand, another combination was prepared containing a monomeric unit of acrylates (EA or HEA) and a monomeric unit of methacrylates (EMA or HEMA). **Figure 4.1** shows the structural formula of the homopolymers that were synthesised by bulk free radical copolymerisation.

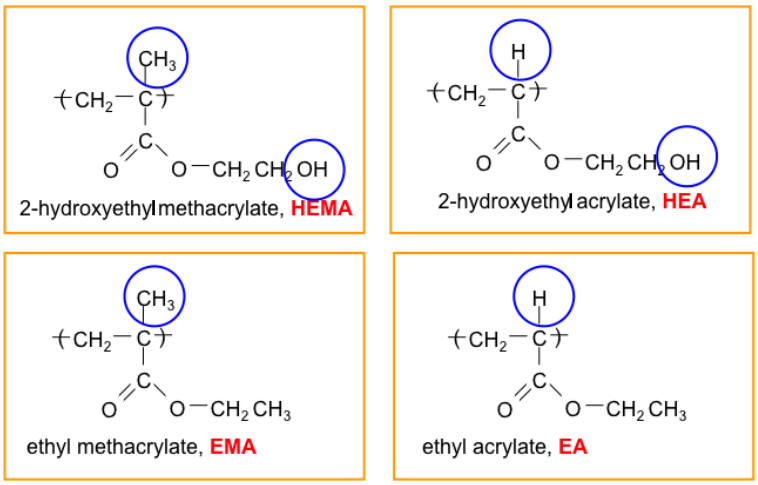

Figure 4.1 Structural formula of HEMA, HEA, EMA and EA monomeric units.

Table 3.1 (in chapter **3**) shows the different compositions prepared for each series of copolymer networks, together with the short designation used in the text.

The difference between polyacrylates and polymethacrylates is in the methyl group bonded to the main chain in each monomeric unit (**Figure 4.1**). This group modifies the flexibility of the chain and is responsible, for example, for making the glass transition temperature (T_g) in polymethacrylates to be in the order of 100°C higher than in its analogous polyacrylate. However, in this work, special attention is given to the difference in monomer reactivity.

When polymerisation takes place in a mixture of monomers of different reactivity, a richer copolymer chain of the most reactive monomer can be formed. Because the most reactive monomer is the first to be consumed, at the end of the process a stock of the less reactive monomer remains, which incorporates into the polymer chains or the polymer network in the form of homopolymer blocks. Depending on the sizes of the blocks, a phase separation can take place, forming aggregates of different composition – in our case, since hydrophobic monomers results less reactive, hydrophobic domains may appear in the final copolymer structure.

4.1.1.2 Polymer characterisation

The first step in this work was to test if, in our series of copolymers, a phase separation did actually occur and if more hydrophilic aggregates were formed in alternation with others less hydrophilic.

The existence of a single glass transition in a multicomponent polymer system is a generally accepted criterion for the homogeneity of the material. When domains only a few nanometres in dimension and with a composition differing from the average are present in a matrix material, a glass transition is produced. This glass transition is separated from that of the matrix, provided that the mass fraction of such domains is significant (around 10 wt%), and the glass transition

temperature of both phases is separated by at least about 10ºC [133]. This glass transition is detectable by calorimetry or dilatometry.

The main dynamic-mechanical relaxation process associated with the glass transition [134] is even more sensitive to this phase heterogeneity, *i.e*, the glass transition of the domains dispersed in the matrix can be detected with a smaller mass fraction of the dispersed phase.

Figure 4.2 shows the loss tangent of the homopolymer networks used in this work and the copolymers P(EA-co-HEMA), P(EA-co-HEA) and P(EMA-co-HEA) with 50 wt% of each component. PEA homopolymer shows a single peak, with a maximum at around 0ºC, due to its main relaxation process. On the other hand, PHEMA has its main relaxation at around 140ºC, and, at lower temperatures, in the glassy state, there is a smooth increase in the loss tangent that is ascribed to the secondary relaxation associated with local movements of the side chains of the polymer: the β relaxation [135].

In random copolymers in which one component is an acrylate and the other a methacrylate, the intensity of the β relaxation of the methacrylate component rapidly decreases with an increasing amount of acrylate monomeric units, and at the same time it shifts towards lower temperatures [136, 137]. Thus in P(EA-co-HEMA) copolymers, the β relaxation should play no role in the temperature interval of the measurements. Whereas in the case of copolymers of the series P(EA-co-EMA) and P(EMA-co-HEMA), the peak in the loss tangent that characterises the main relaxation process associated with the glass transition is clearly a single narrow peak (like in the homopolymer networks), the P(EA-co-HEMA) copolymers have a double peak that is representative of the presence of two separated phases.

More evidence of phase separation in P(EA-co-HEMA) copolymers was obtained using DSC and AFM [131, 138]. It was shown that hydrophobic, irregular PEA domains with sizes in the order of nanometers are dispersed in a matrix of a P(EA-co-HEMA) copolymer with a composition richer in HEMA than the average. It can be assumed that P(EA-co-HEA) and P(EMA-co-HEA) copolymers are not phase separated and as a consequence the distribution of the hydrophilic groups in them is homogeneous.

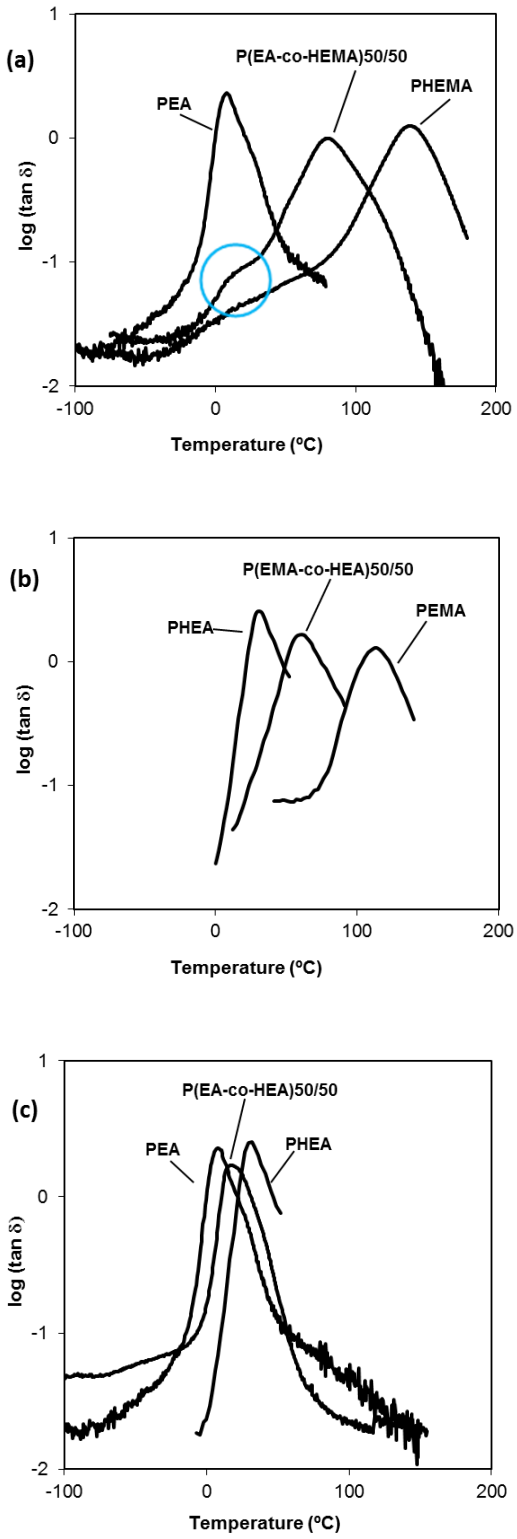

Figure 4.2 Temperature dependence of the mechanical loss tangent of three copolymer networks compared with those of the pure component networks.

(a) P(EA-co-HEMA) 50/50 wt% is compared with PEA and PHEMA homopolymer networks. The blue circle indicates the zone of the low-temperature main relaxation of disperse domains of poly(ethyl acrylate) in the P(EA-co-HEMA) 50/50 wt%.

(b) P(EMA-co-HEA) 50/50 wt% is compared with PHEA and PEMA homopolymer networks.

(c) P(EA-co-HEA) 50/50 wt% is compared with PEA and PHEA homopolymer networks.

The EWC is measured on dry basis, *i.e*. mass of absorbed water per unit mass of polymer. The EWC of the copolymer networks are listed in **Table 4.1**.

Table 4.1 Sample composition, EWC and surface energy measurements

Sample	Composition	EWC	γ^p (mN/m)	γ^d (mN/m)	γ_s (mN/m)
A1	PEA	0.6	0.04	32.22	32.26
A2	P(EA-co-HEMA) 70/30 wt%	7.7	0.40	32.05	32.46
A3	P(EA-co-HEMA) 50/50 wt%	15.1	2.08	31.53	33.61
A4	P(EA-co-HEMA) 30/70 wt%	26.4	4.83	35.47	40.30
A5	PHEMA	52.6	26.05	27.06	42.07
B1	PEMA	1.1	4.13	27.67	31.81
B2	P(EMA-co-HEA) 70/30 wt%	6.9	3.46	37.41	40.87
B3	P(EMA-co-HEA) 50/50 wt%	16.2	4.43	24.77	29.20
B4	P(EMA-co-HEA) 30/70 wt%	45.6	5.40	25.05	30.45
B5	PHEA	142.2	18.81	27.39	46.20
C1	PEA	0.6	0.04	32.22	32.26
C2	P(EA-co-HEA) 70/30 wt%	7.6	0.59	31.24	31.83
C3	P(EA-co-HEA) 50/50 wt%	18.2	3.17	33.32	36.49
C4	P(EA-co-HEA) 30/70 wt%	40.6	2.82	34.45	37.26
C5	PHEA	142.2	18.81	27.39	46.20

Pure PHEA networks absorb more water than pure PHEMA with the same cross-linking density, whereas the pure PEA or PEMA absorb around or less than 1 wt% water measured on dry basis. Thus, PEA and PEMA can be considered hydrophobic materials. The water absorption decreases uniformly with an increase in the hydrophobic component in all of the three-copolymer series studied.

Surface energy of the substrate is probably more related to the cell response in monolayer culture than EWC. The surface energy or surface tension of the polymeric substrate can be determined from the contact angle of a drop of liquids of known surface tension deposited on the solid surface as represented in **Figure 4.3**.

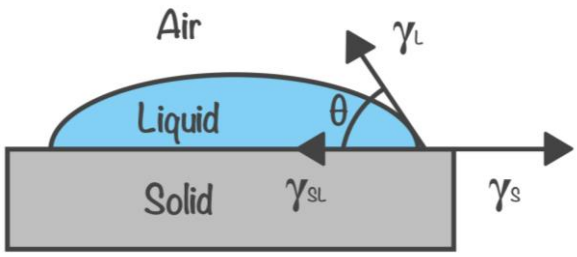

Figure 4.3 Diagram of the sessile-drop contact angle system

Young's Equation (equation 4.1.) [139] relates surface energy of a given solid (γ_S) with the surface energy of a liquid (γ_L) and its corresponding liquid-solid interfacial energy (γ_{SL}) (**Figure 4.3**).

$$\gamma_S = \gamma_{SL} + \gamma_L \cos\theta \quad (4.1)$$

The experimental property is the contact angle (θ) and it can be measured for a variety of liquids with a more or less broad range of surface tension. The calculation of the surface tension of the solid surface requires an evaluation of the experimental results with the aid of a theoretical development. In the case of our materials, the method described by Owens and Wendt (Equation 4.3) [132] is especially adequate since it allows the two components of the surface tension to be determined: the polar component, γ^p, (derived from polar interactions between molecules) and the dispersive component, γ^d, (resulting from the rest of the molecular interactions) (Equation 4.2):

$$\gamma = \gamma^p + \gamma^d \quad (4.2)$$

$$\gamma_{SL} = \gamma_L + \gamma_S - 2(\gamma_L^d \cdot \gamma_S^d)^{1/2} - 2(\gamma_L^p \cdot \gamma_S^p)^{1/2} \quad (4.3)$$

Thus, the combination of Owens & Wendt's hypothesis (equation 4.3) and Young's equation (4.1) results in equation (4.4).

$$\frac{1+\cos\theta}{2}\frac{\gamma_L}{\left(\gamma_L^d\right)^{1/2}} = \left(\gamma_S^p\right)^{1/2}\left(\frac{\gamma_L^p}{\gamma_L^d}\right)^{1/2} + \left(\gamma_S^d\right)^{1/2} \quad (4.4)$$

Representing the experimental data of the contact angle of liquids of varying surface tension in a graphic (**Figure 4.4**):

in **x** axis $\left(\frac{\gamma_L^p}{\gamma_L^d}\right)^{1/2}$ and, in **y** axis $\frac{1+\cos\theta}{2}\frac{\gamma_L}{\left(\gamma_L^d\right)^{1/2}}$,

the linear fit **y = mx + b** allows the polar and dispersive components of the surface tension of the polymer to be determined from the slope and the intercept in the y-axis, respectively.

As an example, the representation for the copolymer P(EA-co-HEMA) 50/50 is shown in **Figure 4.4**. **Table 4.2** shows the contact angle results obtained for P(EA-co-HEMA) 50/50 with four different liquids. The uncertainty of the measurements is representative of that of the rest of the samples. The mean values ± standard deviation (SD) is represented in **Table 4.2**. The same procedure was followed with the rest of samples and the results are listed in **Table 4.1.**

Table 4.2 P(EA-co-HEMA) 50/50 contact angle measurements

P(EA-co-HEMA) 50/50						
Nº	**Right angle (degrees)**	**Left angle (degrees)**	**Individual mean value (degrees)**	**MEAN VALUE ± SD**	**RANGE**	**LIQUID**
1	82,2	82,1	82,1	**81,76** ± 1,90	4,60	Glycerol
2	82,2	82,1	82,1			
3	80,8	80	80,4			
4	80,8	80	80,4			
5	83	84,6	83,8			
6	47,4	50	48,7	**46,70** ± 1,92	4,90	Diiodomethane
7	41,7	46,1	43,9			
8	41	45,1	43			
9	43,4	46,6	45			
10	45,5	45,7	45,6			
11	74,2	76,5	75,3	**76,90** ± 1,80	4,20	Formamide
12	73,2	73,9	73,6			
13	79,4	78,1	78,8			
14	77,3	78	77,7			
15	77,3	78	77,7			
16	50,4	49,3	49,9	**50,76** ± 3,36	9,10	Diethilenglycol
17	50,8	55,7	53,2			
18	58,3	51,8	55			
19	48,9	50,4	49,7			
20	49	46,6	47,8			

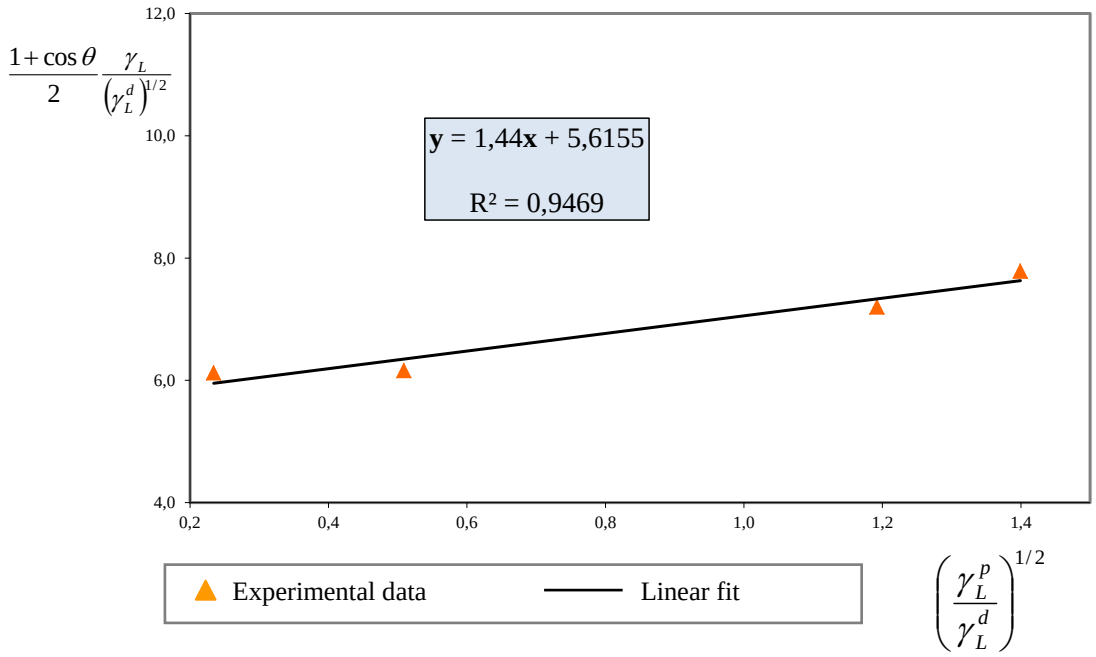

Figure 4.4 Graphic representation of experimental data according to equation (4.4) for the P(EA-co-HEMA) 50/50 copolymer.

The surface energy (**Table 4.1**) of the copolymer networks decreases uniformly with an increasing amount of the hydrophobic polymer. The composition dependence of the dispersion component of the surface energy is modest, increasing slightly with the content of the hydrophobic components, whereas the polar component that has a high value for the pure hydrophylic homopolymers decreases sharply with very small amounts of the hydrophobic component of the copolymer networks. The only copolymer network that seems to behave differently from the rest of the samples is the P(EMA-co-HEA) containing 30 wt% of HEA, whose surface tension is higher than that of pure PEMA and copolymers richer in HEA. The reason is not clear, but this feature might be due to the high glass transition temperature of this copolymer in the dry state and its low EWC.

4.1.1.3 Cell seeding and morphology

Once the materials were characterised, the next step was to culture cells on the surface of the materials to test their biocompatibility and biological response. Cells were seeded on the flat substrates and cultured for 7 and 14 days onto all the material's compositions.

The cells cultured onto the biomaterials were stained with Mayer's haematoxylin in order to assess their adhesion capacity. The observations with optical microscopy showed a diverse spreading of the cells on the different biomaterials (**Figure 4.5**). Pure PEA (**Figure 4.5(a)**) and pure PEMA (not shown) were mainly colonised with round shaped cell clusters at 7 days of

culture, whereas copolymer networks showed a homogeneous distribution of cells with a fibroblast-like shape as in the CPS control.

Pure PHEMA, even though it is unfavourable to cell adhesion, was cytocompatible (**Figure 4.5(i)** and **Figure 4.5(j)**) whereas pure PHEA gave the worst results, with very few cells attached to the substrate (data not shown). There was no appreciable increase in the cell number in pure PHEMA culture from 7 to 14 days after seeding. At 14 days from seeding, the cells cultured onto hydrophobic materials became flattened and had more homogeneous distribution.

Both 7 and 14 days after seeding, the materials that showed the best results were P(EA-co-HEMA) 50/50 wt% (sample A3) followed by the hydrophobic networks. The results obtained in P(EA-co-HEMA) 50/50wt% 14 days after seeding were similar to the control polystyrene results (**Figure 4.5(k)** and **Figure 4.5(l)**). To further clarify this point, **Figure 4.6** shows the culture results at 7 days after seeding on samples P(EMA-co-HEA) and P(EA-co-HEA) corresponding to the 50/50 wt% homogeneous copolymers to be compared with the corresponding result of sample P(EA-co-HEMA) in **Figure 4.5**.

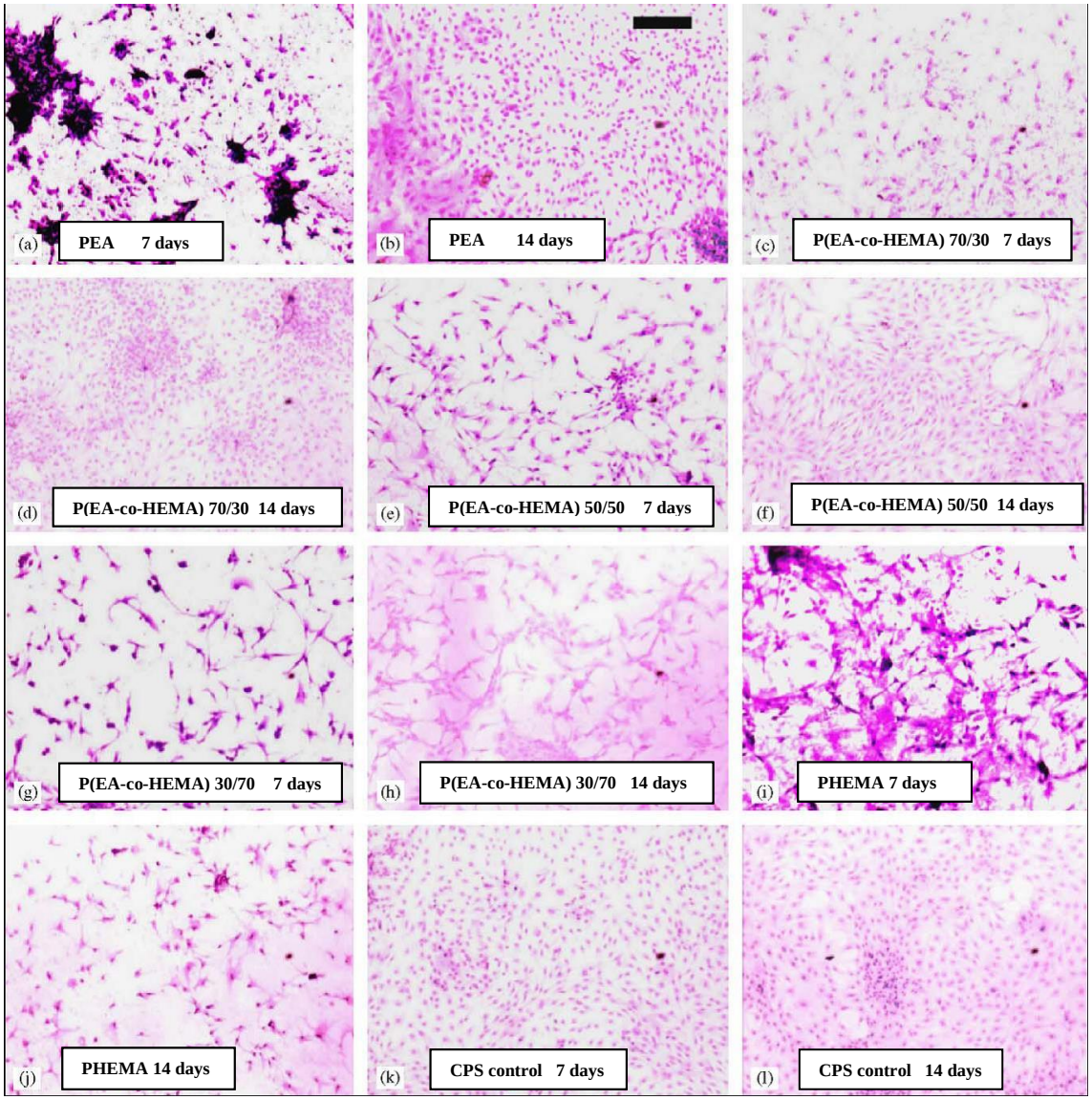

Figure 4.5 Optical microscope pictures of Mayer's haematoxylin stained chondrocytes seeded onto P(EA-co-HEMA) biomaterial set

(a) and **(b)** PEA network, **(c)** and **(d)** P(EA-co-HEMA) 70/30 wt%, **(e)** and **(f)** P(EA-co-HEMA) 50/50 wt%, **(g)** and **(h)** P(EA-co-HEMA) 30/70 wt%, **(i)** and **(j)** PHEMA, **(k)** and **(l)** CPS control. The pictures **(a)**, **(c)**, **(e)**, **(g)**, **(i)**, **(k)** show the culture at 7 days and the pictures **(b)**, **(d)**, **(f)**, **(h)**, **(j)**, **(l)** show the culture at 14 days. The dimension bar corresponds to 200 µm.

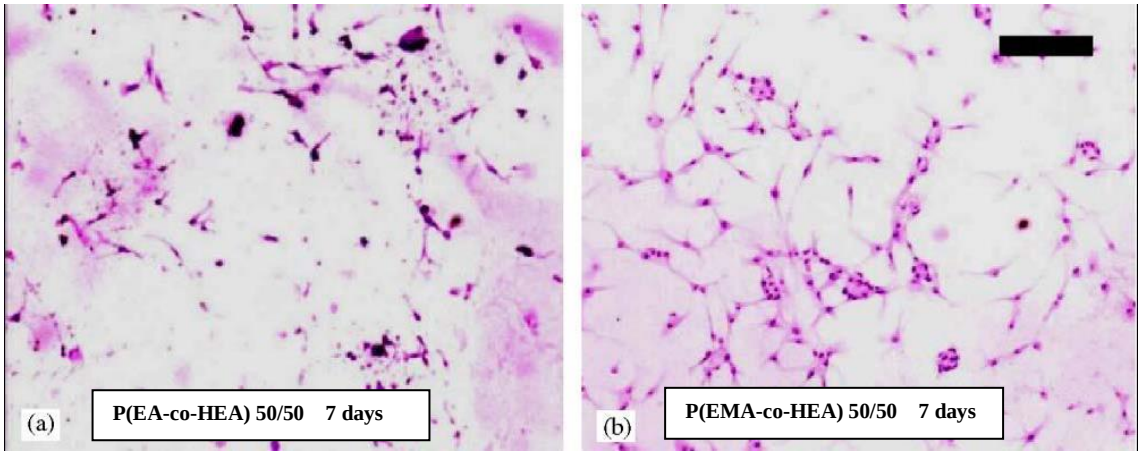

Figure 4.6 Optical microscope pictures of Mayer's haematoxylin stained chondrocytes seeded onto P(EA-co-HEA) and P(EMA-co- HEA)

Chondrocytes were seeded onto **(a)** P(EA-co-HEA) 50/50 wt%, and **(b)** P(EMA-co- HEA) 50/50 wt%, 7 days after seeding, to be compared with the picture **(e)** of **Figure 4.5**, corresponding to P(EA-co-HEMA) 50/50 wt%, 7 days after seeding. The dimension bar shown corresponds to 200 µm.

4.1.1.4 Chondrocytes proliferation and viability

BrdU assays and MTT tests were used to assess the proliferative activity and the cellular viability of human chondrocytes cultured on the polymer substrates over 7 days, respectively. The results are shown in **Figure 4.7**. The data were normalised in each experiment with the value obtained in the sample containing 30 wt% of the hydrophobous component (samples A4, B4 and C4). Hence, a copolymer with intermediate hydrophilic/hydrophobic composition was preferred as the reference for normalisation since the hydrophilic homopolymer network showed lower adhesion.

The normalisation allowed experiments performed at different days and with different chondrocyte lines to be compared. **Figure 4.7** shows the results of both assays in pure PEA. **Figure 4.7(a)** and **Figure 4.7(c)** show the results for samples A1 and C1, which are the same material (PEA; see **Table 3.1**). The results for samples A1 and C1 looked quite different, despite being the same material. The reason for the differences observed was that the proliferation and viability of the chondrocytes on sample A4 containing PHEMA as the hydrophilic component was higher than in sample C4 containing PHEA.

No control values are shown for the MTT results because the measurements were performed on the material's surface, and the absorbance was greater than in the CPS, and not suitable for comparison.

Both assays, MTT and BrdU, showed complementary results, which were consistent with cellular adhesion on the material (**Figure 4.5**). Thus, the materials with better cellular adhesion had higher MTT and BrdU values. Chondrocyte proliferation levels at 14 days post-seeding

decreased with respect to those at 7 days, whereas similar cell viability values were observed (**Figure 4.8**).

4.1.1.5 Chondrocytes characterisation

Aggrecan synthesis was quantified at 7 and 14 days from seeding. A first subculture was used to seed biomaterials; aggrecan production was tested to control the chondrocyte's phenotype (**Figure 4.9**).

The ELISA results demonstrated the presence of aggrecan in the medium supernatants. However, aggrecan synthesis slightly decreased at 14 days compared with 7 days values (data not shown). Expansion of chondrocytes in two-dimensional culture systems resulted in their dedifferentiation. Accordingly, expression of specific hyaline cartilage markers such as aggrecan decreased at 14 days of culture.

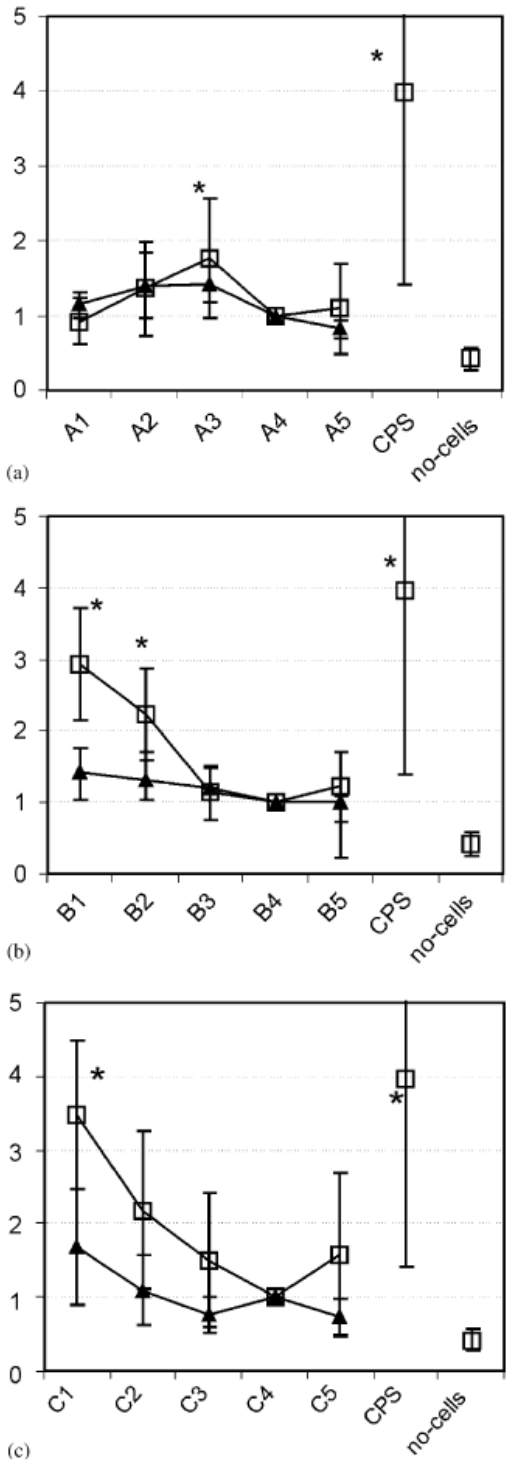

Figure 4.7 MTT and BrdU assays of the three copolymer series at 7 days from seeding.

A550 (MTT) (▲) and A450 (BrdU) (□) values are presented as normalised means±SD from five independent experiments. (*) indicates the data with probability less than 0.05 compared to the other materials within the same series (ANOVA-T3 Dunnet). **(a)** P(EA-co- HEMA), **(b)** P(EMA-co-HEA), **(c)** P(EA-co-HEA)

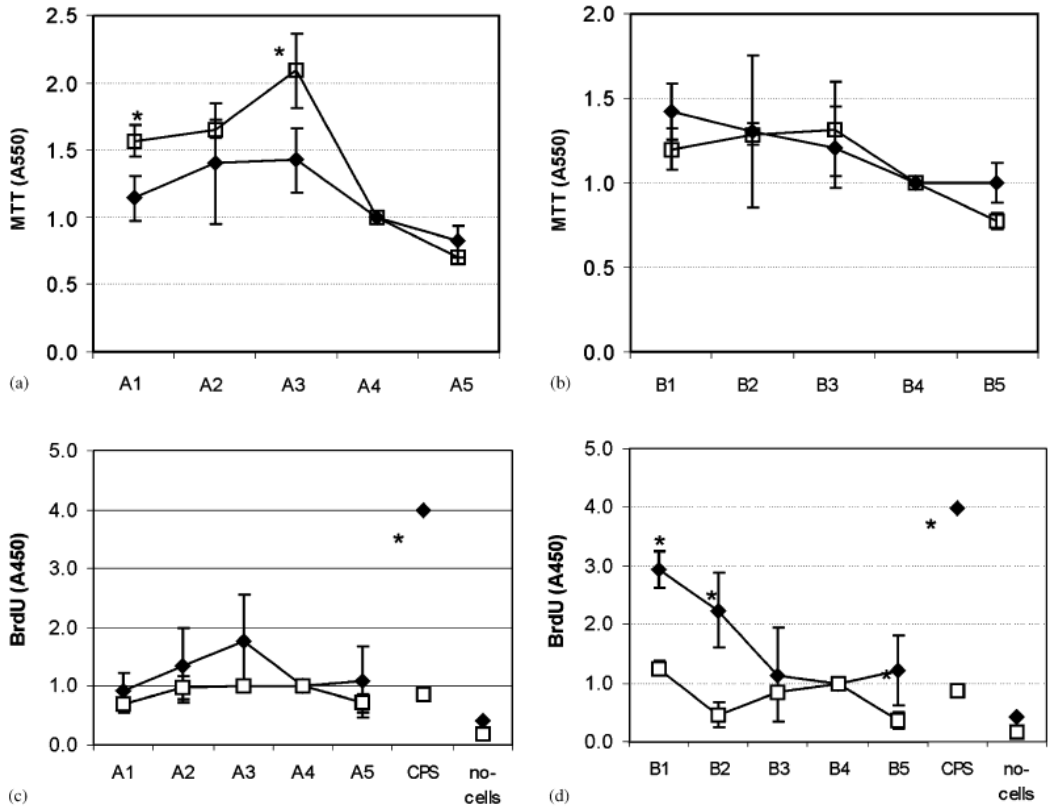

Figure 4.8 Cell viability and proliferation

Cell viability **(a)** and **(b)**, and proliferation **(c)** and **(d)** measurement at 7 (♦) and 14 (□) days. Absorbance values are presented as normalised means±SD from two independent experiments at 14 days from seeding. (*) indicates the data with probability less than 0.05 compared to 7 days of culture (ANOVA-T3 Dunnet).

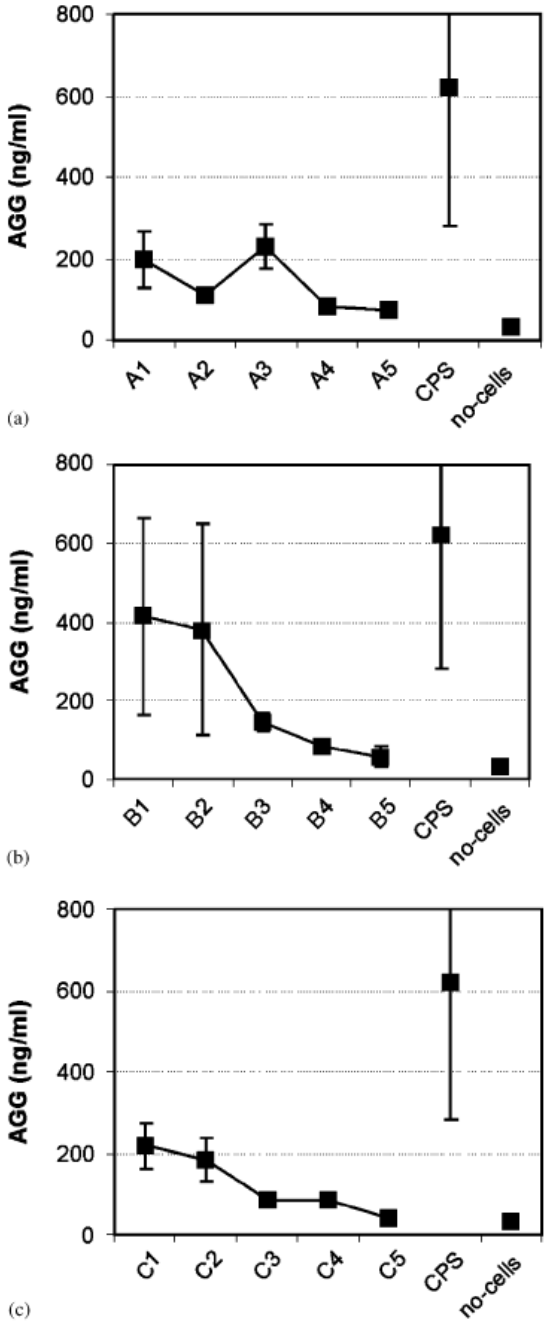

Figure 4.9 Quantification of aggrecan synthesis of the three copolymer series at 7 days from seeding
The values (ng/ml) are presented as normalised means±SD. No significant differences were found among the different biomaterials: **(a)** P(EA-co-HEMA), **(b)** P(EMA-co-HEA), **(c)** P(EA-co-HEA)

4.1.2 Discussion

This study shows that the presence of a single and narrow main relaxation process in the copolymer whose components have their own glass transitions separated by around 50ºC, as is the case of the P(EMA-co-HEA) series, is a strong indication of spatial composition homogeneity in the material (**Figure 4.2**). Contrarily, the presence of two overlapped relaxations indicates the existence of phase separation in the P(EA-co-HEMA) copolymer

series. Phase separation in these copolymers has been confirmed by other experimental techniques such as DSC and AFM in other studies published by our group [131, 138].

Likewise, the different behaviour of the P(EA-co-HEMA) copolymers comes from the fact that the reactivity of hydroxyethyl methacrylate is much higher than that of ethyl acrylate, and thus the former is first consumed in the free radical polymerisation. The remaining ethyl acrylate polymerises at the end of the reaction nearly as a pure PEA domain with nanometric dimensions.

Cells seeded on biomaterials showed reduced chondrocyte attachment capacity as compared with cells seeded on CPS (**Figure 4.7**). However, only the most hydrophilic materials can be considered to have adverse conditions. In fact, the reduced BrdU values observed in the cells seeded onto hydrophilic materials are mainly due to the small amount of cells attached. It is well known that the cell proliferation depends on adhesion capacity onto biomaterials.

A qualitatively different behaviour was found in chondrocyte culture on the copolymers of the series P(EMA-co-HEA) and P(EA-co-HEA) on the one hand, and series P(EA-co-HEMA) on the other. It is worth noting that the polar groups in the polymer networks of the three series reside in the methyl or hydroxyl groups of the side chains, which were exactly the same in the three series since the monomeric units differ only in the presence of the methyl groups attached to the main chain in the methacrylate monomers. Thus, the distribution of functional groups in the substrate surface depends only on the distribution of monomeric units along the polymer chain.

The surface roughness was also similar in all the samples as probed by AFM; the average roughness in all samples was 15±3 nm.

EWC also shows that hydrophilicity depends monotonously on the fraction of hydrophilic component in the copolymer. Something similar occurs with the surface tension dependence on the copolymer composition. Thus, out of all the factors referred to in the literature that affect protein adsorption and cell adhesion [86-92, 111, 112, 140, 141], the distinctive characteristic of series P(EA-co-HEMA) with respect to series P(EMA-co-HEA) and P(EA-co-HEA) is the non-homogeneous distribution of the hydroxyl groups in the substrate surface.

The homogeneous copolymer series, P(EA-co-HEA) and P(EMA-co-HEA), allowed a greater adhesion onto more hydrophobic materials (**Figure 4.7(b)** and **Figure 4.7(c)**). Cell viability and proliferation were gradually reduced when hydrophilicity was increased. This result agrees with the literature on fibroblasts culture on P(EMA-co-HEMA) hydrogels [87, 88, 92, 112, 140, 141].

As will be explained in more detail below (in section **4.2.1.2**), when the content of HEA increases in the system, the cell adhesion and proliferation drop very quickly. This phenomenon occurs with different cell types: Human umbilical vein endothelial cells (HUVEC) [142], fibroblast [142] and epithelial [143], among others.

The effect of the hydrophilic groups' decreasing cell adhesion is also very clear in neural cell culture on copolymers coated with laminin [144]. Laminin allows for the monolayer culture of this type of cells [145, 146].

However, in the materials with nano-phase separation in which hydrophilic and hydrophobic domains alternate, the P(EA-co-HEMA) set, the best results were observed in the copolymer containing 50 wt % of each component, sample A3 (**Figure 4.7(a)**).

In this sense, it is also significant that cell response, in terms of cell adhesion, is better in sample A3 than in B3 or C3, all of them copolymers with 50 wt % of hydrophilic component, as shown in the microphotographs in **Figure 4.5** and **Figure 4.6**. These differences are less evident in MTT and BrdU assays due to the normalisation of the data (**Figure 4.7**). However, the non-normalised values showed this differential biological response among materials (data not shown).

The results of the EWC and surface tension show that the dependence of the total amount of water absorbed in the polymer network on the content of the hydrophilic component is monotonous in the copolymer series with homogeneous spatial distribution of the hydrophilic groups, as expected, though also in the series that shows nano-phase separation. This is not an unexpected result since the same behaviour was found in sequential interpenetrated polymer networks containing a hydrophobic polymer network (of poly(methyl acrylate) [147] or PEA [148] as the first, continuous network) and a PHEA network polymerised in second place. These systems also present nano-phase separation. As a consequence, it can be concluded that it is not via the amount of water absorbed that the spatial distribution of the hydrofilic groups influences cell attachment.

The phenomenon of cell anchorage to the kind of polymeric substrate used in this work seems to be more complicated. The role of protein adsorption, in particular fibronectin, to the substrate may be crucial in this sense. Interaction between cell and ECM occurs through highly specific peptide sequences of the proteins of the ECM and particular integrin α-β pairs of the cell. Integrins are transmembrane proteins - once the external part of the integrin recognises a specific ligand in the proteins of its neighbourhood, integrins migrate throughout the cell membrane to cluster. Then, the internal part of the integrins recruit several cytoplasm proteins such as tensin, vinculin and others to form focal adhesions. From the complex protein clusters, actin polymerises forming stress fibres able to sustain external forces, connecting the nucleus

with the ECM and controlling different cell functions, including proliferation, migration and differentiation. Obviously there is nothing in a synthetic substrate that the cell is able to recognise, and consequently cell-material interaction is mediated by the proteins adsorbed on the material surface [149]. The amount and conformation of the proteins adsorbed on the surface determine the exhibition of the protein ligands, and thus their availability for cell attachment. The behaviour found in chondrocyte culture on the different series of our copolymers must thus be explained by the different way in which proteins from the serum adsorb on their surface. Recent experimental works have shown how the physical and chemical characteristics of the substrate determine protein selection and conformation [150-152]. In particular fibronectin, vitronectin, fibrinogen and laminin are important adhesion proteins of the ECMs. Fibronectin is one of the most abundant proteins in culture media and thus responsible for cell attachment in cell culture. Fibronectin adsorbs preferentially on hydrophobic substrates [153]. Not only is the amount of fibronectin adsorbed on the substrate important for cell attachment but its mobility [154] and the conformation adopted by the molecule on the polymer surface are as well. Cell activity rearrange fibronectin molecules to form networks that exhibit the adhesion domains contained in the fibronectin fragment $III_{7\text{-}10}$, in particular the peptide sequence RGD. This process is called fibrillogenesis and has been found in fibronectin adsorbed on certain polymeric substrates, in particular PEA, in the absence of cell activity [155]. Fibrillogenesis has even been observerd on PEA nanofibers obtained by electrospinning [156]. Nevertheless the presence of even a small amount of HEA in P(EA-co-HEA) copolymers hinders the formation of the fibronectin network. Campillo *et al.* showed a similar effect in the surface of P(EA-co-HEA) 3D scaffolds [142]. Interestingly, in the case of other adhesion proteins, conformation of the protein on P(EA-co-HEA) copolymers substrates is not monotonous. This laminin adopts globular forms on pure PEA (hyrophobous) and on pure PHEA (hydrophilic) but clearly spreads on 50/50 copolymers [157]. Correlation between adsorbed protein conformation and cell attachment has been demonstrated in different 2D materials [64, 158, 159]. It has been shown [160] that small amounts of a poly(ethylene glycol) can regulate the fibronectin bioactivity since the presence of hydrophilic aggregates on the hydrophobic substrate induces an extended conformation of adsorbed fibronectin, which exposes more amino acid adhesion sequences of the protein to the external medium. If the distribution of the hydrophilic groups on the surface is homogeneous, a globular fibronectin conformation results and the cell adhesion decreases.

The role of a microstructure in which hydrophilic and hydrophobic domains alternate in enhancing cell adhesion has been reported for other cell-substrate situations [141, 161].

The increased cell viability in the most hydrophobic materials of the PEA-co-PHEMA series, A1, A2, A3 at 14 days of culture with respect to 7 days, shown in **Figure 4.8(a)**, corresponds to

a much higher proliferation than sample A4, which was used to normalise the experiment. This feature can also be observed in the microphotographs of **Figure 4.5**. Both MTT and BrdU values showed a similar tendency at the two measurement times with minor variations. In the case of the P(EMA-co-HEA) series, the most hydrophobic materials B1, B2 and B3 showed similar MTT values at 14 days (**Figure 4.8(a)**). Optical microscopy observations showed a similar amount of cells on these materials (data not shown) and it could explain these MTT values. On the other hand, the materials with good cell attachment showed a greater decrease in proliferation values from 7 to 14 days culture (**Figure 4.8(b)**). These reduced values were due to a saturated proliferation when the culture reaches confluence.

All materials tested except the most hydrophilic (pure PHEMA and pure PHEA) showed an increase in cell number between 7 and 14 days (**Figure 4.5**). In pure PHEMA, no proliferation was detected, and it even decreased in cell number due to unfavourable adhesion conditions. Schiraldi *et al*. [162] obtained similar results when a murine fibroblast line and human primary osteoblasts were seeded on PHEMA films.

The chondrocytes cultured *in vitro* are capable of forming aggregates with round shaped cells like native cartilage. These cells are functional and express specific markers of chondrocyte phenotype. Other authors have demonstrated that cell clusters keep the differentiated phenotype and favour the formation of cartilage extracellular matrix [163, 164]. At 7 days, cells seeded on pure PEA and PEMA showed cell clusters capable of proliferating and synthesising aggrecan.

The different aggrecan values found among substrates are consistent with the differences in cell number according to the values obtained in MTT and BrdU assays. These results suggest that there are no differences in cell differentiation among substrates.

4.1.3 Conclusions

The spatial distribution of hydrophilic domains in a polymer substrate can be crucial for the cell adhesion, viability and proliferation of human chondrocytes cultured *in vitro*. Good biological response was obtained in monolayer culture on a P(EA-co-HEMA) copolymer network containing 50 wt% of each component, which presents phase separation with hydrophobous domains of nanometric dimensions dispersed in a hydrophilic matrix consisting in a copolymer richer in PHEMA than the average composition.

4.2 SCAFFOLDS WITH INTERCONNECTED SPHERICAL PORES: SPHERE TEMPLATE METHOD

The first part of this chapter (section **4.2.1.1**) is based on the work: R. Brígido Diego, M. Pérez Olmedilla, A. Serrano Aroca, J.L. Gómez Ribelles, M. Monleón Pradas, G. Gallego Ferrer, M. Salmerón Sánchez. *Acrylic scaffolds with interconnected spherical pores and controlled hydrophilicity for tissue engineering*. Journal of Materials Science. Materials in Medicine 16, 693-698 (2005).

In section **4.2.1.1**, 3D scaffolds were obtained with the copolymer networks characterised in section **4.1**. Scaffolds used in the following sections of this work and that were prepared with the same techniques but with different compositions are also presented. In section **4.2.1.2**, scaffolds made from CLMA-PHEA copolymers were prepared by Jorge Luis Escobar Ivirico while polycaprolactone scaffolds were prepared by Myriam Lebourg at the CBIT.

4.2.1 Results and Discussion

4.2.1.1 Acrylic scaffolds of P(EA-co-HEMA) with controlled hydrophilicity

The methodology employed made it possible to obtain a macroporous structure of interconnected spherical pores in a whole range of compositions, from pure hydrophilic PHEMA to pure hydrophobic PEA. PHEMA is a biocompatible material that has been used in a wide variety of biomedical applications, such as ophthalmologic prostheses, vascular prostheses, drug delivery system and soft-tissue replacement [165].

When HEMA is polymerised, the resulting material is hard and glassy with a glass transition temperature around 90ºC [138]. When swollen in water, it becomes a soft and flexible rubber. The copolymerisation with a hydrophobic component plays a double role. On the one hand, mechanical reinforcement is obtained in the swollen state and, on the other hand, copolymerisation allows the desired hydrophobicity of the material to be optimised with a specific application in mind.

As shown in section **4.1**, the molecular structure of the system obtained after copolymerisation of EA and HEMA, through bulk copolymerised from the monomer mixture, consists of a distribution of nano-aggregates of alternating HEMA-rich and pure hydrophobic domains, a structure that seems to favour both cell adhesion and diffusion of nutrients [166].

SEM micrographs of the resulting scaffolds (**Figure 4.10**, **Figure 4.11** and **Figure 4.12**) show the 3D spherical interconnected porous network. The same geometrical structure can be

obtained with a broad range of compositions, from pure hydrophobic PEA (**Figure 4.10**) to pure hydrophilic PHEMA (**Figure 4.12**); the average diameter of the pores, between 65-85 µm, does not depend on the chemical composition of the material but rather on the size of the PMMA spheres used as a template.

This is the reason the pore size and connectivity could be easily modified by changing both the sphere diameter and the sintering process: by changing the temperature and pressure, the contact between the spheres can be regulated, which results in a controlled variation of the porous structure of the polymer scaffold (**Figure 4.11**). This fact has already been proven with paraffin spheres [109, 167] and with similar PMMA spheres of different diameters. For instance, Brígido Diego and co-workers [168] reported that the porosity of PEA scaffolds could be modulated from 70% to 85% by applying different degrees of compression in the sintering process of the PMMA porogen templates. Moreover, the pores sizes were also controlled by using spheres with different diameters 35, 90 and 250 µm. By using this methodology, the mechanical properties of the PEA scaffolds could be regulated according to application. An exhaustive study by Microfinite Element Modeling about the regulation of scaffold mechanical properties by pores architecture can be read in the publication by Alberich-Bayarri [169].

When the porogen template method is used to obtain macroporous scaffolds of rubbery networks as PEA with quite large pores diameters, the porous structure tends to collapse during the removal of the porogen spheres. A systematic increase of the network crosslinking degree demonstrated to be appropriate for keeping pores open after porogen removal [170]. Pore collapse has been recently used to develop macroporous thin membranes for cell transplant used in cornea regeneration [171]. This is not the case of our scaffolds, which retained the open structure when drying (**Figure 4.10**, **Figure 4.11** and **Figure 4.12**). Impregnating sphere templates by liquid monomers and their subsequent polymerisation has been an excellent method for the manufacture of acrylic polymer scaffolds with good response in the culture of different cell lines [172].

The polymerisation method in the presence of templates is versatile and enables scaffolds with different geometries of the pores to be developed; in the form of channels using porogens [173] of aligned polymeric fibres or in the shape of cross-channels by using sintered polymer fabrics [174], both with good results in animal models in rat brains [175]. These templates also allow for the synthesis of scaffolds of acrylate hybrid nanocomposites reinforced by silica networks, with great promise in bone regeneration, as they have an improved bioactivity [176].

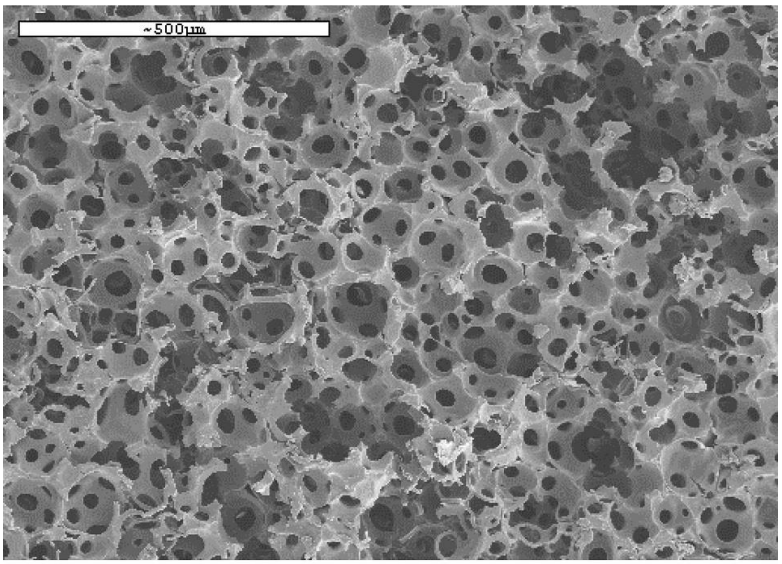

(a)

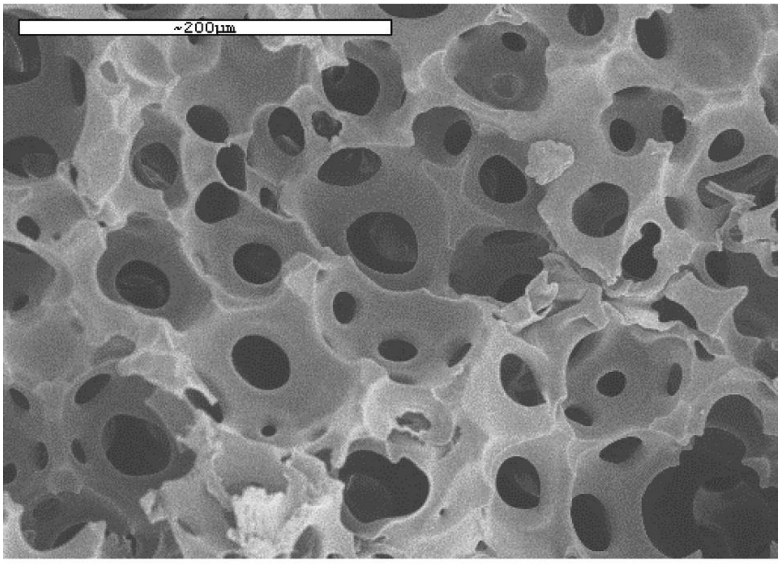

(b)

Figure 4.10 SEM micrographs of hydrophobic PEA scaffolds at different magnifications

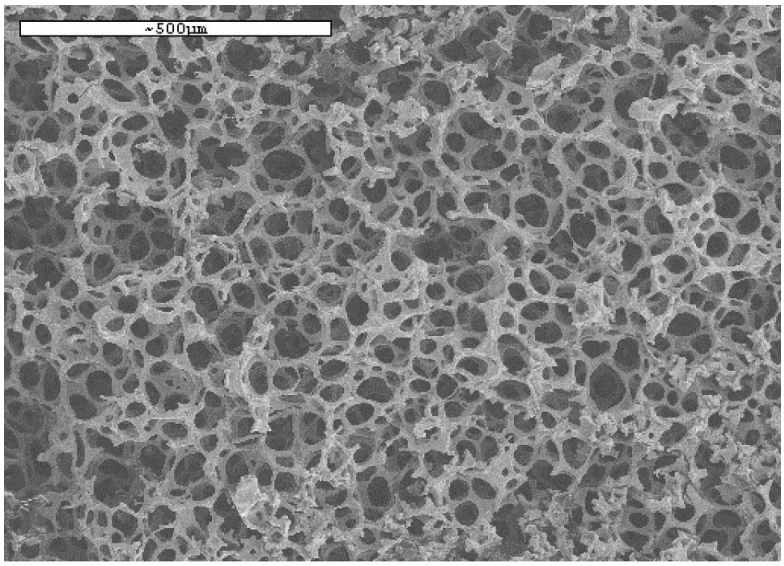

(a)

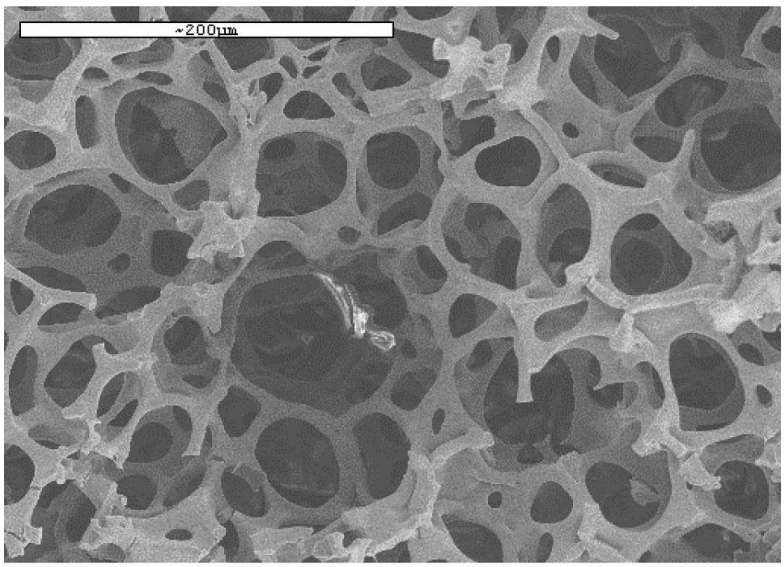

(b)

Figure 4.11 SEM micrographs of P(EA-co-HEMA) copolymer scaffolds (30% HEMA) at different magnifications

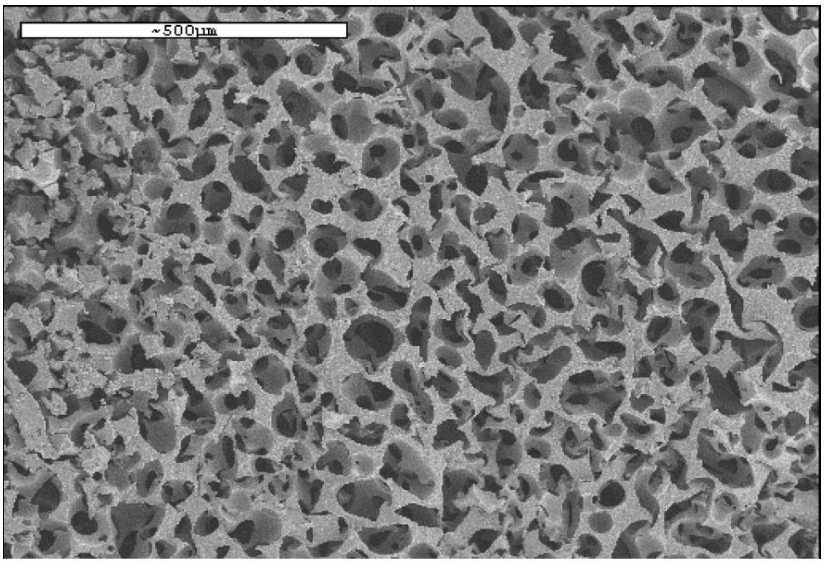

(a)

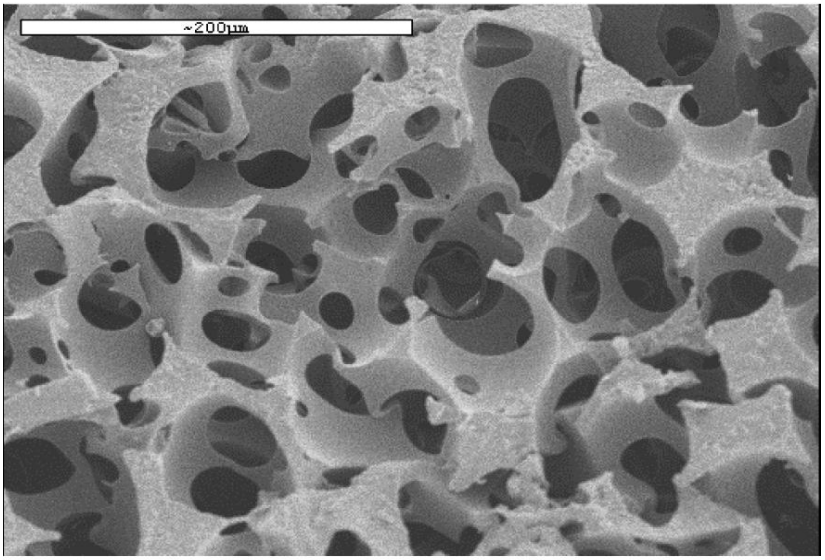

(b)

Figure 4.12 SEM micrographs of hydrophilic PHEMA scaffolds at different magnifications

Porosity of the scaffolds is shown in **Table 4.3** and was calculated as described in chapter **3.**

Table 4.3 Density, porosity and EWC of the bulk-copolymerised systems and of the scaffolds[a]

Copolymer composition	Bulk density (g/cm^3)	w^*	w^*_s	Porosity (%)
PEA	1.13	0.007	2.25	78±2
P(EA-co-HEMA) 70/30 wt%	1.17	0.06	2.50	83±2
P(EA-co-HEMA) 50/50 wt%	1.18	0.13	2.80	81±1
P(EA-co-HEMA) 30/70 wt%	1.19	0.19	3.30	76±3
PHEMA	1.21	0.35	4.50	75±2

[a] EWC w^* (the mass of water absorbed in equilibrium by the polymer divided by the mass of the dry polymer) of the bulk-copolymerised systems and of the scaffolds w^*_s. The porosity of the scaffolds with different compositions is shown in the last column.

Volume fraction of pores is around 80%, independent of the chemical composition of the material, *i.e.* while keeping the same percentage of pores, the hydrophilic/hydrophobic ratio of the material of the scaffold can be changed in the whole range. Such a high porosity is reflected in the lowering of the mechanical properties of the porous systems when compared with those of the same bulk material [169]. Dynamic mechanical spectroscopy (DMS) of the copolymers scaffolds compared with those obtained in the bulk copolymerised systems shows that the rubbery modulus is much lower in the porous systems (**Figure 4.13(a)**). In addition, since the rubbery modulus depends very closely on the geometric architecture of the porous solid [177], the fact that the same reduction with respect to the bulk is obtained for different copolymer compositions of the scaffolds supports the hypothesis that the same pore distribution and interconnectivity is obtained for the different copolymer compositions.

From a more fundamental point of view, it is noteworthy that the main relaxation of the material polymerised in presence of the PMMA template shows a broader relaxation than the corresponding bulk polymer. The effect is also independent of composition and takes place in both pure systems (PEA, PHEMA) and copolymers (**Figure 4.13**). This broadening suggests a different molecular architecture of the porous material from that of the bulk polymer, and must be related to the much higher surface to volume ratio in the material polymerised in the free spaces of the template. In general, the surface free energy contribution to the modulus is non-negligible in materials with high porosity. This contribution alone can account for differences in the mechanical properties of porous and bulky samples of the same material composition.

Additionally, in this case one should also take into account that the material in the immediate vicinity of the pore surfaces has been polymerised out of monomer units that might have penetrated to some extent the PMMA spheres. Thus, the surface layer of the matrix network may have a different structure from the network in the bulk region of the material. These facts would broaden the dynamics of the system and the regions of the material capable of undergoing cooperative motions shows a broader distribution of sizes, which results in a broader relaxation process.

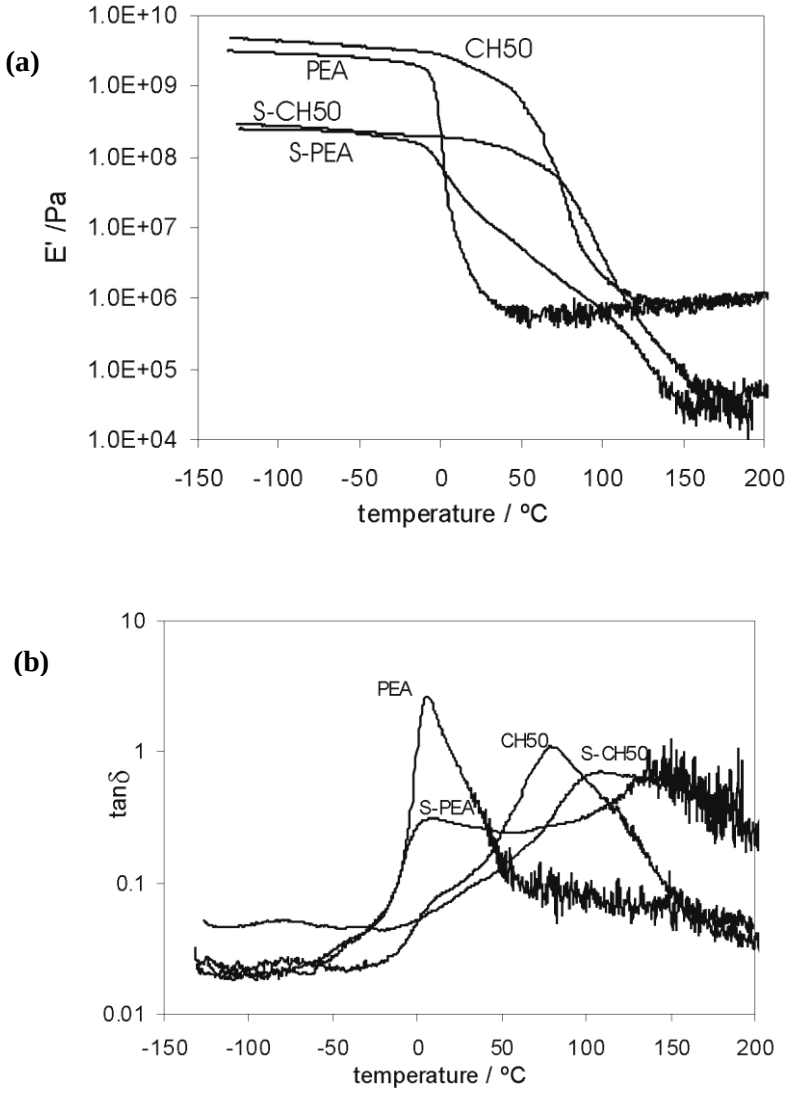

Figure 4.13 Dynamic-mechanical relaxation and mechanical loss tangent of polymers

Dynamic-mechanical relaxation spectra of bulk (PEA) and porous (S-PEA) PEA and the copolymerised systems with 50% HEMA (bulk CH50, scaffold S-CH50) measured at 1Hz.
(a) Storage modulus (E') as a function of temperature. **(b)** Mechanical loss tangent (tanδ) as a function of temperature.

4.2.1.2 Modified-caprolactone scaffolds with varying hydrophilicity and porosity

- **P(CLMA-co-HEA)**

Pore structure of P(CLMA-co-HEA) scaffolds is the same in all the scaffolds, independent of the chemical composition of the material (see **Figure 4.14**). Porosity is 77±3% and mean diameter of pores around 100 µm. Both PCLMA and PHEA are amorphous polymers with glass transition temperatures, T_g, below room temperature as shown in **Table 4.4**. The T_g of the copolymer networks is between those of the homopolymers. Thus, all the copolymers behave as elastomers at the temperature of the cell culture even if they are in the dry state. On the other hand, the equilibrium water content of the samples immersed in water at 37ºC or in culture medium rapidly increases with increasing content of HEA. Values range from that of PCLMA which is 10% (measured on dry basis) typical of hydrophobic materials up to around 370% for the hydrophilic PHEA homopolymer network. Thus, all the copolymer sponges are soft and deform easily when swollen in water or in culture medium. More details about the physical behaviour of P(CLMA-co-HEA) copolymers can be obtained from references [129] and [178].

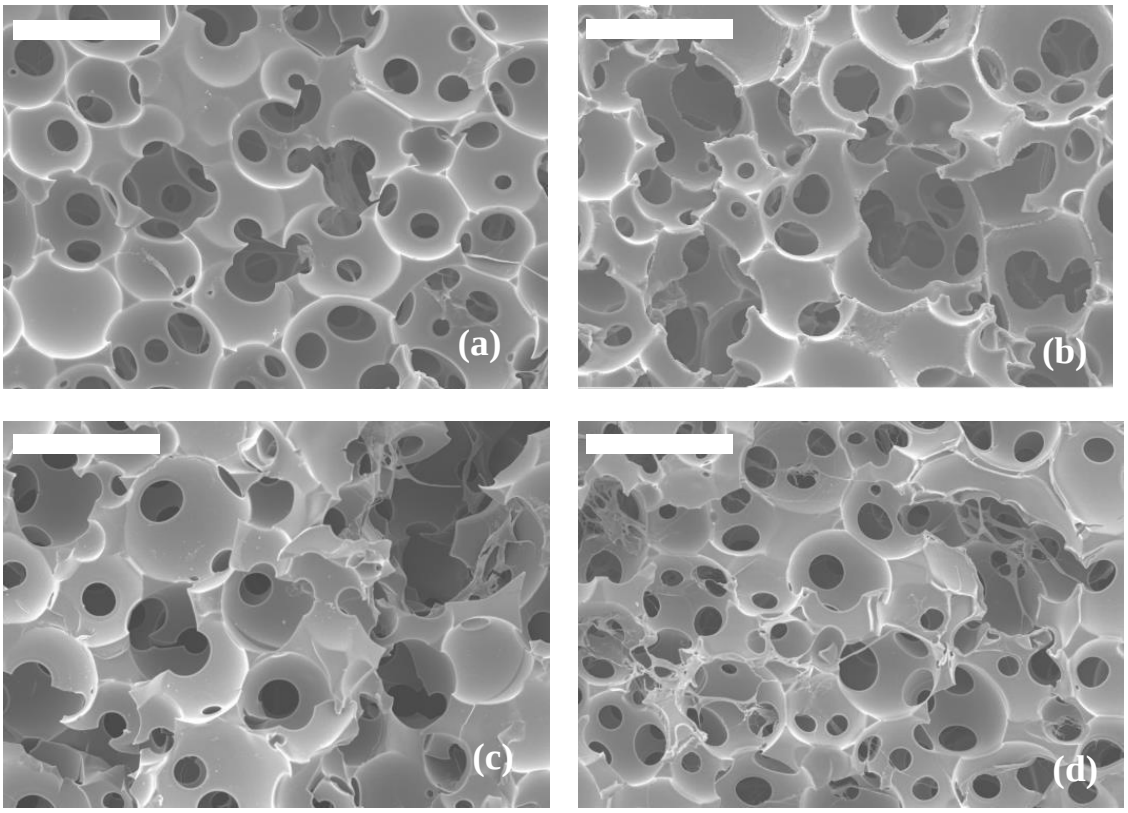

Figure 4.14 SEM micrographs of caprolactone-based scaffolds
(a) PCLMA, **(b)** P(CLMA-co-HEA) 70/30, **(c)** P(CLMA-co-HEA) 50/50, **(d)** P(CLMA-co-HEA) 30/70. Dimension bar 100 µm.

Table 4.4 Composition of the feeding mixture, glass transition temperatures and apparent diffusion coefficients

Sample	HEA (wt %)	T_g (ºC)	$D_{ap} \times 10^7$ (cm^2/s)
PCLMA	0	-13.6	2.34
P(CLMA-co-HEA) 70/30	30	-5.7	3.57
P(CLMA-co-HEA) 50/50	50	-3.1	4.69
P(CLMA-co-HEA) 30/70	70	3.1	4.86
PHEA	100	9	8.39

- **PCL**

When the starting material for developing scaffolds is not a monomer, but a polymer, it is also possible to employ templates of sintered spheres for the manufacture of these scaffolds, but the method gets complicated because the polymer must permeate the template molten and its high viscosity makes the process difficult. Such has been the case of PCL scaffolds presented below [179], where a high pressure has been employed to facilitate the penetration of the molten PCL in the template, or similar PCL scaffolds where the polymer has been injected with the help of a vacuum [119].

The pore architecture of PCL scaffolds of different porosity can be seen in **Figure 4.15**. In PCL scaffolds, the porosity was varied by changing the compression ratio when sintering the porogen particles in the preparation of the template. Pore interconnectivity increases with scaffold porosity. The structure of the PCL 85 scaffold can be observed in detail in **Figure 4.24** (in section **4.4.1.1**).

Since the porogen particles were identical for all samples, the pore size, that is, the diameter of the spherical cavities is the same in all the series. That is to say, higher porosity is achieved by increasing the compression ratio, which leads to larger pore throats and higher interconnectivity. The porosity of the PCL scaffolds (volume fraction of pores) was 60±2%, 70±2%, and 85±2% for PCL60, PCL70, and PCL85 respectively.

Polycaprolactone is a semicrystalline polymer with a melting temperature around 60ºC and glass transition temperature around -60ºC. So in spite of the high porosity, these scaffolds are rather stiff materials.

Their compression modulus measured in stress–strain compressive tests with dry samples ranged from 0.6 MPa for the most porous to 8.1 MPa for the scaffold with 60% porosity [179]. All produced scaffolds were homogeneous with well-interconnected pores, nevertheless the mean size of the throats between pores in PCL60 is quite small, 38±9 μm in average, whereas in

PCL70 and PCL85 (**Figure 4.15**) pore throats are larger with mean values 52±13 and 80±25 μm, respectively.

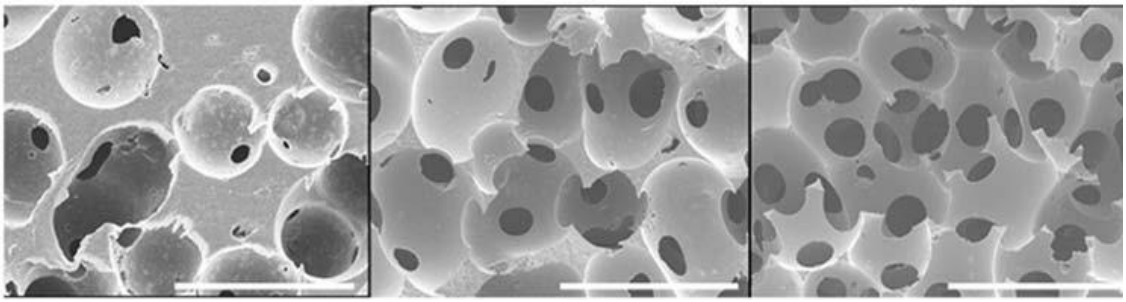

Figure 4.15 SEM microphotographs of PCL scaffolds

SEM microphotographs of PCL60 (left), PCL 70 (center), and PCL85 (right) scaffolds. Dimension bar 300 μm.

This manufacturing process can be simplified by the technique of "freeze gelation", in which the polymer is mixed with the spherical porogen in solution (and not in a molten state). By doing this, the process of preparation of the sintered template is avoided and in consequence, the manufacturing of scaffolds is simplified. Once the spheres have been mixed with the polymer solution, the structure is frozen and the crystals remaining in the polymer solvent are cold removed for subsequently hot removal of the spherical porogen, saving the polymer that will form the scaffold from dissolving. In this way, dual porosity scaffolds are obtained, macropores of the size of the spheres with microporous wall, pores which are the same size as the crystals produced by freezing the solvent. This procedure has been applied in the case of PLA and PCL [180-182] or in the case of chitosan through cold gelation in the presence of porogen [183]. The porosity can be regulated by the amount of spheres with respect to the mass of polymer solution and by the concentration of the polymer solution.

4.2.1.3 Cell seeding in porogen template scaffolds

Cell seeding in 3D scaffold highly depends on pore connectivity. The scaffolds developed in this work are really versatile with respect to pore shape, pore size and the size of pore throats. This procedure of scaffold fabrication allows a variety of porogen particles to be used and to graduate sintering. For cell culture testing, a cell suspension was injected into the core of the macroporous scaffold using a Hamilton syringe. The flow of the cell suspension through the tortuous path from the center of the scaffold piece to its borders allows cells to attach to the pore walls and remain inside the sample. To test that, several preliminary experiments were conducted just to check cell distribution inside the scaffold. **Figure 4.16** shows a cross section of the P(EA-co-HEA) 50/50 scaffold into which a chondrocyte suspension was injected. Cells

were cultured for 14 days in culture medium containing FBS. The cross section of the sample was stained with DAPI to observe the cell nuclei. Due to the autofluorescence of the material or the florescence produced by the absorption of DAPI by the material, the shape of the pores can be clearly observed, and show that the cells attach to the pore walls and are well distributed throughout the sample.

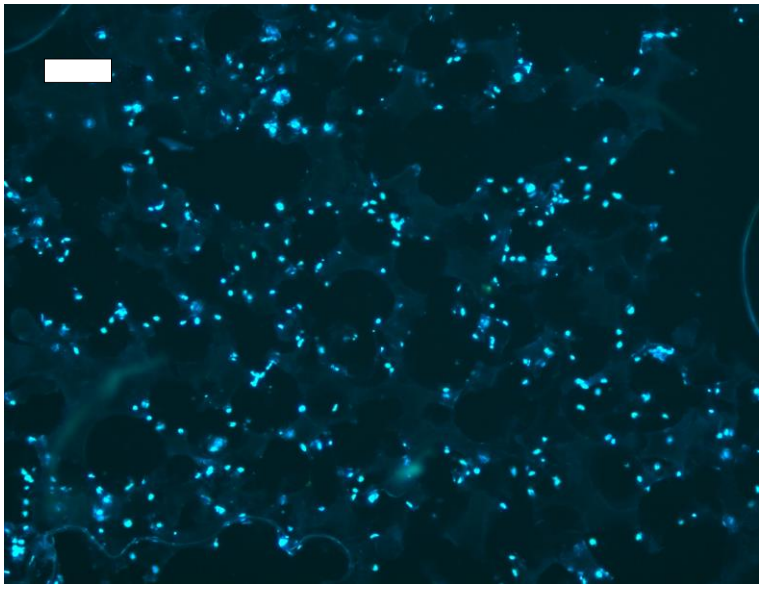

Figure 4.16 Confocal microscopic image of the cross section of the P(EA-co-HEA) 50/50 scaffold
A chondrocyte suspension was injected into the scaffold and cultured for 14 days. DAPI staining in blue. Dimension scale 100 μm

Nevertheless, cell distribution was not always uniform, especially when the pores' size and the size of the interconnection throats are smaller than 100μm. Thus, it is frequent to find situations in which chondrocytes appear close to the surface. **Figure 4.17** shows the superposition of a fluorescence image of the cross-section with the cell nuclei in red and an image of light microscopy obtained simultaneously to show the pores' structure. In this structure, cells could not invade the porous structure due to the small dimension of pores and interconnection throats.

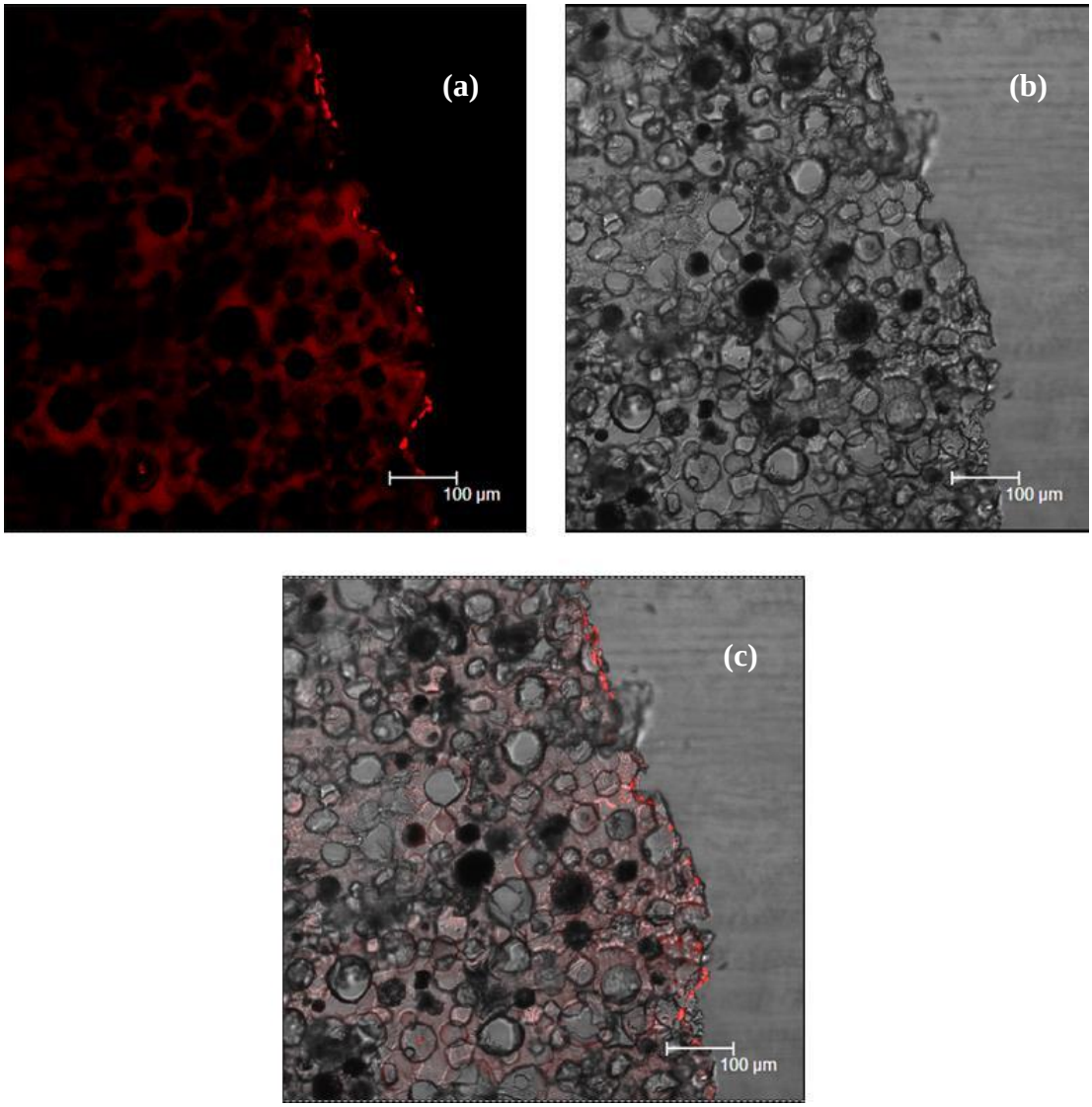

Figure 4.17 Microscopy pictures of a cross-section of a P(EA-co-HEA) 50/50 scaffold with small pore size.

(a) Fluorescence image of the cross-section showing the cell nuclei in red, **(b)** image of light microscopy of the same cross-section and **(c)** combination picture of (a) and (b). Chondrocytes cultured for 28 days.

4.2.2 Conclusions

A methodology that makes it possible to obtain scaffolds with a pore architecture consisting of spherical interconnected pores was applied. Pore size and pore connectivity depends mainly on the template produced by sintering porogen microspheres with thermal and mechanical treatments. Interestingly, in this way one can compare the effect of the scaffolding material composition without changing the pore architecture. For this study in particular, we were interested in the effect of hydrophilicity on cell response in 3D environments. Highly periodic and regular pore architectures can be obtained in this way. The mechanical behaviour of the porous samples is significantly different from that of the bulky material of the same

composition: not only is the modulus lower, but there are also indications of a distinct relaxational behaviour due to the effect of the surface layer. The template technique allows PCL scaffolds to be manufactured from a commercial PCL by introducing molten polymer into the free volume of the template with the aid of a pressure gradient. Pore size and interconnectivity is sufficient to allow for cell seeding by injection in the centre of the scaffold sample of a cell suspension.

4.3 A POROUS PCL SCAFFOLD PROMOTES HUMAN CHONDROCYTES REDIFFERENTIATION AND HYALINE-SPECIFIC EXTRACELLULAR MATRIX PROTEIN SYNTHESIS.

This chapter is based on the work by N. Garcia-Giralt, R. Izquierdo, X. Nogués, M. Perez-Olmedilla, P. Benito, J. L. Gómez-Ribelles, M.A. Checa, J. Suay, E. Caceres, J.C. Monllau. *A porous PCL scaffold promotes the human chondrocytes redifferentiation and hyaline-specific extracellular matrix protein synthesis*. Journal of Biomedical Materials Research. Part A 85A, 1082-1089 (2008).

4.3.1 Results

4.3.1.1 Mature chondrocyte redifferentiation

The aim of study was to assess chondrogenic function in 3D scaffolds of human mature chondrocytes previously expanded in monolayer. The purpose was to test a strategy for articular cartilage regeneration with TE techniques as close as possible to the clinical practice. In this sense, cell sources selected were mature chondrocytes of which there is broad clinical experience and the scaffold selected was made of PCL. PCL was selected for being a semi-crystalline material with good mechanical properties and degradation rate slower than other polyesters [116]. Because of the mechanical and degradation properties of PCL [117], it can be used for long-term *in vitro* cell culture before implantation into the injury site. The scaffold would thus maintain its architectural integrity and mechanical properties during the preimplantation period while chondrocytes are both redifferentiating and synthesising new cartilage matrix. Section **4.2** has shown that the pore architecture of these scaffolds favours cell seeding with a quite simple technique; by direct injection of the cell suspension in the centre of the scaffold piece.

Chondrocyte expansion in monolayer cultures before seeding the scaffold induces the loss of the chondrocytic phenotype. Redifferentiation is achieved by subsequently seeding the dedifferentiated chondrocytes in a 3D environment [184, 185]. In this section we analyse the cell functionality of previously expanded human chondrocytes by culturing in the PCL scaffolds in the adequate chondrogenic medium. This step would thus be previous to implantation in the cartilage defect of the patient in order to implant chondrocytes with a phenotype as close as possible to that of the hyaline cartilage.

Mature hyaline cartilage chondrocytes are characterised by their spherical cell morphology as well as expression of the genes for type II collagen and aggrecan. The response of chondrocytes in our scaffolds will therefore be evaluated for biological parameters including *in vitro* cell attachment, proliferation, gene expression, and matrix deposition. We have previously described the physical properties of the porous 3D PCL structure, in which the pores are fully connected throughout the foam structure after the filler material has been leached (see section **4.2** and references [119, 179] as well). The resulting motif of the scaffolds used in this section consists of spherical cavities having a mean size of 130 ± 25 μm, with the same shapes as the original filler porogen beads, and linked to each other by circular throats. The porosity of the scaffolds was 70% [119]. The scaffold has a high surface area to volume ratio, which provides a favourable environment for high-density accommodation of chondrocytes, similar to that in pellet cultures.

Human chondrocytes were isolated from osteoarthritic knee joints as explained in section **3.3.1**, they were cultured in monolayer after one or two passages and a cell suspension was injected in the centre of the scaffolds, fabricated according to the procedure described in section **3.1.2.3**.

4.3.1.2 Cell culture and phenotype characterisation

The proliferation and differentiation of human chondrocytes cultured in PCL scaffolds were characterised for determining the suitability of this biomaterial for cartilage regeneration.

To assess the ability of porous PCL scaffolds to promote chondrogenic redifferentiation, the expression levels of cartilage-associated genes at days 7, 14 and 28 were analysed and compared to cells cultured in monolayer and pellet (controls). All experiments were performed in medium with FBS (FBS-containing medium:FCM) or without FBS and supplemented with 1% ITS (ITS-containing medium: ICM). Both mediums were supplemented with 50 μg/ml ascorbic acid. Expression of the type II collagen (*COL2A1*) and aggrecan genes was assessed by real-time PCR.

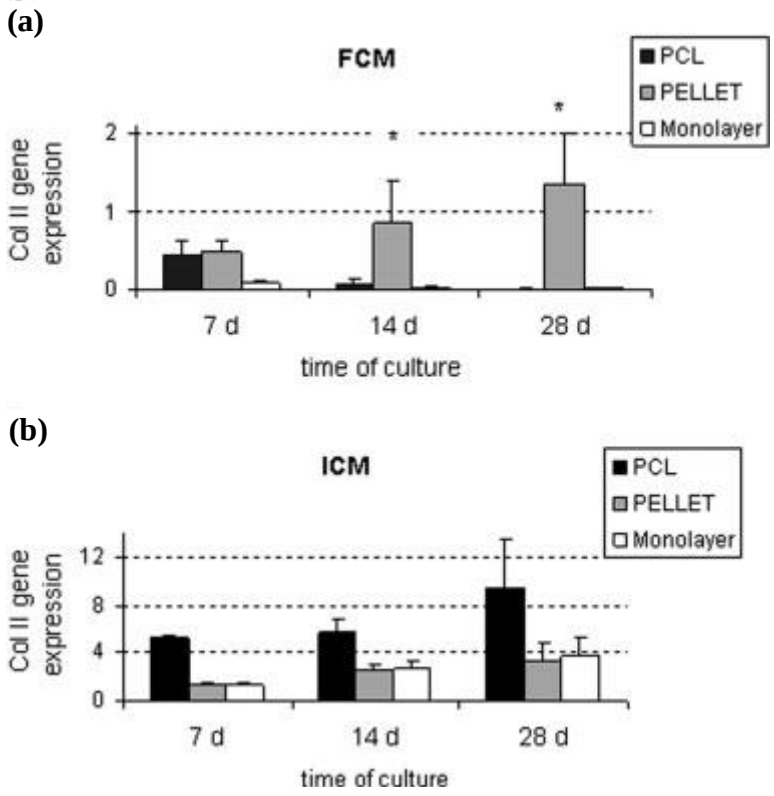

Figure 4.18 Relative quantification of the expression of the type II collagen gene

The specimens were cultured with **(a)** FBS-containing medium (FCM) and ascorbate, or **(b)** ITS-containing medium (ICM) and ascorbate. Note that the *y*-axis has a different scale in each figure. (*) Significant differences among culture systems were found ($p < 0.05$).

Expression of the type II collagen gene was higher ($p<0.05$) in all ICM culture systems than in all FCM culture systems at all times of measurement (**Figure 4.18**). In FCM cultures, only the pellet systems induced redifferentiation during the cell culture period (**Figure 4.18(a)**). The worst result was found in monolayer cultures, and the expression of the type II collagen gene was null in both PCL and monolayer cultures at 28 days.

In contrast, in ICM cultures (**Figure 4.18(b)**), the PCL scaffolds had higher increases in expression of the type II collagen gene than did the pellet and monolayer cultures, which behaved similarly at all times. This result indicates that PCL scaffolds induced chondrocyte redifferentiation more efficiently than did the pellet and monolayer cultures in ICM cultures (**Figure 4.18(b)**).

Expression of the aggrecan gene did not differ between ICM and FCM cultures for both PCL and pellet cultures (**Figure 4.19**), although PCL cultures had half the expression levels than pellet cultures. For ICM cultures, monolayer cultures always showed significantly higher expression levels than PCL or pellet systems (**Figure 4.19(b)**). The relative gene expression

levels in both culture media for the three systems (monolayer > pellet > PCL) were constant at all times of measurement.

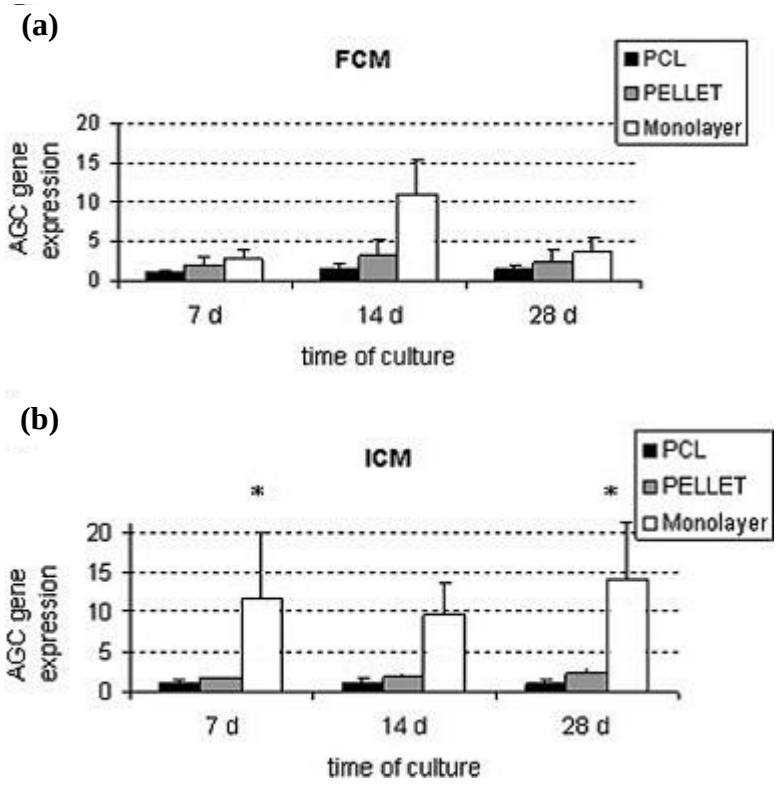

Figure 4.19 Relative quantification of the expression of the aggrecan gene

The specimens were cultured with **(a)** FCM or **(b)** ICM. (*****) Significant differences among culture systems were found ($p < 0.05$).

To assess the proliferation of cells cultured in PCL scaffolds and in pellets, Ki-67 detection was used at 7, 14 and 28 days of culture in FCM and in ICM (**Figure 4.20**). Results showed low proliferation in FCM for both specimens and very reduced proliferation was detected in ICM at any time.

Chondrocytic differentiation was evaluated using S-100 immuno detection (**Figure 4.21**). All cultures tested positive at all times of analysis. The PCL chondrocytes were round and formed aggregates within the scaffold pores. The pellet chondrocytes were similar in appearance.

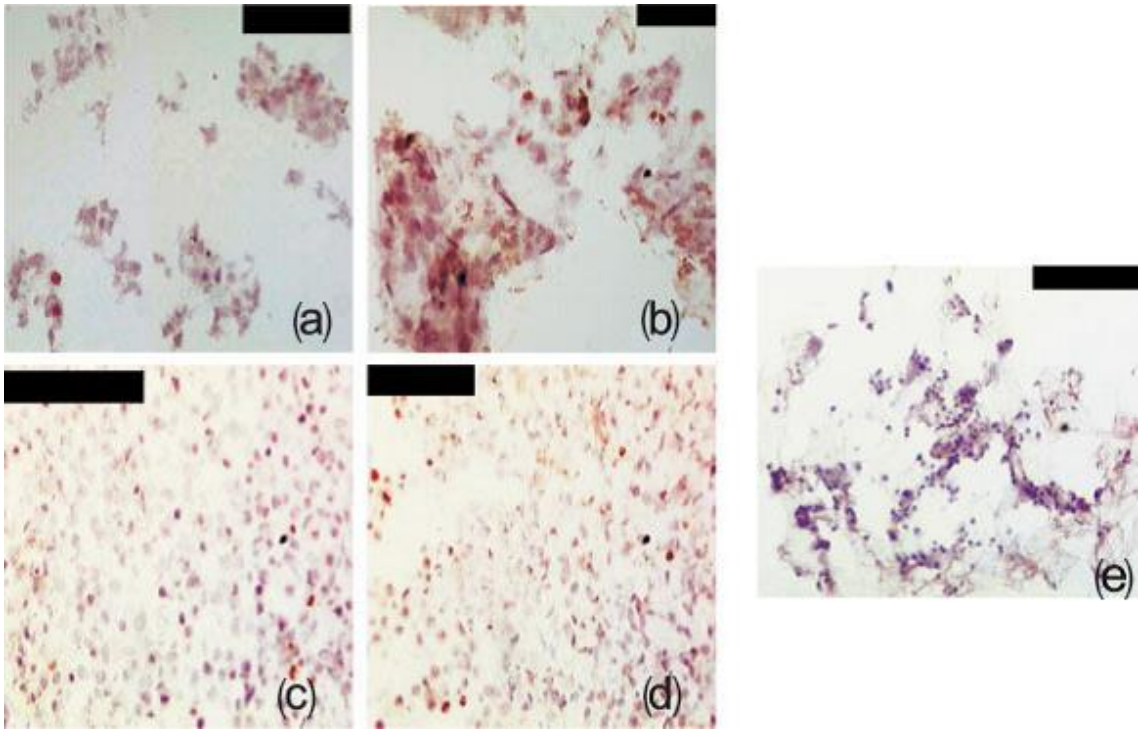

Figure 4.20 Immunohistochemical staining of Ki-67

Immunohistochemical staining of Ki-67 was performed on sections of human chondrocytes cultured into PCL scaffolds (**(a)** and **(b))** or in pellet (**(c)** and **(d))**. Specimens were cultured in FBS-containing medium (FCM) at 7 (**(a)** and **(c))** and 28 days (**(b)** and **(d))** of culture or ITS-containing medium (ICM) at 14 days **(e)** of culture. Bar scale is 50 µm.

In addition to gene expression quantification, synthesis of type II collagen protein and glycosaminglycans (GAG) deposition were also analysed inside the scaffold pores. Type II collagen was assessed by immunohistochemistry using a specific antibody (**Figure 4.22**), and GAG was assessed by Alcian blue staining (**Figure 4.23**).

Specimens were cultured in FCM or ICM and were analysed at 7, 14 and 28 days post-seeding.

Figure 4.22 and **Figure 4.23** show histological sections at 7 and 28 days of culture. Protein synthesis and deposition within scaffold pores were found to be similar between FCM and ICM cultures. Similar results were obtained at 14 days. Moreover, the amount of synthesised matrix in the scaffold was comparable to that in pellet cultures (used as 3D positive control).

4.3.2 Discussion

The cartilage engineering strategy planned in this study consists of extracting chondrocytes from minimal donor cartilage by enzymatic digestion, allowing for the construction of autologous transplant grafts. The free cells obtained are grown *in vitro* to a desired population level and then seeded in a scaffold, which in turn is transplanted into the defect site to restore

normal function. The most favourable scaffold materials are biodegradable synthetic polymers, which offer a controllable degradation rate, high reproducibility, and are readily fabricated to obtain specific shapes and pore sizes.

This study expands upon previous work in which a porous PCL scaffold was designed and tested for human chondrocyte adhesion and viability [119]. In the present study, this PCL scaffold was evaluated for cell proliferation and the synthesis of hyaline cartilage specific ECM proteins. Pellet cultures were used as a positive control for chondrocyte redifferentiation. Currently, the most common method for promoting *in vitro* chondrogenesis of mesenchymal stem cells is to maintain them as a high-density pellet culture [187].

Pellets are formed by centrifugation, which compresses the cells into a high density environment to promote cell-cell interaction, mimicking the cellular condensation observed in precartilage during embryonic limb bud development [188].

Monolayer cultures were used as a negative control for chondrocyte differentiation, and as a positive control for proliferation. Numerous cells can be quickly generated with monolayer cultures. However, chondrocytes cultured in monolayers tend to dedifferentiate due to cytoskeletal modifications resulting from the 2D culture environment.

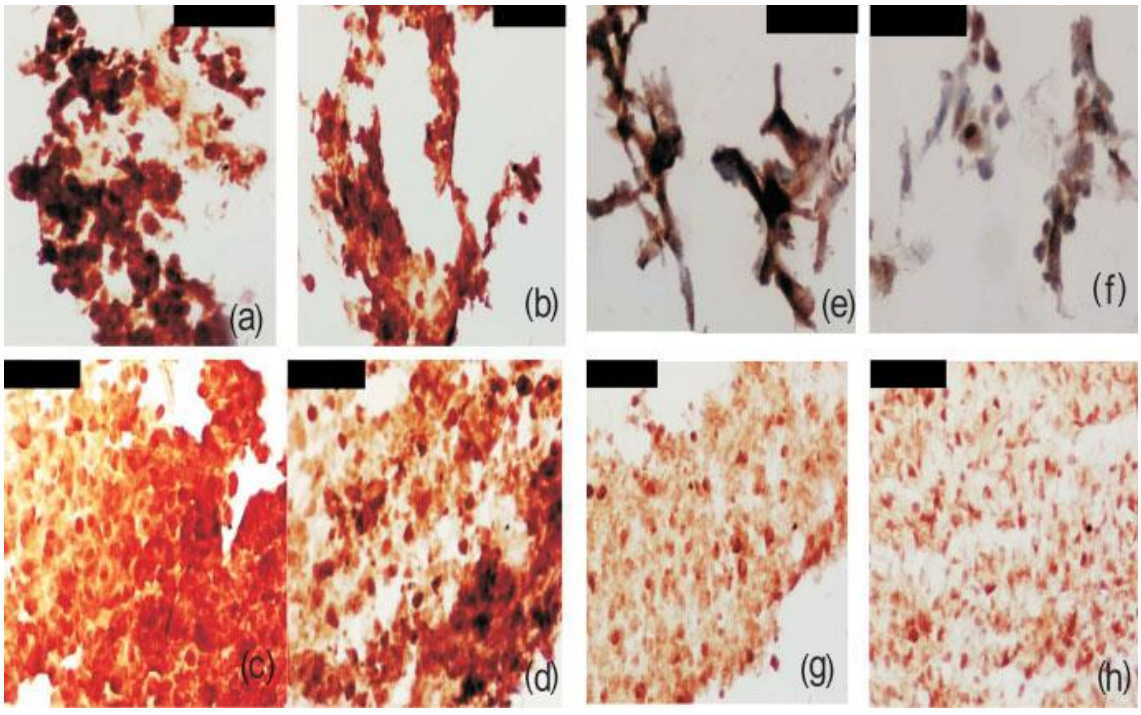

Figure 4.21 S-100 Immunohistochemical staining

Sections of sections of human chondrocytes cultured in PCL scaffolds (**(a)**, **(b)**, **(e)**, and **(f)**) or in pellets (**(c)**, **(d)**, **(g)**, and **(h)**). Specimens were cultured in FCM and ascorbate at 7 (**(a)** and **(c)**) and 28 days (**(b)** and **(d)**) of culture or in ICM and ascorbate at 7 (**(e)** and **(g)**) and 28 days (**(f)** and **(h)**) of culture. Bar scale is 50 µm.

Cell redifferentiation and chondrocyte functionality is usually characterised by production of tissue-specific ECM proteins. In this study, production of cartilage-specific ECM proteins were evaluated at gene transcriptional level and at protein synthesis level. A positive correlation between these two levels was usually found in previous studies [121].

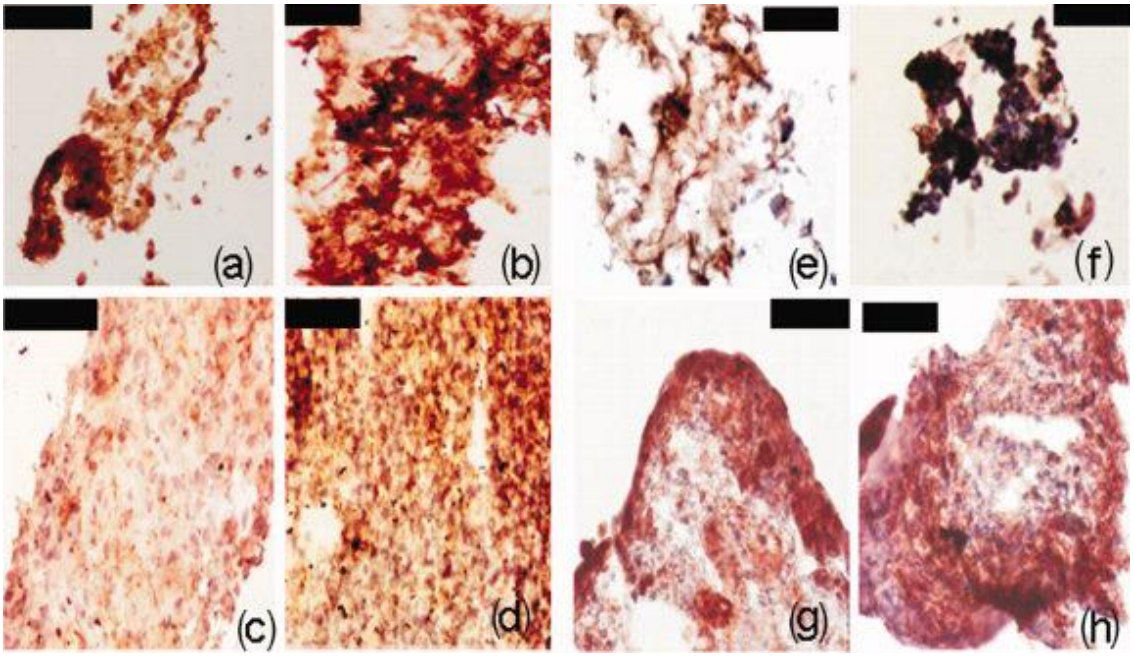

Figure 4.22 Type II collagen immunohistochemical staining

Sections of sections of human chondrocytes cultured in PCL scaffolds (**(a)**, **(b)**, **(e)**, and **(f)**) or in pellets (**(c)**, **(d)**, **(g)** and **(h)**). Specimens were cultured in FCM and ascorbate at 7 (**(a)** and **(c)**) and 28 days (**(b)** and **(d)**) of culture or in ICM and ascorbate at 7 (**(e)** and **(g)**) and 28 days (**(f)** and **(h)**) of culture. Bar scale is 50 µm.

These results highlight that a 3D environment can significantly improve the redifferentiation capacity of human chondrocytes. However, for cultures grown in FCM, chondrocytes could only redifferentiate in a pellet culture system, as determined by measurements of type II collagen gene expression. Alternatively, all culture systems could redifferentiate when grown in ICM, wherein the greatest redifferentiation was found for PCL cultures. Although pellet cultures grown in FCM showed increases in the expression of the type II collagen gene, much higher increases were observed for those grown in ICM, suggesting that expression is enhanced by the absence of FBS and its substitution by ITS.

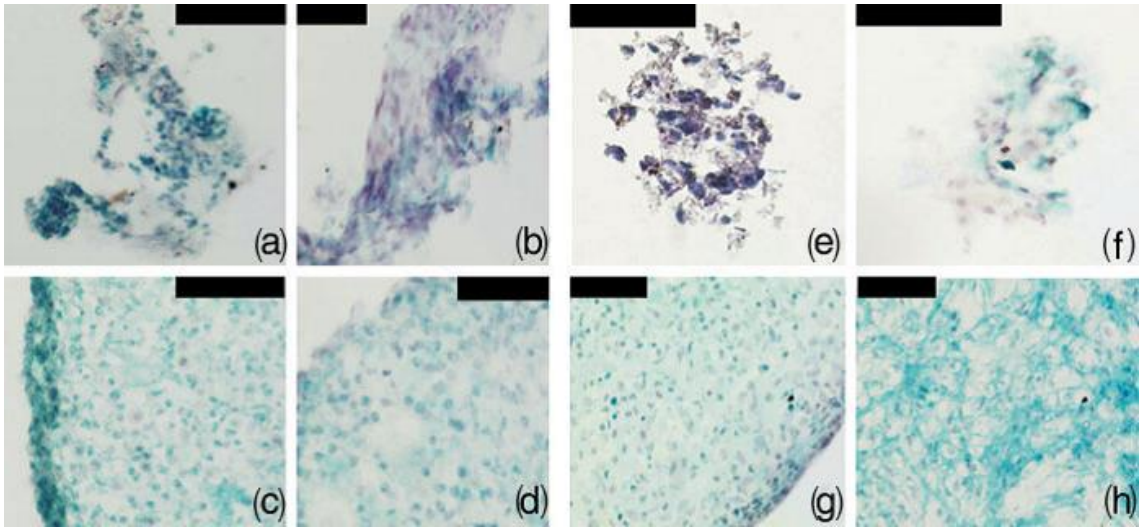

Figure 4.23 Alcian blue stained and hematoxylin counterstained histological sections

Sections of human chondrocytes cultured in PCL scaffolds (**(a)**,**(b)**, **(e)** and **(f)**) or in pellets **((c)**, **(d)**, **(g)** and **(h)**). Specimens were cultured in FCM and ascorbate (**(a)**, **(b)**, **(c) and (d)**) or ICM and ascorbate (**(e)**, **(f)**, **(g) and (h)**), and GAGs were analysed at 7 (**(a)**, **(c)**, **(e)** and **(g)**) and 28 days (**(b)**, **(d)**, **(f)** and **(h)**) of culture. Bar scale is 50 μm.

Despite the gradual disappearance of *COL2A1* gene expression in PCL-cultured cells over time grown in FCM at 28 days post-seeding, it was observed by immunodetection that type II collagen accumulated in the scaffolds' pores. This suggests that whatever small amount of type II collagen mRNA was translated into protein early on then this protein was in turn deposited into the pores, which remains throughout the culture period.

Since immunohistochemistry is not quantitative, it makes it difficult to determine which culture system or medium provided the most efficient synthesis of cartilage ECM proteins. Only gene expression could be quantified at each time of measurement. Therefore it can be hypothesised that among the experimental conditions tested, PCL scaffolds cultured in ICM provided the best support for chondrocytes.

The expression of the aggrecan gene did not differ significantly among the FCM cultures, although the maximum gene expression was found in monolayer cultures, and pellet cultures had twice the level of aggrecan expression than did PCL cultures.

The levels of aggrecan gene in ICM cultures were similar to those in the FCM cultures, but the monolayer cultures had significantly higher levels than did the three-dimensional cultures. Interestingly, aggrecan gene expression was independent of culture medium for PCL and pellet cultures. This result is in concordance with the fact that no differences in the levels of GAG deposited in the PCL scaffold pores were found by histological staining between cultures grown in FCM and those grown in ICM at 28 days culture.

Monolayer cultures had significantly higher levels of aggrecan expression than did the 3D cultures. These results are corroborated by the findings of Grunder *et al*. [189], who studied cells cultured for two weeks in FCM. The authors found that type II collagen transcription was higher in cells embedded in alginate beads than in cells grown in a monolayer. In contrast, they did not observe any difference in expression of the aggrecan gene among the culture systems. Lastly, they found that cells embedded in alginate beads had a very low rate of proliferation.

The gene expression results show that by culturing the monolayer-expanded chondrocytes in PCL scaffolds in ICM, chondrocytes can redifferentiate by increasing their production of type II collagen. These results agree with those of previous studies using human chondrocytes encapsulated in alginate beads in ICM [190].

Serum (FBS) is a complex supplement containing growth factors, hormones, enzyme inhibitors, etc. Although the major constituents of serum are known such as albumin and transferrin, the exact composition and their effect on cell growth and physiology have not been determined. Therefore, serum can contain several factors that may interfere with normal cellular functions, such as differentiation [191].

Using a serum free-medium chemically defined (ICM) allows the experiment parameters to be controlled more accurately. The studies of chondrocytes cultured in a 3D environment without FBS and ITS presence generally improved cell differentiation levels [115, 189, 192]. However, cell cultures in the defined serum free-medium show minimal proliferation activity because of the lack of mitogenic factors present in serum. In any case, human primary chondrocytes cultured in either PCL scaffolds or pellets in FCM do not have a high rate of proliferation but are not able to synthesise type II collagen in long-term cultures.

Homicz *et al*. [193] demonstrated that human chondrocytes divided more rapidly in monolayers than they did in alginate or biodegradable polymer scaffold forms. Tsai *et al*. [194] obtained similar results for chondrocytes cultured on PCL polymer films, which proliferated at a lower rate than did chondrocytes cultured on polystyrene plates. In this study, the chondrocytes were cultured with 10% FBS, and the authors observed the same pattern of expression of the type II collagen gene as the one in this thesis: the expression of type II collagen in PCL substrates that had been observed on day 7 had totally ceased by day 14.

Cells grown in PCL scaffolds are rounded and proliferate slowly. These results suggest that disperse monolayer cells proliferate, whereas rounded 3D cells differentiate. Therefore, the rounded chondrocytes of PCL and pellet cultures switch from a proliferative state to a non-proliferative state. This behaviour was observed for both FCM and ICM cultures. The study performed by Li *et al*. [195] suggests that the suppression of cellular proliferation in PCL

scaffolds and pellets that results from the use of serum-free medium and a high cell-density environment appears to favour mesenchymal chondrogenic differentiation.

Analysing the S-100 production, the chondrocytic phenotype remains after 28 days post-seeding in both FCM and ICM cultures, but the expression of the type II collagen gene was particularly striking in ICM cultures, thus demonstrating that the PCL scaffolds are suitable for chondrocyte culture in serum-free medium conditions.

It is worth noting that this research line has been continued in the CBIT and IMIM- Hospital del Mar with experiments in a knee rabbit model, implanting PCL scaffolds like those shown in this study with very promising results [196, 197].

4.3.3 Conclusions

It has been demonstrated that chondrocytes seeded in PCL scaffolds and then cultured in medium supplemented with ITS and ascorbate efficiently maintained their differentiated phenotype and were able to synthesise cartilage-specific ECM proteins. Based on previous experiences, it was concluded that PCL scaffolds are not a good culture substrate for promoting chondrocyte proliferation, regardless of the growth medium used. Moreover, FCM leads to a loss in expression of the type II collagen gene that is not compensated by chondrocyte proliferation. Therefore, for *in vivo* implant studies, the use of monolayer-expanded chondrocytes cultured in an organised 3D scaffold using serum-free medium supplemented with ITS was proposed.

4.4 IN VITRO 3D CULTURE OF HUMAN CHONDROCYTES USING MODIFIED-CAPROLACTONE SCAFFOLDS WITH VARYING HYDROPHILICITY AND POROSITY

This chapter is based on the work by M. Pérez Olmedilla, M. Lebourg, J.L. Escobar Ivirico, I. Nebot, N. Garcia Giralt, G. Gallego Ferrer, J.M. Soria and J. L. Gómez Ribelles. *In vitro 3D culture of human chondrocytes using modified ε-caprolactone scaffolds with varying hydrophilicity and porosity*. Journal of Biomaterials Applications 27, 299-309 (2012).

In this section the role of cell-material interaction in the culture of human chondrocytes in macroporous scaffolds is explored. As in the previous section (**4.3**), in order to be close to possible clinical application, we concentrate on biodegradable PCL as base material, but we modified it by introducing hydrophilic poly(hydroxyethyl acrylate) blocks into the polymer chains, P(CLMA-co-HEA) copolymers. In this way, we were able to tune the hydrophylicity of the pore walls with which the cells are in contact. The preparation of materials is described in chapter **3** and more detailed information can be found in the other works of the CBIT [129, 198, 199]. Additionally, porosity and pore interconnectivity seems to be crucial for cell seeding and neo-formed tissue organisation. Thus, we explore the viability of chondrocytes cultured on PCL scaffolds with varying porosity.

4.4.1 Results and Discussion

4.4.1.1 Cell viability of chondrocytes into PCL and P(CLMA-co-HEA) scaffolds *in vitro*

Cell seeding into the scaffolds by injection of a cell suspension in the middle of the scaffold piece has proven to be effective for introducing chondrocytes into the pore structure [119, 200]. Nevertheless, a fraction of the cells adhered to the external surface.

Cells adhered to the surface of the scaffold behave as monolayer cultures in terms of shape and proliferation confluence. If the hydrophilicity of the scaffolds is not too high (as in PCL series or in P(CLMA-co-HEA) copolymers up to 30% HEA), after 28 days culture, the complete surface of the scaffold appears covered by a layer of cells and ECM (as seen in **Figure 4.24(a)** and **Figure 4.25(a)**).

In P(CLMA-co-HEA) 50/50 and 30/70, the cell layer could still be seen by SEM. However, the sample containing 70% HEA was partially covering the scaffold surface as shown in **Figure 4.26(a)**.

The behaviour of the cells inside the pores is different and the cross-sections of the scaffolds observed after 28 days culture show a much smaller cell density than that of the surface. Cells and ECM spread inside the spherical cavities, showing a large number of adhesion points to the pore walls as can be seen in **Figure 4.24(b)** and **Figure 4.24(c)** for PCL80 and in **Figure 4.25(b)** and **Figure 4.25(c)** for P(CLMA-co-HEA) 70/30. Some round cells could be seen bulging under a carpet of matrix. In most hydrophilic copolymers, the number of cells found in the pores of the scaffolds is very small, but their morphology resembles that of the hydrophobic polymers.

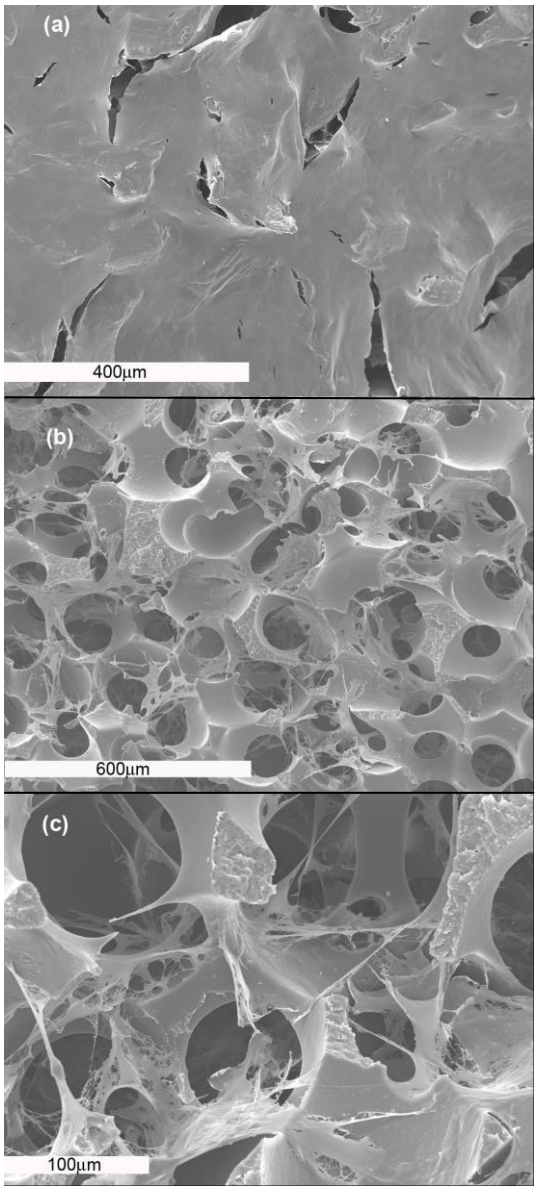

Figure 4.24 SEM pictures of the surface (a) **and cross sections** (b) **and** (c) **of 85% porosity PCL scaffold after 28 days culture**

The scaffolds are covered by a compact layer of cells and ECM. Inside, the cells seem to be uniformly distributed in the pore structure and adhere to the pore walls. The shape of the cells is characteristic of strong adhesion to the synthetic material. No cells with the rounded morphology characteristic of chondrocytes *in vivo* were observed.

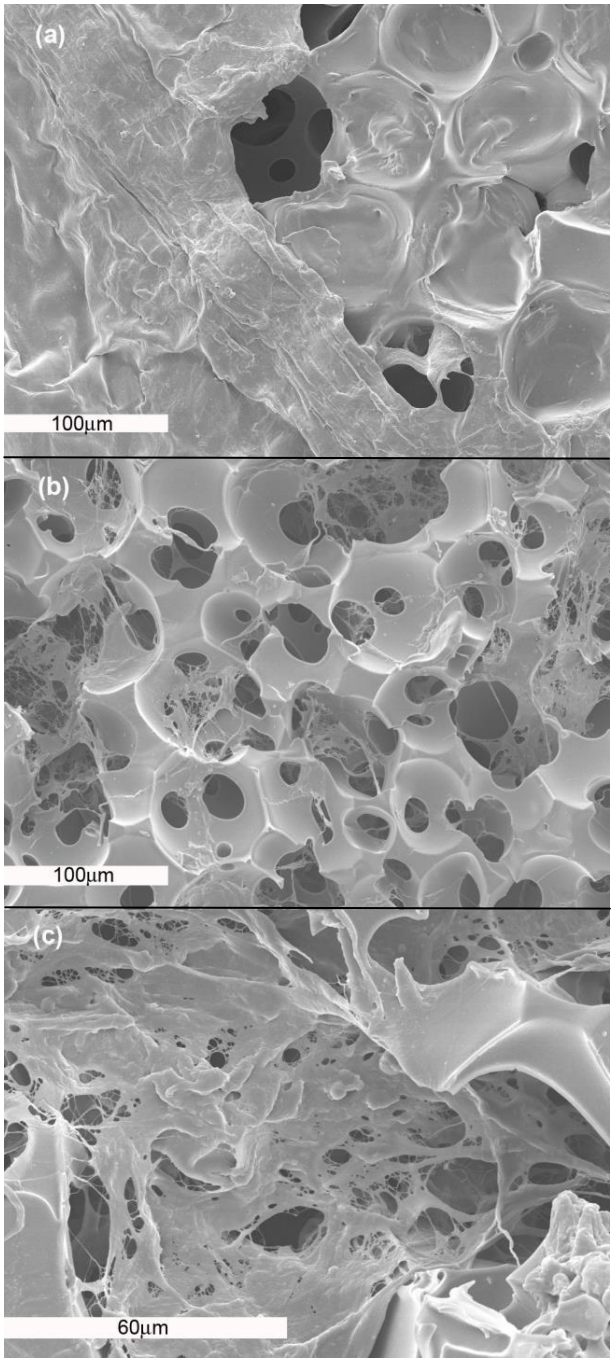

Figure 4.25 SEM pictures of the surface (a) **and cross sections** (b) **and** (c) **of P(CLMA-co-HEA) 70/30 after 28 days culture**

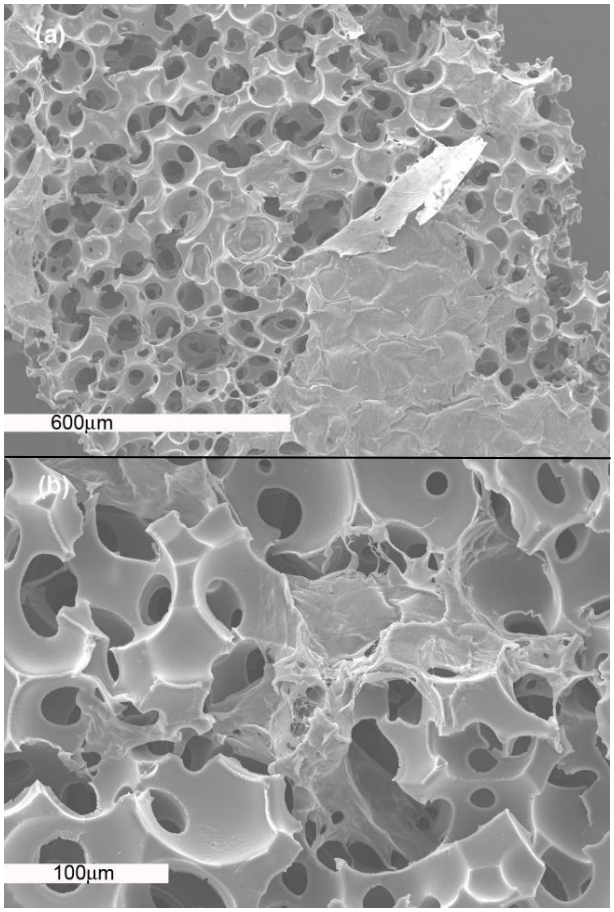

Figure 4.26 SEM pictures of the surface (a) **and cross section** (b) **of P(CLMA-co-HEA) 30/70 after 28 days culture**

The different behaviour of cells inside the pores and on the surface prevents any attempt of quantification of the number of cells in the different materials. Nevertheless, a qualitative approach obtained by inmunostaining shows a clear dependence of the number of chondrocytes located inside the scaffolds as a function of porosity and hydrophylicity of the materials.

Figure 4.27 shows confocal microscopy images of cross sections of PCL70 and PCL80 scaffolds after 7 or 14 days culture. The cell nuclei were stained with DAPI. Although no quantitative evaluation with sufficient accuracy was possible, it can be observed that the number of cells inside the scaffolds decreases with decreasing volume fraction of pores due to the lack of interconnectivity between the spherical cavities. Very few cells were found in PCL60 scaffolds, with 60% volume fraction of pores. Non-specific staining of PCL allowed the pores contour to be seen. Chondrocytes seemed to form clusters close to the pore walls.

In a previous work it was shown that cell adhesion and proliferation of human chondrocytes in monolayer culture on PCLMA and P(CLMA-co-HEA) 70/30 was similar and only slightly lower than in the CPS cultures. In 3D culture inside the scaffolds, the results also seem to be

analogous in these two macroporous materials, as can be seen in the confocal pictures of cross-sections after culture at 7 or 14 days (**Figure 4.28**).

The number of cells in these materials seems to be of the same order as that in PCL scaffolds. However, for higher HEA content in P(CLMA-co-HEA) copolymer scaffolds, only a few cells can be localised in the immunostained cross sections, which confirms the SEM results. The SEM pictures clearly show that even in the most hydrophilic copolymers, cell attachment to the substrate is possible, although the adhesion forces are probably weaker than those in hydrophobic materials.

The adhesion force to the scaffold has been shown to play an important role in the morphology of chondrocytes seeded in macroporous 3D scaffolds. Miot *et al*. [201] found that scaffolds made of polyethylene glycol terephtalate/polybutylene terephtalate hydrophilic materials, chondrocytes better maintain the differentiated phenotype *in vitro* in the scaffolds with the highest hydrophilicity, which was ascribed to a reduced fibronectin adsorption to the substrate.

However, as in the case of monolayer culture, dedifferentiation of the cultured chondrocytes does not take place in all the materials at the same culture time. It has been shown that the development of actin cytoskeleton takes place in monolayer culture on PLLA at longer culture periods than in control substrates [64]. This behaviour was also found in monolayer culture on foamed or unfoamed poly(ethyl methacrylate) substrates [202]. On the other hand, the average density of hydrophilic groups on the surface is not the key factor; their distribution and the way in which they are exposed for protein adsorption also play an important role, as explained in section **4.1**.

In 3D culture in macroporous scaffolds, the pore architecture seems to be very important as well. The adhesion to micro or nanofiber 3D biomaterials could be different from that to scaffolds with pore cavities made of the same materials. A round morphology was better preserved in the micro or nanofibres 3D biomaterials [203, 204].

The hydrophilic/hydrophobic copolymers of reference Miot *et al.* [201] and also the series presented in this work seem to sustain cell attachment even for high hydrophilicity.

The biological response, however, is quite different between the two series. In the P(CLMA-co-HEA) series of scaffolds, the results obtained in the copolymer containing 30% HEA groups were very similar to those in PCLMA with low hydrophilicity or PCL80, which is hydrophobic.

A further increase of the HEA content seems to avoid the viability of the cells inside the scaffold. This behaviour could be related to the need of cell attachment to the pore walls at least in the initial phases of cell seeding.

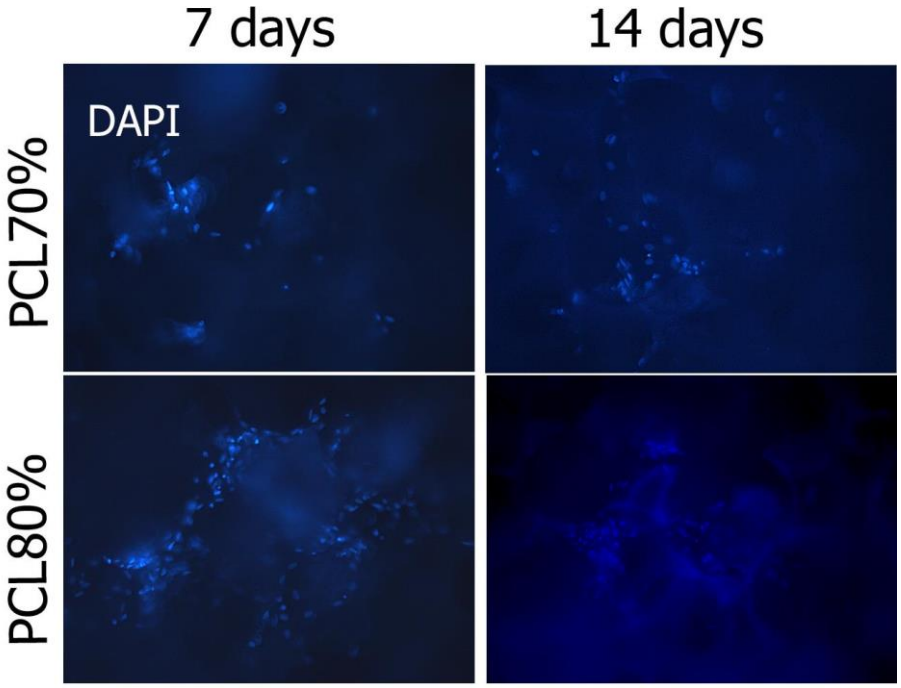

Figure 4.27 Representative cross sections of the PCL scaffolds observed with confocal microscopy at 7 and 14 days

Cell nuclei were stained with DAPI.

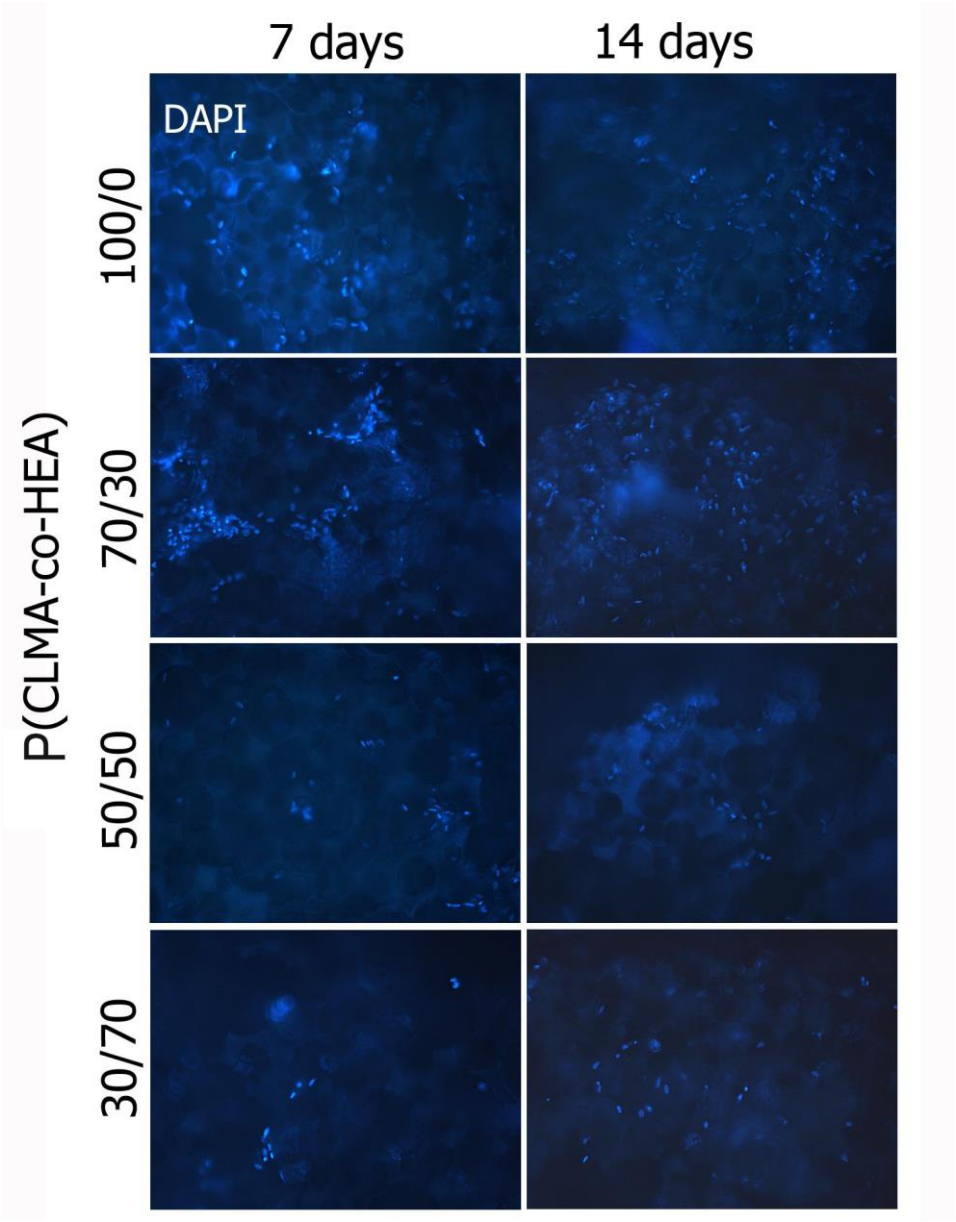

Figure 4.28 Representative cross sections of the P(CLMA-co-HEA) scaffolds observed with confocal microscopy at days 7 and 14

Cell nuclei were stained with DAPI. The pictures show cell clusters inside PCLMA scaffold or the P(CLMA-co-HEA) 70/30 scaffolds. Nevertheless, more hydrophilic polymers show a much smaller number of cells.

4.4.1.2 Morphological and inmunocytochemical analysis

Immunofluorescent staining showed that cells clustered close to the pore walls and expressed both collagen type I and collagen type II (green colour in **Figure 4.29**), and aggrecan (red colour in **Figure 4.30**).

Figure 4.29 and **Figure 4.30** provide the results of representative cross sections of PCL80 and P(CLMA-co-HEA) 70/30 scaffolds, both with a significant number of cells.

In all materials, collagen type I and collagen type II were expressed by all cell clusters observed up to 14 days culture. The adhesion of a chondrocyte to a substrate starts with the recognition by the cell's transmembrane integrins of some binding sequences of the proteins adsorbed on the biomaterial surface, which triggers a sequence of events that includes the aggregation of the integrins, the formation of focal adhesions and the development of the actin cytoskeleton, which changes the rounded physiological morphology of the cell into the spread morphology characteristic of the dedifferentiated cell, yielding the change of the cell phenotype. The change of phenotype is mainly characterised by the switch from expressing collagen type II to expressing collagen type I since it is believed that a single dedifferentiating cell is not able to produce both types of collagen simultaneously [61, 205].

The pores of the scaffold are large enough compared with the size of the cells, such that when chondrocytes are seeded into the 3D pore structure, at least part of them adhere to the surfaces of the pore walls and maintain the dedifferentiated phenotype, while others redifferentiate and produce collagen type II and aggrecan.

Another point of interest is the ability that the cells adhered to the substrate have for proliferating. As mentioned above, the results of tests such as MTT, MTS or DNA quantification are representative mainly of the proliferative cells in the external surfaces of the scaffold. Nevertheless, Ki67 positive cells were detected in the cell clusters inside the pores, as shown in **Figure 4.30** by the green points, which indicates some mitotic capacity of cells adhered to the scaffold walls (observable at higher magnification in **Figure 4.31**).

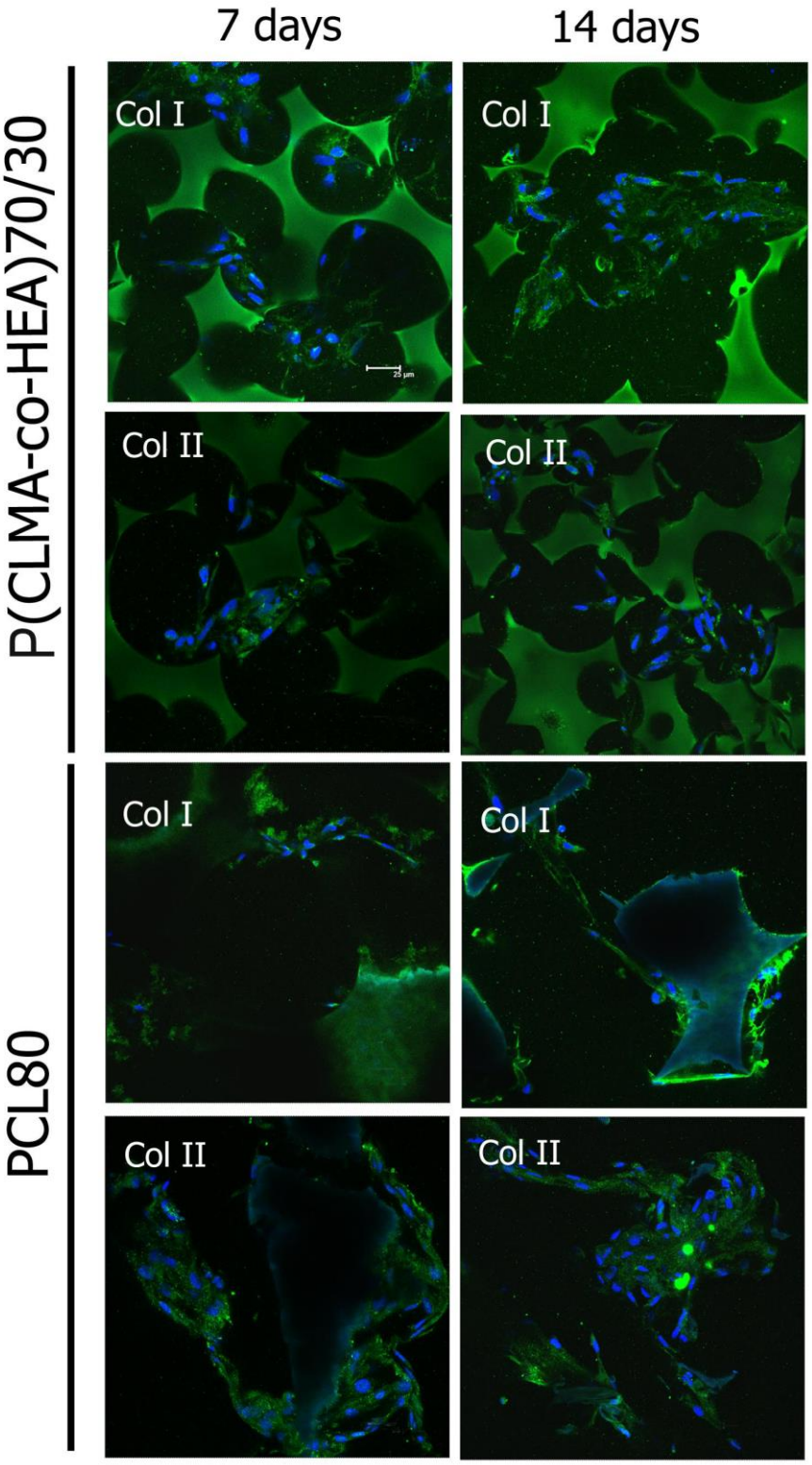

Figure 4.29 Immunocytochemistry assay of collagen type I and type II in cross sections of PCL80 and P(CLMA-co-HEA) 70/30 after 7 and 14 days culture

The cell nuclei are counterstained with DAPI (blue). Unspecific staining of the polymer marks the pore walls. Cell clusters appear close to the pore walls expressing both collagen type I and type II (green).

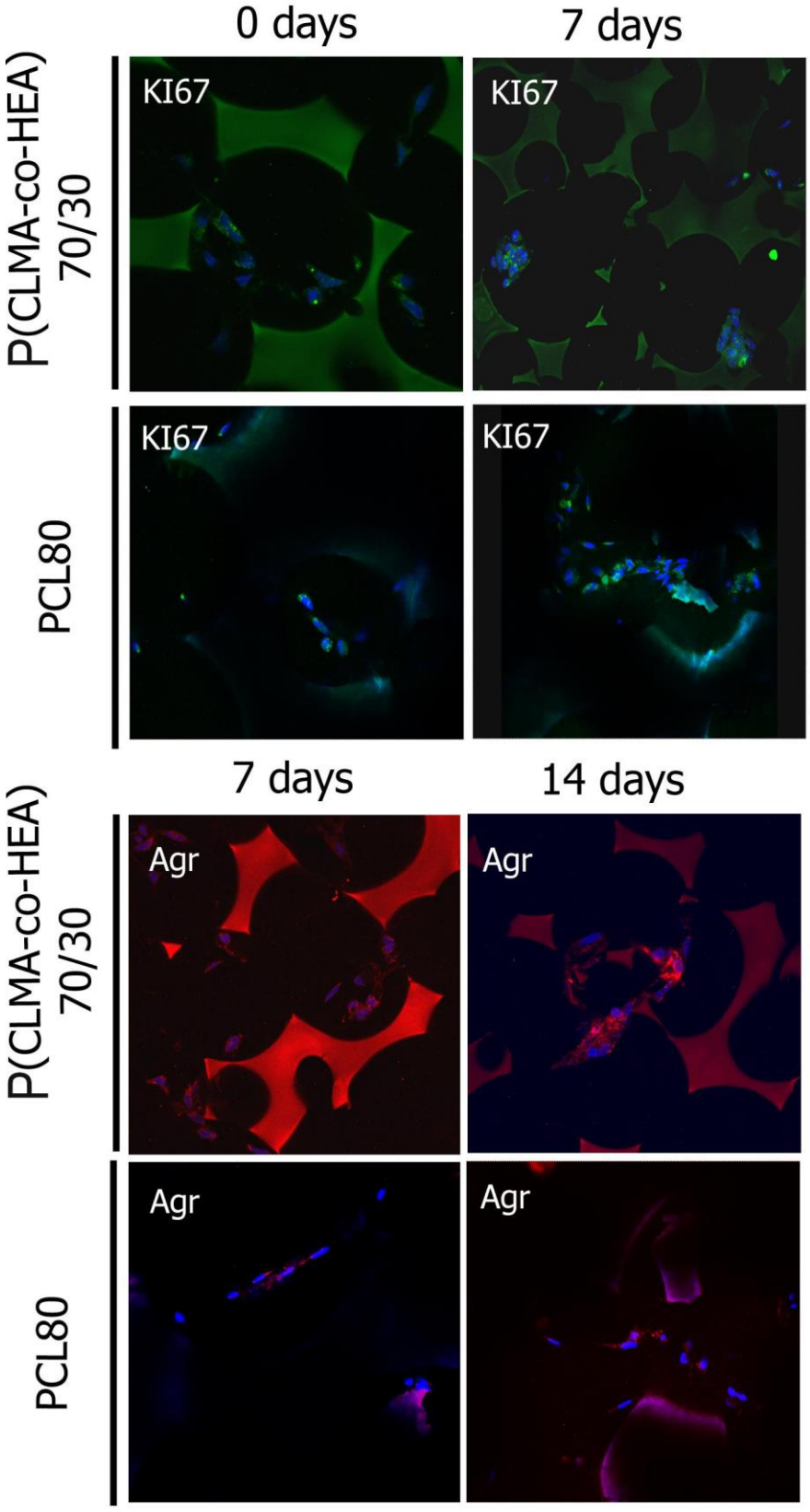

Figure 4.30 Immunocytochemistry assay of cross sections of PCL80 and P(CLMA-co-HEA) 70/30 after 7 and 14 days culture

Clusters of cells can be observed with some Ki67 positive cells (green points within or close to the cell nuclei). Aggrecan expression (red) is also detected.

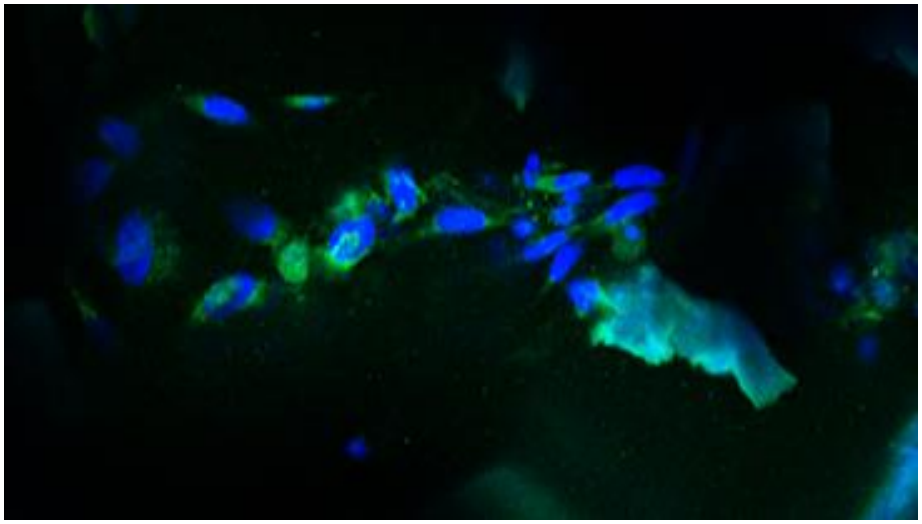

Figure 4.31 A detail of the Ki67 staining of PCL80 scaffold at 14 days culture from Figure 4.30

4.4.2 Conclusions

Two series of polycaprolactone based scaffolds were prepared, one of them of varying porosity and the other with copolymers in which the ratio of hydrophilic/hydrophobic component varied. The number of cells inside polycaprolactone scaffolds clearly increased as porosity was increased, as expected. A minimum of around 70% porosity seems to be necessary for this scaffold architecture to allow seeding and viability of the cells inside the scaffold. Almost no cells were observed inside the copolymer scaffolds with 50% or more of the hydrophilic component. Nevertheless, the scaffold made by the copolymer containing 30% of the hydrophilic monomeric units showed a result as good as pure polycaprolactone. Interestingly, both SEM and non specific staining of the scaffold material by the inmunofluorescent antibodies allowed for the observation of chondrocytes inside the scaffold forming aggregates adhered to, or very close to, the pore walls. In addition a fraction of cells were Ki67 positive, thus showing some proliferation inside the scaffold despite the fact that the major part of the culture was performed in medium without FBS and with ITS. Moreover, chondrocytes expressed both type I and type II collagen in addition to aggrecan. It can be inferred that part of the cells inside the scaffold adhered to the pore walls and kept the dedifferentiated phenotype characteristic of chondrocytes cultured in monolayer, while others redifferentiate.

Chapter 5

CONCLUSIONS

"Nunca consideres el estudio como una obligación, sino como una oportunidad para penetrar en el bello y maravilloso mundo del saber."

"Hay dos maneras de vivir su vida: una como si nada es un milagro, la otra es como si todo es un milagro."

"Si tu intención es describir la verdad, hazlo con sencillez y la elegancia déjasela al sastre."

Albert Einstein (Físico teórico. 1879-1955)

CONCLUSIONS

The conclusions drawn from this study can be stated as follows:

1.- The presence of hydrophilic and hydrophobic domains at the surface of the culture 2D material can be obtained by radical polymerisation of two monomers of different reactivity. In this way polymerisation produces firstly a copolymer rich in the more reactive monomer that is consumed, while a fraction of the less reactive monomer still remains. This less reactive monomer then produces homopolymer chains that aggregate in nanometric domains. In our work we produced surfaces with nano-domains of hydrophobic polymer and showed a favourable effect, on average, on cell adhesion to a hydrophilic surface.

2.- Hydrophilicity and surface distribution of hydrophilic and hydrophobic domains highly affect cell-material interaction. Introducing a fraction of hydrophilic groups homogeneously distributed at the surface at molecular level hinders cell attachment, which can limits cell expansion in monolayer but can also be highly favourable for chondrocytes redifferentiation in macroporous scaffolds. An increase in hydrophilicity also facilitates cell seeding into the pores of the scaffold, as well as diffusion of nutrients and other water soluble molecules through the scaffold-cell construct.

3.- Template techniques are useful for producing macroporous scaffolds from a variety of biostable or biodegradable materials. Mechanical properties of these scaffolds are adequate for many TE applications including cartilage regeneration.

4.- The behaviour of chondrocytes after seeding in the macropores of the scaffold can depend very significantly on pore size and pore interconnectivity. Furthermore, the interaction between cells and the pore walls is also a key factor for chondrocytes behaviour in the scaffold.

5.- In polycaprolactone scaffolds with pore architecture consisting of spherical interconnected pores, a minimum porosity of around 70% (and minimum pore throats of 50μm) appears to be a requirement for cell seeding and viability.

6.- In polycaprolactone scaffolds with pore diameter in the order of 100 μm ,the highly adherent nature of the polymer results in chondrocyte adhesion to the pore walls and the response is quite similar to that of a monolayer culture, *i.e.* cells spread, developing the actin cytoskeleton without adopting the characteristic spherical morphology, and proliferate. However, despite

these adhesive properties of polycaprolactone, when chondrogenic medium is used in the culture, they produce an ECM containing collagen type II and aggrecan.

7.- Thus, the study of cell-material interaction is very important, not only for chondrocyte expansion in monolayer, but also for cell redifferentiation in 3D macroporous scaffolds.

8.- Redifferentiation of mature chondrocytes by culture in 3D macroporous scaffolds is feasible in the absence of FBS and in ITS containing medium (ICM). Chondrocytes previously expanded in monolayer culture were redifferentiated and expressed chondrogenic markers (type II collagen and aggrecan).

Chapter 6

REFERENCES

"La manera como se presentan las cosas no es la manera como son; y si las cosas fueran como se presentan la ciencia entera sobraría."

Karl Marx (filósofo, economista y político. 1818-1883)

REFERENCES

[1] Gentili C, Cancedda R. Cartilage and bone extracellular matrix. Current pharmaceutical design. 2009;15:1334-48.

[2] Fawcett DW. Tratado de Histología–Bloom Fawcett. 12th ed: Mc Graw Hill-Interamericana; 1995.

[3] Gallik S. The on-line lab manual for mammalial histology. http://histologyolmstevegallikorg/node/412009.

[4] Sophia Fox AJ, Bedi A, Rodeo SA. The basic science of articular cartilage: structure, composition, and function. Sports health. 2009;1:461-8.

[5] Sopena J, Carrillo JM, Rubio M, Redondo JI, Serra I, Soler C. Estructura y función del cartílago articular. In: articular EP-Afalp, editor. http://wwwtraumatologiaveterinariacom/articulaciones/docs/cartilago_articularpdf1995. p. 24-6.

[6] Mar Vista Animal Medical Center. Normal Joint Structure. http://www.marvistavet.com/html/body_normal_joint_structure.html2015.

[7] Landínez-Parra NS, Garzón-Alvarado DA, Vanegas-Acosta JC. Mechanical Behavior of Articular Cartilage: Intech; 2012.

[8] Flik KR, Verma N, Cole BJ, Bach BR. Articular Cartilage: Structure, Biology, and Function. Cartilage Repair Strategies. Totowa, New Jersey: Humana Press Inc; 2007. p. 1-12.

[9] Athanasiou KA, Darling EM, Hu JC. Articular Cartilage Tissue Engineering. University of California, Davis: Morgan and Claypool Publishers; 2009.

[10] Meachim G, Sheffield SR. Surface ultrastructure of mature adult human articular cartilage. The Journal of bone and joint surgery British volume. 1969;51:529-39.

[11] Ulrich-Vinther M, Maloney MD, Schwarz EM, Rosier R, O'Keefe RJ. Articular cartilage biology. The Journal of the American Academy of Orthopaedic Surgeons. 2003;11:421-30.

[12] Poole CA, Flint MH, Beaumont BW. Chondrons in cartilage: ultrastructural analysis of the pericellular microenvironment in adult human articular cartilages. Journal of orthopaedic research : official publication of the Orthopaedic Research Society. 1987;5:509-22.

[13] Buckwalter JA, Mankin HJ. Articular cartilage, part 1: tissue design and chondrocyte-matrix interaction. The Journal of bone and joint surgery American volume. 1997;79:600-11.

[14] Eyre DR, Weis MA, Wu JJ. Articular cartilage collagen: an irreplaceable framework? Eur Cell Mater. 2006;12:57-63.

[15] Hardingham T, Bayliss M. Proteoglycans of articular cartilage: changes in aging and in joint disease. Seminars in arthritis and rheumatism. 1990;20:12-33.

[16] Martin JA, Buckwalter JA. Telomere erosion and senescence in human articular cartilage chondrocytes. The journals of gerontology Series A, Biological sciences and medical sciences. 2001;56:B172-9.

[17] Buckwalter JA. Articular cartilage injuries. Clin Orthop Relat Res. 2002:21-37.

[18] San Roman F. El Cartilago Articular. Iams Nutrition Symposium. Chicago2000.

[19] Kelc R, Naranda J, Kuhta M, Vogrin M. The Physiology of Sports Injuries and Repair Processes. In: (Ed.) APMH, editor. Current Issues in Sports and Exercise Medicine: InTech; 2013.

[20] Outerbridge RE. The etiology of chondromalacia patellae. The Journal of bone and joint surgery British volume. 1961;43-B:752-7.

[21] Browne JE, Branch TP. Surgical alternatives for treatment of articular cartilage lesions. The Journal of the American Academy of Orthopaedic Surgeons. 2000;8:180-9.

[22] Barber FA. Chondral injuries in the knee. In: Johnson DH, Pedowitz RA, editors. Practical Orthopaedic Sports Medicine and Arthroscopy. Philadelphia: Lippincott Williams & Wilkins; 2007. p. 741-57.

[23] Mila E. Long-Term Treatment of Osteoarthritis Pain: Achieving a Balance Between Efficacy and Tolerability for a Successful Chronic Therapy. In: Chen PQ, editor. Osteoarthritis - Diagnosis, Treatment and Surgery: InTech; 2012.

[24] Martel-Pelletier J, Pelletier JP. Is osteoarthritis a disease involving only cartilage or other articular tissues? Eklem hastaliklari ve cerrahisi = Joint diseases & related surgery. 2010;21:2-14.

[25] Takahashi I, Masuda T, Kohsaka K, Terao F, Anada T, Sasano Y, et al. Molecular mechanisms of the response to mechanical stimulation during chondrocyte differentiation. In: Sasano T, Suzuki O, editors. Interface Oral Health Science. Tokyo: Springer; 2010. p. 53-9.

[26] Hunziker EB. Articular cartilage repair: basic science and clinical progress. A review of the current status and prospects. Osteoarthritis Cartilage. 2002;10:432-63.

[27] Rodríguez-Merchán EC, De la Corte-García H. Regeneration of Articular Cartilage of the Knee: Basic Concepts. In: Rodríguez-Merchán EC, editor. Articular Cartilage Defects of the Knee. Italia: Springer; 2012.

[28] Rodriguez-Merchan EC. Regeneration of articular cartilage of the knee. Rheumatology international. 2013;33:837-45.

[29] Curl WW, Krome J, Gordon ES, Rushing J, Smith BP, Poehling GG. Cartilage injuries: a review of 31,516 knee arthroscopies. Arthroscopy : the journal of arthroscopic & related surgery : official publication of the Arthroscopy Association of North America and the International Arthroscopy Association. 1997;13:456-60.

[30] Bhosale AM, Richardson JB. Articular cartilage: structure, injuries and review of management. British medical bulletin. 2008;87:77-95.

[31] Bos PK, van Melle ML, van Osch GJ. Articular cartilage repair and the evolving role of regenerative medicine. Open Access Surg. 2013;3:109–22.

[32] Steadman JR, Rodkey WG, Briggs KK, Rodrigo JJ. The microfracture technique to treat full thickness articular cartilage defects of the knee. Orthopade. 1999;28:26-32.

[33] Mithoefer K, Williams RJ, 3rd, Warren RF, Potter HG, Spock CR, Jones EC, et al. Chondral resurfacing of articular cartilage defects in the knee with the microfracture technique. Surgical technique. The Journal of bone and joint surgery American volume. 2006;88 Suppl 1 Pt 2:294-304.

[34] Insall J. Pridie debridement operation for osteoarthritis of knee Clinical Orthopaedics and Related Research. 1974:61-7.

[35] Pridie KH. A method of resurfacing osteoarthritic knee joints. . J Bone Joint Surg [Br] 1959;41-B:618-19.

[36] Smith GD, Knutsen G, Richardson JB. A clinical review of cartilage repair techniques. The Journal of Bone and Joint Surgery (Br). 2005;87B:445-9.

[37] Hunziker EB. Articular cartilage repair: basic science and clinical progress. A review of the current status and prospects. Osteoarthritis Cartilage. 2001;10:432-63.

[38] Ficat RP, Ficat C, Gedeon P, Toussaint JB. Spongialization: a new treatment for diseased patellae. Clin Orthop Relat Res. 1979:74-83.

[39] Kreuz PC, Steinwachs MR, Erggelet C, Krause SJ, Konrad G, Uhl M, et al. Results after microfracture of full-thickness chondral defects in different compartments in the knee. Osteoarthritis Cartilage. 2006;14:1119-25.

[40] Langer R, Vacanti JP. Tissue engineering. Science. 1993;260:920-6.

[41] Peterson L, Minas T, Brittberg M, Nilsson A, Sjogren-Jansson E, Lindahl A. Two- to 9-year outcome after autologous chondrocyte transplantation of the knee. Clin Orthop Relat Res. 2000:212-34.

[42] Bentley G, Biant LC, Carrington RW, Akmal M, Goldberg A, Williams AM, et al. A prospective, randomised comparison of autologous chondrocyte implantation versus mosaicplasty for osteochondral defects in the knee. The Journal of bone and joint surgery British volume. 2003;85:223-30.

[43] Knutsen G, Engebretsen L, Ludvigsen TC, Drogset JO, Grontvedt T, Solheim E, et al. Autologous chondrocyte implantation compared with microfracture in the knee. A randomized trial. The Journal of bone and joint surgery American volume. 2004;86-A:455-64.

[44] Chen G, Liu D, Tadokoro M, Hirochika R, Ohgushi H, Tanaka J, et al. Chondrogenic differentiation of human mesenchymal stem cells cultured in a cobweb-like biodegradable scaffold. Biochem Biophys Res Commun. 2004;322:50-5.

[45] Patrick CW, Mikos AG, McIntire LV. Frontiers in Tissue Engineering. . First ed. London Pergamon; 1998.

[46] Brittberg M, Peterson L, Sjogren-Jansson E, Tallheden T, Lindahl A. Articular cartilage engineering with autologous chondrocyte transplantation - A review of recent developments. Journal of Bone and Joint Surgery-American Volume. 2003;85A:109-15.

[47] Redman SN, Oldfield SF, Archer CW. Current strategies for articular cartilage repair. Eur Cell Mater. 2005;9:23-32; discussion 23-32.

[48] Ochi M, Adachi N, Nobuto H, Yanada S, Ito Y, Agung M. Articular cartilage repair using tissue engineering technique--novel approach with minimally invasive procedure. Artif Organs. 2004;28:28-32.

[49] Makris EA, Gomoll AH, Malizos KN, Hu JC, Athanasiou KA. Repair and tissue engineering techniques for articular cartilage. Nature reviews Rheumatology. 2015;11:21-34.

[50] Matsiko A, Levingstone TJ, O'Brien FJ. Advanced Strategies for Articular Cartilage Defect Repair. Materials 2013;6:637-68.

[51] Oseni AO, Crowley C, Boland MZ, Butler PE, Seifalian AM. Cartilage Tissue Engineering: the Application of Nanomaterials and Stem Cell Technology, Tissue Engineering for Tissue and Organ Regeneration. In: (Ed.) PDE, editor.: InTech; 2011.

[52] Johnstone B, Alini M, Cucchiarini M, Dodge GR, Eglin D, Guilak F, et al. Tissue engineering for articular cartilage repair--the state of the art. Eur Cell Mater. 2013;25:248-67.

[53] Chung C, Burdick JA. Engineering cartilage tissue. Advanced Drug Delivery Reviews. 2008;60:243-62.

[54] Cancedda R, Dozin B, Giannoni P, Quarto R. Tissue engineering and cell therapy of cartilage and bone. Matrix biology : journal of the International Society for Matrix Biology. 2003;22:81-91.

[55] Buckley CT, Vinardell T, Thorpe SD, Haugh MG, Jones E, McGonagle D, et al. Functional properties of cartilaginous tissues engineered from infrapatellar fat pad-derived mesenchymal stem cells. J Biomech. 2010;43:920-6.

[56] De Bari C, Dell'Accio F, Tylzanowski P, Luyten FP. Multipotent mesenchymal stem cells from adult human synovial membrane. Arthritis Rheum. 2001;44:1928-42.

[57] Kelc R, Naranda J, Kuhta M, Vogrin M. Novel Therapies for the Management of Sports Injuries. In: (Ed.) APMH, editor. Current Issues in Sports and Exercise Medicine: InTech; 2013.

[58] Lin Z, Fitzgerald JB, Xu J, Willers C, Wood D, Grodzinsky AJ, et al. Gene expression profiles of human chondrocytes during passaged monolayer cultivation. Journal of orthopaedic research : official publication of the Orthopaedic Research Society. 2008;26:1230-7.

[59] Schulze-Tanzil G. Activation and dedifferentiation of chondrocytes: implications in cartilage injury and repair. Annals of anatomy = Anatomischer Anzeiger : official organ of the Anatomische Gesellschaft. 2009;191:325-38.

[60] Marlovits S, Hombauer M, Tamandl D, Vecsei V, Schlegel W. Quantitative analysis of gene expression in human articular chondrocytes in monolayer culture. International journal of molecular medicine. 2004;13:281-7.

[61] Brodkin KR, Garcia AJ, Levenston ME. Chondrocyte phenotypes on different extracellular matrix monolayers. Biomaterials. 2004;25:5929-38.

[62] Freemont AJ, Hoyland J. Lineage plasticity and cell biology of fibrocartilage and hyaline cartilage: Its significance in cartilage repair and replacement. European Journal of Radiology. 2006;57:32-6.

[63] Boyan BD, Hummert TW, Dean DD, Schwartz Z. Role of material surfaces in regulating bone and cartilage cell response. Biomaterials. 1996;17:137-46.

[64] Costa Martinez E, Rodriguez Hernandez JC, Machado M, Mano JF, Gomez Ribelles JL, Monleon Pradas M, et al. Human chondrocyte morphology, its dedifferentiation, and fibronectin conformation on different PLLA microtopographies. Tissue engineering Part A. 2008;14:1751-62.

[65] Martinez EC, Hernandez JCR, Machado M, Mano JF, Ribelles JLG, Pradas MM, et al. Human Chondrocyte Morphology, Its Dedifferentiation, and Fibronectin Conformation on Different PLLA Microtopographies. Tissue Eng Part A. 2008;14:1751-62.

[66] Hutcheon GA, Downes S, Davies MC. Interactions of chondrocytes with methacrylate copolymers. Journal of materials science Materials in medicine. 1998;9:815-8.

[67] Schmal H, Mehlhorn AT, Fehrenbach M, Muller CA, Finkenzeller G, Sudkamp NP. Regulative mechanisms of chondrocyte adhesion. Tissue Eng. 2006;12:741-50.

[68] Wyre RM, Downes S. An in vitro investigation of the PEMA/THFMA polymer system as a biomaterial for cartilage repair. Biomaterials. 2000;21:335-43.

[69] Temenoff JS, Mikos AG. Review: tissue engineering for regeneration of articular cartilage. Biomaterials. 2000;21:431-40.

[70] Chua KH, Aminuddin BS, Fuzina NH, Ruszymah BH. Insulin-transferrin-selenium prevent human chondrocyte dedifferentiation and promote the formation of high quality tissue engineered human hyaline cartilage. Eur Cell Mater. 2005;9:58-67; discussion

[71] Caron MM, Emans PJ, Coolsen MM, Voss L, Surtel DA, Cremers A, et al. Redifferentiation of dedifferentiated human articular chondrocytes: comparison of 2D and 3D cultures. Osteoarthritis Cartilage. 2012;20:1170-8.

[72] Stevens MM, Qanadilo HF, Langer R, Shastri VP. A rapid-curing alginate gel system: utility in periosteum-derived cartilage tissue engineering. Biomaterials. 2004;25:887-94.

[73] Schagemann JC, Chung HW, Mrosek EH, Stone JJ, Fitzsimmons JS, O'Driscoll SW, et al. Poly-epsilon-caprolactone/gel hybrid scaffolds for cartilage tissue engineering. Journal of biomedical materials research Part A. 2010;93:454-63.

[74] Bolgen N, Vargel I, Korkusuz P, Guzel E, Plieva F, Galaev I, et al. Tissue responses to novel tissue engineering biodegradable cryogel scaffolds: an animal model. Journal of biomedical materials research Part A. 2009;91:60-8.

[75] Jeong CG, Hollister SJ. A comparison of the influence of material on in vitro cartilage tissue engineering with PCL, PGS, and POC 3D scaffold architecture seeded with chondrocytes. Biomaterials. 2010;31:4304-12.

[76] Gantenbein-Ritter B, Potier E, Zeiter S, van der Werf M, Sprecher CM, Ito K. Accuracy of three techniques to determine cell viability in 3D tissues or scaffolds. Tissue engineering Part C, Methods. 2008;14:353-8.

[77] Jones JR, Atwood RC, Poologasundarampillai G, Yue S, Lee PD. Quantifying the 3D macrostructure of tissue scaffolds. Journal of materials science Materials in medicine. 2009;20:463-71.

[78] Sarkar S, Isenberg BC, Hodis E, Leach JB, Desai TA, Wong JY. Fabrication of a layered microstructured polycaprolactone construct for 3-D tissue engineering. Journal of biomaterials science Polymer edition. 2008;19:1347-62.

[79] Giannini S, Buda R, Vannini F, Di Caprio F, Grigolo B. Arthroscopic autologous chondrocyte implantation in osteochondral lesions of the talus: surgical technique and results. The American journal of sports medicine. 2008;36:873-80.

[80] Manfredini M, Zerbinati F, Gildone A, Faccini R. Autologous chondrocyte implantation: a comparison between an open periosteal-covered and an arthroscopic matrix-guided technique. Acta orthopaedica Belgica. 2007;73:207-18.

[81] O'Conor CJ, Case N, Guilak F. Mechanical regulation of chondrogenesis. Stem cell research & therapy. 2013;4:61.

[82] Ribelles JLG. Bio-Inspired 3D Environments for Cartilage Engineering. Biomimetic Approaches for Biomaterials Development: Wiley-VCH Verlag GmbH & Co. KGaA; 2012. p. 515-36.

[83] Hutmacher DW. Scaffolds in tissue engineering bone and cartilage. Biomaterials. 2000;21:2529-43.

[84] Zhang R, Ma PX. Synthetic nano-fibrillar extracellular matrices with predesigned macroporous architectures. J Biomed Mater Res. 2000;52:430-8.

[85] Ma PX, Choi JW. Biodegradable polymer scaffolds with well-defined interconnected spherical pore network. Tissue Eng. 2001;7:23-33.

[86] Singhvi R, Stephanopoulos G, Wang DI. Effects of substratum morphology on cell physiology. Biotechnol Bioeng. 1994;43:764-71.

[87] Lyndon MJ. Synthetic Hydrogels as Substrata for Cell Adhesion Studies. Brit Poly J. 1986;18:22–7.

[88] Lyndon MJ, Minett TW, Tighe BJ. Cellular interactions with synthetic polymer surfaces in culture Biomaterials. 1985;6:396–402.

[89] De Bartolo L, Morelli S, Bader A, Drioli E. Evaluation of cell behaviour related to physico-chemical properties of polymeric membranes to be used in bioartificial organs. Biomaterials. 2002;23:2485-97.

[90] Zheng Z, Bei FF, Tian HL, Chen GQ. Effects of crystallization of polyhydroxyalkanoate blend on surface physicochemical properties and interactions with rabbit articular cartilage chondrocytes. Biomaterials. 2005;26:3537-48.

[91] Schakenraad JM, Busscher HJ, Wildevuur CR, Arends J. The influence of substratum surface free energy on growth and spreading of human fibroblasts in the presence and absence of serum proteins. J Biomed Mater Res. 1986;20:773-84.

[92] Rosen JJ, Schway MB. Kinetics of cell adhesion to a hydrophilic–hydrophobic copolymer model system. Polym Sci Technol. 1980;12:667–75.

[93] Arora KA, Lesser AJ, McCarthy TJ. Compressive behavior of microcellular polystyrene foams processed in supercritical carbon dioxide. Polymer Engineering and Science. 1998;38:2055-62.

[94] Thomson RC, Wake MC, Yaszemski MJ, Mikos AG. Biodegradable polymer scaffolds to regenerate organs. In: Peppas NA, Langer, R. S. (Eds.), editor. Biopolymers II Springer Berlin Heidelberg; 1995. p. 245-74.

[95] Arica MY, Hasirci NV. Permeability of PHEMA Membranes Prepared by Photoinitiation. Polymer International. 1993;32:177–82.

[96] Andrianova G, Parkhomov S. Porous materials from crystallizable polyolefins produced by gel technology. Polym Eng Sci 1997;37:1367–80.

[97] Okay O. Formation of Macroporous Styrene–Divinylbenzene Copolymer Networks: Theory vs. Experiments. Journal of Applied Polymer Science. 1999;74:2181–95.

[98] Okay O. Macroporous copolymer networks. Progress in Polymer Science. 2000;25:711-79.

[99] Shapiro L, Cohen S. Novel alginate sponges for cell culture and transplantation. Biomaterials. 1997;18:583-90.

[100] Song SW, Torkelson JM. Coarsening Effects on Microstructure Formation in Isopycnic Polymer Solutions and Membranes Produced via Thermally Induced Phase Separation. Macromolecules. 1994;27:6389-97.

[101] Lu L, Mikos AG. The importance of new processing techniques in tissue engineering. MRS bulletin / Materials Research Society. 1996;21:28-32.

[102] Thomson RC, Shung AK, Yaszemski MJ, Mikos AG. Polymer Scaffold Processing. In: Lanza RP LR, Vacan ti J, editors, editor. Principles of Tissue Engineering. Second ed. California: Elsevier Science; 2000. p. 251-62.

[103] Dhandayuthapani B, Yoshida Y, Maekawa T, Sakthi Kumar DS. Polymeric Scaffolds in Tissue Engineering Application: A Review. International Journal of Polymer Science. 2011;2011.

[104] Getgood A, Brooks R, Fortier L, Rushton N. Articular cartilage tissue engineering: today's research, tomorrow's practice? The Journal of bone and joint surgery British volume. 2009;91:565-76.

[105] Woodfield TB, Bezemer JM, Pieper JS, van Blitterswijk CA, Riesle J. Scaffolds for tissue engineering of cartilage. Critical reviews in eukaryotic gene expression. 2002;12:209-36.

[106] Cao T, Ho KH, Teoh SH. Scaffold design and in vitro study of osteochondral coculture in a three-dimensional porous polycaprolactone scaffold fabricated by fused deposition modeling. Tissue Eng. 2003;9 Suppl 1:S103-12.

[107] Giordano RA, Wu BM, Borland SW, Cima LG, Sachs EM, Cima MJ. Mechanical properties of dense polylactic acid structures fabricated by three dimensional printing. Journal of biomaterials science Polymer edition. 1996;8:63-75.

[108] Chen VJ, Ma PX. Nano-fibrous poly(L-lactic acid) scaffolds with interconnected spherical macropores. Biomaterials. 2004;25:2065-73.

[109] Ma Z, Gao C, Gong Y, Shen J. Paraffin spheres as porogen to fabricate poly(L-lactic acid) scaffolds with improved cytocompatibility for cartilage tissue engineering. Journal of biomedical materials research Part B, Applied biomaterials. 2003;67:610-7.

[110] Gross KA, Rodriguez-Lorenzo LM. Biodegradable composite scaffolds with an interconnected spherical network for bone tissue engineering. Biomaterials. 2004;25:4955-62.

[111] Kiremitci M, Serbetci AI, Colak R, Piskin E. Cell attachment to PU and PHEMA based biomaterials: Relation to structural properties. Clinical Materials. 1991;8:9–16.

[112] Horbett TA, Schway MB, Ratner BD. Hydrophilic–hydrophobic copolymers as cell substrates: effect on 3T3 cell growth rates. J Colloid Interf Sci 1985;104:28–39.

[113] Agrawal CM, Ray RB. Biodegradable polymeric scaffolds for musculoskeletal tissue engineering. J Biomed Mater Res. 2001;55:141-50.

[114] Ishaug SL, Yaszemski MJ, Bizios R, Mikos AG. Osteoblast function on synthetic biodegradable polymers. J Biomed Mater Res. 1994;28:1445-53.

[115] Li WJ, Danielson KG, Alexander PG, Tuan RS. Biological response of chondrocytes cultured in three-dimensional nanofibrous poly(epsilon-caprolactone) scaffolds. Journal of biomedical materials research Part A. 2003;67:1105-14.

[116] Pitt CG, Marks TA, Schindler A. In: Baker R, editor. Controlled Release of Bioactive Materials. New York: Academic Press; 1980. p. 19.

[117] Williams JM, Adewunmi A, Schek RM, Flanagan CL, Krebsbach PH, Feinberg SE, et al. Bone tissue engineering using polycaprolactone scaffolds fabricated via selective laser sintering. Biomaterials. 2005;26:4817-27.

[118] Buckwalter JA, Mankin HJ. Articular cartilage: tissue design and chondrocyte-matrix interactions. Instructional course lectures. 1998;47:477-86.

[119] Izquierdo R, Garcia-Giralt N, Rodriguez MT, Caceres E, Garcia SJ, Ribelles JLG, et al. Biodegradable PCL scaffolds with an interconnected spherical pore network for tissue engineering. Journal of Biomedical Materials Research Part A. 2008;85A:25-35.

[120] Schulze-Tanzil G, de Souza P, Villegas Castrejon H, John T, Merker HJ, Scheid A, et al. Redifferentiation of dedifferentiated human chondrocytes in high-density cultures. Cell Tissue Res. 2002;308:371-9.

[121] Saldanha V, Grande DA. Extracellular matrix protein gene expression of bovine chondrocytes cultured on resorbable scaffolds. Biomaterials. 2000;21:2427-31.

[122] Martin I, Jakob M, Schafer D, Dick W, Spagnoli G, Heberer M. Quantitative analysis of gene expression in human articular cartilage from normal and osteoarthritic joints. Osteoarthritis Cartilage. 2001;9:112-8.

[123] Klangjorhor J, Nimkingratana P, Settakorn J, Pruksakorn D, Leerapun T, Arpornchayanon O, et al. Hyaluronan production and chondrogenic properties of primary human chondrocyte on gelatin based hematostatic spongostan scaffold. Journal of orthopaedic surgery and research. 2012;7:40.

[124] Klangjorhor J, Phitak T, Pruksakorn D, Pothacharoen P, Kongtawelert P. Comparison of growth factor adsorbed scaffold and conventional scaffold with growth factor supplemented media for primary human articular chondrocyte 3D culture. BMC biotechnology. 2014;14:108.

[125] Antonioli E, Lobo AO, Ferretti M, Cohen M, Marciano FR, Corat EJ, et al. An evaluation of chondrocyte morphology and gene expression on superhydrophilic vertically-aligned multi-walled carbon nanotube films. Materials science & engineering C, Materials for biological applications. 2013;33:641-7.

[126] Zeng L, Chen X, Zhang Q, Yu F, Li Y, Yao Y. Redifferentiation of dedifferentiated chondrocytes in a novel three-dimensional microcavitary hydrogel. Journal of biomedical materials research Part A. 2015;103:1693-702.

[127] Mardani M, Hashemibeni B, Ansar MM, Zarkesh Esfahani SH, Kazemi M, Goharian V, et al. Comparison between Chondrogenic Markers of Differentiated Chondrocytes from Adipose Derived Stem Cells and Articular Chondrocytes In Vitro. Iranian journal of basic medical sciences. 2013;16:763-73.

[128] Barlic A, Drobnic M, Malicev E, Kregar-Velikonja N. Quantitative analysis of gene expression in human articular chondrocytes assigned for autologous implantation. Journal of orthopaedic research : official publication of the Orthopaedic Research Society. 2008;26:847-53.

[129] Ivirico JL, Martinez EC, Sanchez MS, Criado IM, Ribelles JLG, Pradas MM. Structure and properties of methacrylate-endcapped caprolactone networks with modulated water uptake for biomedical applications. Journal of Biomedical Materials Research Part B-Applied Biomaterials. 2007;83B:266-75.

[130] Lebourg M, Anton JS, Ribelles JLG. Porous membranes of PLLA-PCL blend for tissue engineering applications. European Polymer Journal. 2008;44:2207-18.

[131] Salmerón Sánchez M, Molina Mateo J, Romero Colomer FJ, Gómez Ribelles JL. Nanoindentation and tapping mode AFM study of phase separation in poly(ethyl acrylate-co-hydroxyethyl methacrylate) copolymer networks. European Polymer Journal. 2006;42:1378–83.

[132] Owens DK, Wendt RC. Estimation of the surface free energy of polymers. J Appl Polym Sci. 1969;13:1741–47.

[133] Paul DR. Background and Perspective. In: Paul DR, Newman S, editors. Polymer Blends. New York: Academic Press; 1978.

[134] Ward IM, Hadley DW. An introduction to the mechanical properties of solid polymers. Chichester, UK: Wiley; 1993.

[135] Lednicky F, Janacek J. Relaxation behavior of the ester groups (β dispersion) in some swollen polymethacrylates J Macromol Sci Phys. 1971;B5:335–54.

[136] Espadero Berzosa A, Gómez Ribelles JL, Kripotou S, Pissis P. Relaxation Spectrum of Polymer Networks Formed from Butyl Acrylate and Methyl Methacrylate Monomeric Units. Macromolecules. 2004;37:6472-79.

[137] McCrum NG, Read BE, Williams G. Anelastic and dielectric effects in polymeric solids. New York: Dover Publications Inc; 1967.

[138] Salmerón Sánchez M, Brígido Diego R, Iannazzo SAM, Gómez Ribelles JL, Monleón Pradas M. The structure of poly(ethyl acrylate-co-hydroxyethyl methacrylate) copolymer networks by segmental dynamics studies based on structural relaxation experiments. Polymer. 2004;45:2349–55.

[139] van Krevelen DW, te Nijenhuis K. Properties of Polymers. Their Correlation with Chemical Structure; their Numerical Estimation and Prediction from Additive Group Contributions. 4th Edition ed. Amsterdam: Elsevier; 2009.

[140] Horbett TA, Waldburger JJ, Ratner BD, Hoffman AS. Cell adhesion to a series of hydrophilic-hydrophobic copolymers studied with a spinning disc apparatus. J Biomed Mater Res. 1988;22:383-404.

[141] Eskin SG, Horbett TA, McIntire LV, Mitchell RN, Ratner BD, Schoen FJ, et al. Some background concepts. In: Ratner BD, Hoffman AS, Schoen FJ, Lemons JE, editors. Biomaterials science: an introduction to materials in medicine. Second ed. London: Elsevier Academic Press; 2004. p. 237-91.

[142] Campillo-Fernandez AJ, Unger RE, Peters K, Halstenberg S, Santos M, Salmeron Sanchez M, et al. Analysis of the biological response of endothelial and fibroblast cells cultured on synthetic scaffolds with various hydrophilic/hydrophobic ratios: influence of fibronectin adsorption and conformation. Tissue engineering Part A. 2009;15:1331-41.

[143] Campillo-Fernandez AJ, Pastor S, Abad-Collado M, Bataille L, Gomez-Ribelles JL, Meseguer-Duenas JM, et al. Future design of a new keratoprosthesis. Physical and biological analysis of polymeric substrates for epithelial cell growth. Biomacromolecules. 2007;8:2429-36.

[144] Soria JM, Martinez Ramos C, Bahamonde O, Garcia Cruz DM, Salmeron Sanchez M, Garcia Esparza MA, et al. Influence of the substrate's hydrophilicity on the in vitro Schwann cells viability. Journal of biomedical materials research Part A. 2007;83:463-70.

[145] Soria JM, Martinez Ramos C, Salmeron Sanchez M, Benavent V, Campillo Fernandez A, Gomez Ribelles JL, et al. Survival and differentiation of embryonic neural explants on different biomaterials. Journal of biomedical materials research Part A. 2006;79:495-502.

[146] Martinez-Ramos C, Lainez S, Sancho F, Garcia Esparza MA, Planells-Cases R, Garcia Verdugo JM, et al. Differentiation of postnatal neural stem cells into glia and functional neurons on laminin-coated polymeric substrates. Tissue engineering Part A. 2008;14:1365-75.

[147] Gómez Ribelles JL, Monleón Pradas M, Gallego Ferrer G, Peidro Torres N, Pérez Giménez V, Pissis P, et al. Poly(methyl acrylate)/poly(hydroxyethyl acrylate) sequential interpenetrating polymer networks. Miscibility and water sorption behavior. J Polym Sci B Polym Phys. 1999;37.

[148] Gallego Ferrer G, Soria Meliá JM, Hernández Canales J, Meseguer Dueñas JM, Romero Colomer F, Monleón Pradas M, et al. Poly(2-hydroxyethyl acrylate) hydrogel confined in a hydrophobous porous matrix. Colloid and Polymer Science. 2005;283:681-90.

[149] Garcia AJ. Get a grip: integrins in cell-biomaterial interactions. Biomaterials. 2005;26:7525-9.

[150] Gugutkov D, Altankov G, Hernandez JCR, Pradas MM, Sanchez MS. Fibronectin activity on substrates with controlled -OH density. Journal of Biomedical Materials Research Part A. 2010;92A:322-31.

[151] Keselowsky BG, Collard DM, Garcia AJ. Surface chemistry modulates fibronectin conformation and directs integrin binding and specificity to control cell adhesion. Journal of Biomedical Materials Research Part A. 2003;66A:247-59.

[152] Cutler SM, Garcia AJ. Engineering cell adhesive surfaces that direct integrin alpha(5)beta(1) binding using a recombinant fragment of fibronectin. Biomaterials. 2003;24:1759-70.

[153] Grinnell F, Feld MK. Fibronectin adsorption on hydrophilic and hydrophobic surfaces detected by antibody binding and analyzed during cell adhesion in serum-containing medium. The Journal of biological chemistry. 1982;257:4888-93.

[154] Altankov G, Groth T. Reorganization of substratum-bound fibronectin on hydrophilic and hydrophobic materials is related to biocompatibility. Journal of Materials Science-Materials in Medicine. 1994;5:732-7.

[155] Rico P, Hernandez JCR, Moratal D, Altankov G, Pradas MM, Salmeron-Sanchez M. Substrate-Induced Assembly of Fibronectin into Networks: Influence of Surface Chemistry and Effect on Osteoblast Adhesion. Tissue Eng Part A. 2009;15:3271-81.

[156] Ballester-Beltran J, Cantini M, Lebourg M, Rico P, Moratal D, Garcia AJ, et al. Effect of topological cues on material-driven fibronectin fibrillogenesis and cell differentiation. Journal of materials science Materials in medicine. 2012;23:195-204.

[157] Rodriguez Hernandez JC, Salmeron Sanchez M, Soria JM, Gomez Ribelles JL, Monleon Pradas M. Substrate chemistry-dependent conformations of single laminin molecules on polymer surfaces are revealed by the phase signal of atomic force microscopy. Biophysical Journal. 2007;93:202-7.

[158] Ribeiro C, Panadero JA, Sencadas V, Lanceros-Mendez S, Tamano MN, Moratal D, et al. Fibronectin adsorption and cell response on electroactive poly(vinylidene fluoride) films. Biomed Mater. 2012;7:035004.

[159] Briz N, Antolinos-Turpin CM, Alio J, Garagorri N, Ribelles JL, Gomez-Tejedor JA. Fibronectin fixation on poly(ethyl acrylate)-based copolymers. Journal of biomedical materials research Part B, Applied biomaterials. 2013;101:991-7.

[160] Tziampazis E, Kohn J, Moghe PV. PEG-variant biomaterials as selectively adhesive protein templates: model surfaces for controlled cell adhesion and migration. Biomaterials. 2000;21:511-20.

[161] Klee D, Hocker H. Polymers for biomedical applications: improvement of the interface compatibility. Adv Polym Sci. 1999;149:1-57.

[162] Schiraldi C, D'Agostino A, Oliva A, Flamma F, De Rosa A, Apicella A, et al. Development of hybrid materials based on hydroxyethylmethacrylate as supports for improving cell adhesion and proliferation. Biomaterials. 2004;25:3645-53.

[163] Tanaka H, Murphy CL, Murphy C, Kimura M, Kawai S, Polak JM. Chondrogenic differentiation of murine embryonic stem cells: effects of culture conditions and dexamethasone. J Cell Biochem. 2004;93:454-62.

[164] Bassleer C, Gysen P, Bassleer R, Franchimont P. Proteoglycans synthesized by human chondrocytes cultivated in clusters. The American journal of medicine. 1987;83:25-8.

[165] Montheard JP, Chatzopoulos M, Chappard D. 2-hydroxyethyl methacrylate (HEMA) ; chemical properties and applications in biomedical fields. J Macromol Sci, Macromol Rev. 1992;32:16.

[166] Drury JL, Mooney DJ. Hydrogels for tissue engineering: scaffold design variables and applications. Biomaterials. 2003;24:4337-51.

[167] Silva JM, Georgi N, Costa R, Sher P, Reis RL, Van Blitterswijk CA, et al. Nanostructured 3D constructs based on chitosan and chondroitin sulphate multilayers for cartilage tissue engineering. PLoS One. 2013;8:e55451.

[168] Diego RB, Estelles JM, Sanz JA, Garcia-Aznar JM, Sanchez MS. Polymer scaffolds with interconnected spherical pores and controlled architecture for tissue engineering: fabrication, mechanical properties, and finite element modeling. Journal of biomedical materials research Part B, Applied biomaterials. 2007;81:448-55.

[169] Alberich-Bayarri A, Moratal D, Ivirico JLE, Hernandez JCR, Valles-Lluch A, Marti-Bonmati L, et al. Microcomputed Tomography and Microfinite Element Modeling for Evaluating Polymer Scaffolds Architecture and Their Mechanical Properties. Journal of Biomedical Materials Research Part B-Applied Biomaterials. 2009;91B:191-202.

[170] Diego RB, Ribelles JLG, Sánchez MS. Pore collapse during the fabrication process of rubber-like polymer scaffolds. J Appl Polym Sci 2007;104:1475-81

[171] Alio del Barrio JL, Chiesa M, Gallego Ferrer G, Garagorri N, Briz N, Fernandez-Delgado J, et al. Biointegration of corneal macroporous membranes based on poly(ethyl acrylate) copolymers in an experimental animal model. Journal of biomedical materials research Part A. 2015;103:1106-18.

[172] Veiga DD, Antunes JC, Gomez RG, Mano JF, Ribelles JL, Soria JM. Three-dimensional scaffolds as a model system for neural and endothelial 'in vitro' culture. Journal of biomaterials applications. 2011;26:293-310.

[173] Lluch AV, Fernandez AC, Ferrer GG, Pradas MM. Bioactive scaffolds mimicking natural dentin structure. Journal of biomedical materials research Part B, Applied biomaterials. 2009;90:182-94.

[174] Hernandez JCR, Aroca AS, Ribelles JLG, Pradas MM. Three-dimensional nanocomposite scaffolds with ordered cylindrical orthogonal pores. Journal of Biomedical Materials Research Part B-Applied Biomaterials. 2008;84B:541-9.

[175] Martinez-Ramos C, Valles-Lluch A, Verdugo JM, Ribelles JL, Barcia Albacar JA, Orts AB, et al. Channeled scaffolds implanted in adult rat brain. Journal of biomedical materials research Part A. 2012;100:3276-86.

[176] Valles-Lluch A, Novella-Maestre E, Sancho-Tello M, Pradas MM, Ferrer GG, Batalla CC. Mimicking natural dentin using bioactive nanohybrid scaffolds for dentinal tissue engineering. Tissue engineering Part A. 2010;16:2783-93.

[177] Gibson LJ, Ashby MF. Cellular solids- Structure and properties. Second ed. Cambridge: Cambridge Universyty Press; 1999.

[178] Ivirico JLE, Salmeron-Sanchez M, Ribelles JLG, Pradas MM. Poly(L-lactide) networks with tailored water sorption. Colloid and Polymer Science. 2009;287:671-81.

[179] Lebourg M, Serra RS, Estelles JM, Sanchez FH, Ribelles JLG, Anton JS. Biodegradable polycaprolactone scaffold with controlled porosity obtained by modified particle-leaching technique. Journal of Materials Science-Materials in Medicine. 2008;19:2047-53.

[180] Santamaría VA, Deplaine H, Mariggió D, Villanueva-Molines AR, García-Aznar JM, Gómez Ribelles JL, et al. Influence of the macro and micro-porous structure on the mechanical behavior of poly(l-lactic acid) scaffolds. Journal of Non-Crystalline Solids. 2012;358:3141-9.

[181] Deplaine H, Lebourg M, Ripalda P, Vidaurre A, Sanz-Ramos P, Mora G, et al. Biomimetic hydroxyapatite coating on pore walls improves osteointegration of poly(L-lactic acid) scaffolds. Journal of biomedical materials research Part B, Applied biomaterials. 2013;101:173-86.

[182] Vikingsson L, Gallego Ferrer G, Gomez-Tejedor JA, Gomez Ribelles JL. An "in vitro" experimental model to predict the mechanical behavior of macroporous scaffolds implanted in articular cartilage. J Mech Behav Biomed Mater. 2014;32:125-31.

[183] Cruz DM, Gomes M, Reis RL, Moratal D, Salmeron-Sanchez M, Ribelles JL, et al. Differentiation of mesenchymal stem cells in chitosan scaffolds with double micro and macroporosity. Journal of biomedical materials research Part A. 2010;95:1182-93.

[184] Benya PD, Shaffer JD. Dedifferentiated chondrocytes reexpress the differentiated collagen phenotype when cultured in agarose gels. Cell. 1982;30:215-24.

[185] Bonaventure J, Kadhom N, Cohen-Solal L, Ng KH, Bourguignon J, Lasselin C, et al. Reexpression of cartilage-specific genes by dedifferentiated human articular chondrocytes cultured in alginate beads. Exp Cell Res. 1994;212:97-104.

[186] Giurea A, Klein TJ, Chen AC, Goomer RS, Coutts RD, Akeson WH, et al. Adhesion of perichondrial cells to a polylactic acid scaffold. Journal of orthopaedic research : official publication of the Orthopaedic Research Society. 2003;21:584-9.

[187] Johnstone B, Hering TM, Caplan AI, Goldberg VM, Yoo JU. In vitro chondrogenesis of bone marrow-derived mesenchymal progenitor cells. Experimental Cell Research. 1998;238:265-72.

[188] DeLise AM, Fischer L, Tuan RS. Cellular interactions and signaling in cartilage development. Osteoarthritis Cartilage. 2000;8:309-34.

[189] Grunder T, Gaissmaier C, Fritz J, Stoop R, Hortschansky P, Mollenhauer J, et al. Bone morphogenetic protein (BMP)-2 enhances the expression of type II collagen and aggrecan in chondrocytes embedded in alginate beads. Osteoarthritis Cartilage. 2004;12:559-67.

[190] van Osch GJ, van der Veen SW, Verwoerd-Verhoef HL. In vitro redifferentiation of culture-expanded rabbit and human auricular chondrocytes for cartilage reconstruction. Plastic and reconstructive surgery. 2001;107:433-40.

[191] Jakob M, Demarteau O, Schafer D, Hintermann B, Dick W, Heberer M, et al. Specific growth factors during the expansion and redifferentiation of adult human articular chondrocytes enhance chondrogenesis and cartilaginous tissue formation in vitro. Journal of Cellular Biochemistry. 2001;81:368-77.

[192] Kisiday JD, Kurz B, DiMicco MA, Grodzinsky AJ. Evaluation of medium supplemented with insulin-transferrin-selenium for culture of primary bovine calf chondrocytes in three-dimensional hydrogel scaffolds. Tissue Eng. 2005;11:141-51.

[193] Homicz MR, Chia SH, Schumacher BL, Masuda K, Thonar EJ, Sah RL, et al. Human septal chondrocyte redifferentiation in alginate, polyglycolic acid scaffold, and monolayer culture. The Laryngoscope. 2003;113:25-32.

[194] Tsai WB, Chen CH, Chen JF, Chang KY. The effects of types of degradable polymers on porcine chondrocyte adhesion, proliferation and gene expression. Journal of materials science Materials in medicine. 2006;17:337-43.

[195] Li WJ, Tuli R, Okafor C, Derfoul A, Danielson KG, Hall DJ, et al. A three-dimensional nanofibrous scaffold for cartilage tissue engineering using human mesenchymal stem cells. Biomaterials. 2005;26:599-609.

[196] Martinez-Diaz S, Garcia-Giralt N, Lebourg M, Gomez-Tejedor JA, Vila G, Caceres E, et al. In Vivo Evaluation of 3-Dimensional Polycaprolactone Scaffolds for Cartilage Repair in Rabbits. American Journal of Sports Medicine. 2010;38:509-19.

[197] Lebourg M, Martinez-Diaz S, Garcia-Giralt N, Torres-Claramunt R, Ribelles JL, Vila-Canet G, et al. Cell-free cartilage engineering approach using hyaluronic acid-polycaprolactone scaffolds: a study in vivo. Journal of biomaterials applications. 2014;28:1304-15.

[198] Ivirico JLE, Salmerón Sánchez M, Sabater i Serra R, Meseguer Dueñas JM, Gómez Ribelles JL, Monleón Pradas M. Structure and Properties of Poly(ε-caprolactone) Networks with Modulated Water Uptake. Macromolecular Chemistry and Physics. 2006;207:2195-205.

[199] Sabater i Serra R, Escobar Ivirico JL, Meseguer Duenas JM, Andrio Balado A, Gomez Ribelles JL, Salmeron Sanchez M. Dielectric relaxation spectrum of poly (epsilon-caprolactone) networks hydrophilized by copolymerization with 2-hydroxyethyl acrylate. The European physical journal E, Soft matter. 2007;22:293-302.

[200] Garcia-Giralt N, Izquierdo R, Nogues X, Perez-Olmedilla M, Benito P, Gomez-Ribelles JL, et al. A porous PCL scaffold promotes the human chondrocytes redifferentiation and hyaline-specific extracellular matrix protein synthesis. Journal of Biomedical Materials Research Part A. 2008;85A:1082-9.

[201] Miot S, Woodfield T, Daniels AU, Suetterlin R, Peterschmitt I, Heberer M, et al. Effects of scaffold composition and architecture on human nasal chondrocyte redifferentiation and cartilaginous matrix deposition. Biomaterials. 2005;26:2479-89.

[202] Barry JJA, Gidda HS, Scotchford CA, Howdle SM. Porous methacrylate scaffolds: supercritical fluid fabrication and in vitro chondrocyte responses. Biomaterials. 2004;25:3559-68.

[203] Rudert M, Hirschmann F, Schulze M, Wirth CJ. Bioartificial cartilage. Cells Tissues Organs. 2000;167:95-105.

[204] Yamane S, Iwasaki N, Majima T, Funakoshi T, Masuko T, Harada K, et al. Feasibility of chitosan-based hyaluronic acid hybrid biomaterial for a novel scaffold in cartilage tissue engineering. Biomaterials. 2005;26:611-9.

[205] von der Mark K, Gauss V, von der Mark H, Muller P. Relationship between cell shape and type of collagen synthesised as chondrocytes lose their cartilage phenotype in culture. Nature. 1977;267:531-2.

UNIVERSITAT
POLITÈCNICA
DE VALÈNCIA